FernUniversität in Hagen
Fakultät für Mathematik und Informatik
Lehrgebiet Analysis

Bachelorarbeit

On the Time-Dependent Simplified Spherical Harmonics Equations

André Liemert
(Matrikel-Nr.: 8112860)

Betreuung: Prof. Dr. Delio Mugnolo

Neu-Ulm, 01.04.2025

Acknowledgements

I would like to thank Prof. Dr. Delio Mugnolo very much for giving me the opportunity to work in the frame of this thesis on my proposed topic on the simplified spherical harmonics equations. His kind support during the processing time was very helpful.

Contents

1 Introduction **1**

2 Fundamentals of Radiative Transfer **4**
2.1 The radiative transfer equation 4
2.2 Analytical solutions to the RTE 8
2.2.1 Solution for the fluence in the infinite medium 8
2.2.2 Solution of the RTE in a bounded domain 10

3 On the SP_N Equations in Time Domain **13**
3.1 The spherical harmonics method 13
3.2 The P_N equations under plane symmetry 17
3.2.1 The P_N equations in lossless media 22
3.3 Derivation of the time-dependent SP_N equations 28
3.4 The time-dependent SP_3 equations 30
3.4.1 Considerations in the infinite medium 31
3.4.2 Solution for a bounded domain via the FCT 35
3.4.3 Solution for a bounded domain via the Laplace transform 42
3.4.4 The time-harmonic SP_3 equations 45
3.5 Numerical experiments 47
3.5.1 Simulations for the infinite medium 47
3.5.2 Simulations for the bounded domain 49

4 Conclusion **53**

Bibliography **54**

1 Introduction

The spherical harmonics method is an important approach for representing square-integrable functions on the unit sphere [1] and when it comes to finding solutions to partial differential equations [2, 3]. In the field of radiative transfer, this spectral method is abbreviated as P_N method [4, Section 8.2]. Here, it is used for representing solutions to the radiative transfer equation (RTE) as linear combination of these orthogonal functions [4–6]. However, the determination of the unknown expansion coefficients (that depend on space and time) leads to a complicated system of partial differential equations, known as the P_N equations [5], which are still challenging to solve. In addition, if boundary conditions are taken into account, the resulting systems of linear equations for finding the unknown constants within the homogeneous solution can become difficult to solve, see for example [6, Section 6]. To mitigate the problems associated with the P_N method, the so-called simplified spherical harmonics equations (SP_N equations) were introduced, at first in the steady-state domain about 60 years ago [7]. Not even 20 years ago, the SP_N method was extended for approximating solutions to the time-harmonic RTE [8, 9]. As mentioned in [10], the time-dependent (parabolic) SP_N equations were first introduced by Frank et al. [11] in 2007 via an asymptotic analysis. In 2010, these equations were directly derived from the (hyperbolic) P_N equations, see e.g. [9], in a similar manner as the classical diffusion approximation [5, pp. R46–R49] many years before. We note that the latter kind of derivation (regarding the SP_N equations) is shown within the scope of this thesis. Of course, we will see that the simplifications made do not remain without consequences, especially at short times. In the literature, the fraction of studies focusing on theoretical aspects or reporting on analytical solutions to the SP_N equations is considerably smaller than that dealing with direct applications of these equations e.g. in biomedical optics [9], medical physics [12] and especially in nuclear sciences [13–16]. For example, Zheng and Han investigated the well-posedness of the steady-state SP_N equations under reflective boundary conditions [17] . In their work, which was published in 2011, the authors mentioned in the introduction the lack of mathematical studies on the SP_N method. In the article of McClarren [18], dealing also with theoretical aspects (mainly in the steady-state domain), there was additionally a brief discussion on the SP_N equations in time domain. Until today, there still seems to be a lack of theoretical studies on the SP_N equations, especially with regard to the time-dependent case. A few words about the RTE, for which the P_N and SP_N methods were developed are appropriate in this context. This fundamental equation is involved in many areas of science such as optical tomography [5], heat transfer [19], biophotonics [20] or nuclear physics [21]. However, analytical solutions to this integro-differential equation, which would be of particular importance in view of applications, are very rare. As a consequence, the RTE is mainly solved numerically e.g. via Monte Carlo methods [22], the discrete ordinate method [23] or the finite volume method [24]. Apart from this, the RTE is also approximated by the diffusion equation (DE) [20], which corresponds in the light of the P_N or SP_N methodology with the lowest order approximation. There are well-known shortcomings of the DE (in comparison with the transport theory), which limit its applicability. For example, the diffusion theory fails near sources and in highly absorbing media and it suffers from the unrealistic feature of an infinite speed of propagation, due to the parabolic nature of the DE. In contrast to that, the Telegrapher equation (TE), which represents a second order formulation of the time-dependent P_1 equations, is of the

hyperbolic type that indeed has a finite propagation speed. However, the associated value for the speed (resulting from the P_N method) is too low, namely by a factor of $\sqrt{3}$, see also Example 3.4 and the TE (3.14). The differences between the results obtained from the DE or TE and those predicted by the RTE are generally too large. Consequently, higher order models such as the P_N or SP_N equations must be used. Regarding the applicability of the DE in the field of biomedical optics, we refer to [20, Chapter 3].

Aim and structure of this thesis

According to the relevant literature, the SP_N equations are widely used in different fields of applied science, but there seem to be relatively few publications on theoretical aspects, especially when it comes to the time-dependent case. This also includes the derivation and investigation of concrete (analytical) solutions. In this thesis, we focus on the SP_N equations in the time domain, where our main goal and contribution is the derivation (and partly justification) of exact solutions to the SP_3 equations. This is also motivated by the fact that this kind of solution (if available) is particularly interesting and useful for several reasons. For example, it allows a fast and accurate evaluation, it often permits an insight into the underlying physics and, this is of particular importance, it is usable for verifying results obtained from numerical approaches such as finite differences and/or finite element methods. Another reason for the mentioned goal is that the results predicted by the SP_3 equations have been shown to be sufficiently accurate for several applications, see for example [9,13,15]. We furthermore point out at this stage that we accept (and adopt) the kind of derivation of the SP_N equations without doing further investigations in this direction (e.g. in form of an error analysis). The structure of this thesis is as follows.
In Chapter 2, we give a brief introduction to the basics of radiative transfer and present some computable solutions to the RTE, which are needed in Section 3.5 for comparison purposes. Most of the content in this chapter is known to scientists in the field of radiative transfer. However, the derived Fourier series solutions (2.21) and (2.22) for the bounded domain could not be found by us in the literature.
In Chapter 3, we begin with the spherical harmonics method (P_N method) and derive, in accordance with the relevant literature, the three-dimensional P_N equations (3.6). We then incorporate the simplifications resulting from the plane symmetry and arrive at the (known) hyperbolic system (3.10). In Example 3.4, we look at the lowest order approximation, the P_1 equations (3.13), and derive the Telegrapher equation (3.14) from them. Due to the relevance of the Telegrapher equation (and the P_1 equations) in applied sciences, we present a proof of a known fundamental solution (Theorem 3.5) that has been developed by ourselves. In this context, we only could find Ganapol's paper [25] on the multiple collision method, which goes very roughly in the direction of our proof. Subsection 3.2.1 deals with the P_N equations in lossless media. One reason for this is that solutions for lossless media are usable to construct solutions for the more general case of lossy media, see e.g. the formulation (3.21). We note that this principle is exactly what we have used in proving Theorem 3.5. Moreover, the determination of the characteristics (to the P_N equations) serves as preparation for the classification of the SP_N equations, see Section 3.3, and the derived solution (3.33) to the P_N equations is needed in Section 3.5 for comparisons purposes. We leave the discussion about the P_N equations with a well-posedness result (Corollary 3.10) and with verifying the energy conservation in lossless media. The introduced energy function (3.35) is also used later (in a slightly modified form) in the context of the SP_3 equations (Lemma 3.18).
In Section 3.3, we perform the necessary simplifications to get the time-dependent SP_N equations in form of the vectorial diffusion equation (3.40). So far, this step (regarding the neglect of the time derivatives) is not new and can be reviewed in the relevant literature

such as [9, 14]. However, our derivation differs in the treatment of the absorption. We separate this quantity (by a product ansatz) at the beginning and verify a positive effect on the long-time behavior, see for example (3.58). Next, we confirm with Proposition 3.11 the parabolic nature of the SP_N equations. This classification has been mentioned in the literature, e.g. in [9, 10], but a concrete verification has not been presented.
Section 3.4 constitutes the main part of this thesis in terms of original contributions. Here, we start with some considerations in the infinite medium (Subsection 3.4.1). Of particular importance (with regard to the next subsections) are the moments (3.50) and the estimates (3.52) and (3.53). As a byproduct, we confirm Einstein's formula for the means-square displacement (Proposition 3.14) and the normalization of the zero order moment (Remark 3.15), both for arbitrary orders $N \geq 1$. In Subsection 3.4.2, we present an exact solution to the SP_3 equations in a bounded domain and proof the well-posedness of the obtained expression by verifying existence and uniqueness (Theorem 3.20) as well as the continuous dependence on the initial data (Corollary 3.21). In Subsection 3.4.3, there is the derivation of alternative representations for solutions to the SP_3 equations in Laplace space. The numerical inversion of the Laplace transform is demonstrated in Subsection 3.5.2 by means of the Post-Widder formula. Due to the relevance of time-harmonic sources in diffuse optical tomography, we additionally consider and solve in Subsection 3.4.4 the time-harmonics SP_3 equations, which consist of two coupled Helmholtz equations. To our knowledge, the results presented in Section 3.4 have not yet been reported in the literature on the SP_N equations. In Section 3.5, various numerical experiments are carried out for both the infinite medium and the bounded domain in order to illustrate and verify the theoretical findings.

2 Fundamentals of Radiative Transfer

In this chapter, we give an overview about the quantities, definitions and mathematical concepts that are often used in the field of radiative transfer. In addition, we present computable solutions to the RTE for the infinite medium and for a bounded domain, which are used in Section 3.5 for comparison purposes.

2.1 The radiative transfer equation

The radiative transfer equation (RTE) is widely used for modelling the propagation of particles like photons, neutrons, electrons or molecules in random scattering media [4, 21]. It is a conservation law that governs the gains and losses of the radiance due to scattering and absorption [26]. We note that a solution to the RTE is called specific intensity or radiance. Throughout this thesis we use the latter designation. The time-dependent RTE formulated as integro-differential equation is given by [5, p. R46]

$$\frac{1}{c}\frac{\partial I}{\partial t} + \hat{\mathbf{s}} \cdot \nabla I + (\mu_a + \mu_s) I = \mu_s \int_{\mathbb{S}^2} f(\hat{\mathbf{s}} \cdot \hat{\mathbf{s}}') I(\mathbf{x}, \hat{\mathbf{s}}', t)\, d\hat{\mathbf{s}}', \tag{2.1}$$

for $(\mathbf{x}, \hat{\mathbf{s}}, t) \in V \times \mathbb{S}^2 \times \mathbb{R}_+$. We assume the domain $V = \{(x, y, z) \in \mathbb{R}^3 : x \in \Omega, y \in \mathbb{R}, z \in \mathbb{R}\}$ with $\Omega \subseteq \mathbb{R}$ denoting an open interval. The quantity $I(\mathbf{x}, \hat{\mathbf{s}}, t)$ is the radiance at the position $\mathbf{x} \in V$ evaluated for the direction $\hat{\mathbf{s}} \in \mathbb{S}^2 := \{\mathbf{x} \in \mathbb{R}^3 : \|\mathbf{x}\|_2 = 1\}$ and the time $t \geq 0$. The constant $c > 0$ denotes the speed of light in the medium and $f : [-1, 1] \to [0, \infty)$ is the scattering phase function that is normalized according to $\int_{\mathbb{S}^2} f(\hat{\mathbf{s}} \cdot \hat{\mathbf{s}}')\, d\hat{\mathbf{s}}' = 1$. It describes the probability that a particle travelling along the direction $\hat{\mathbf{s}}$ is scattered within the unit solid angle around $\hat{\mathbf{s}}'$ [20, Chapter 1]. Moreover, $\mu_a \geq 0$ denotes the absorption and $\mu_s \geq 0$ is the scattering coefficient. Both quantities are assumed to be spatially independent. We also note on the streaming operator $\hat{\mathbf{s}} \cdot \nabla = s_1 \partial_x + s_2 \partial_y + s_3 \partial_z$ and the parametrization of the direction variable

$$\hat{\mathbf{s}}(\theta, \varphi) = \begin{pmatrix} \cos\theta \\ \sin\theta\cos\varphi \\ \sin\theta\sin\varphi \end{pmatrix}, \quad (\theta, \varphi) \in [0, \pi] \times [0, 2\pi). \tag{2.2}$$

This means that the polar angle θ is measured from the positive x-axis of a Cartesian reference system. The isotropic[1] initial condition belonging to equation (2.1) is given by

$$I(\mathbf{x}, \hat{\mathbf{s}}, 0) = c\frac{Q(\mathbf{x})}{4\pi}, \quad \mathbf{x} \in V,\ \hat{\mathbf{s}} \in \mathbb{S}^2, \tag{2.3}$$

where $Q \in C^1(V)$. Under the regularity assumption $I \in C^1(V \times \mathbb{S}^2 \times \mathbb{R}_+)$, the radiance that satisfies (2.1) and the initial condition (2.3) can be seen as a classical solution. As usual for the derivation of the SP_N equations, we consider in accordance with the publications [9, 11] an infinitely extended plane source of the form $Q(\mathbf{x}) = Q(x)$, where $x \in \Omega$. Due to the

[1] This means that the source is independent of $\hat{\mathbf{s}}$ and radiates uniformly in all directions.

infinite extend of this source, solutions to (2.1) will be independent of the variables y and z and hence of the form $I = I(x, \hat{\mathbf{s}}, t)$. In view of the phase function, we take into account the uniform distribution $f(\hat{\mathbf{s}} \cdot \hat{\mathbf{s}}') = 1/(4\pi)$ (isotropic scattering), which is often assumed in atmospheric science [4] or nuclear physics [27]. For convenience and without loss of generality, we set $c = 1$ because the case $c \neq 1$ can be readily determined afterwards via scaling. This means that if $I(x, \hat{\mathbf{s}}, t)$ belongs to $c = 1$, then $cI(x, \hat{\mathbf{s}}, ct)$ holds true for $c \neq 1$. Furthermore, we separate the absorption according to $I(x, \hat{\mathbf{s}}, t) := e^{-\mu_a t}\Psi(x, \mu, \varphi, t)$, where $\mu := \hat{\mathbf{s}} \cdot \hat{\mathbf{x}} = \cos\theta \in [-1, 1]$ denoting the cosine of the angle between $\hat{\mathbf{s}}$ and the positive x-direction $\hat{\mathbf{x}} = (1, 0, 0)^T$. Inserting this ansatz into (2.1) and considering the above mentioned conventions results in the transport model

$$\frac{\partial \Psi}{\partial t} + \mu \frac{\partial \Psi}{\partial x} + \mu_s \Psi = \frac{\mu_s}{4\pi} \int_0^{2\pi} \int_{-1}^{1} \Psi(x, \mu', \varphi', t)\, d\mu' d\varphi', \tag{2.4}$$

for $(x, \mu, \varphi, t) \in \Omega \times [-1, 1] \times [0, 2\pi) \times \mathbb{R}_+$ and $\Psi(x, \mu, \varphi, 0) = Q(x)/(4\pi)$. In accordance with the derivations outlined in [10], we integrate equation (2.4) and the initial condition over $\varphi \in [0, 2\pi)$ and define the azimuthally integrated radiance according to [10]

$$\psi(x, \mu, t) := \int_0^{2\pi} \Psi(x, \mu, \varphi, t)\, d\varphi, \tag{2.5}$$

for $(x, \mu, t) \in \overline{\Omega} \times [-1, 1] \times [0, \infty)$.

Remark 2.1. In the present case of an isotropic initial condition, solutions to (2.4) reduce to $\Psi = \Psi(x, \mu, t)$. Concerning (2.5), this means $\psi(x, \mu, t) = 2\pi\Psi(x, \mu, t)$.

As a consequence, we arrive at the following simplified transport equation

$$\frac{\partial \psi}{\partial t} + \mu \frac{\partial \psi}{\partial x} + \mu_s \psi = \frac{\mu_s}{2} \int_{-1}^{1} \psi(x, \mu', t)\, d\mu', \tag{2.6}$$

for $(x, \mu, t) \in \Omega \times [-1, 1] \times \mathbb{R}_+$ and $\psi(x, \mu, 0) = Q(x)/2$. In view of concrete applications, e.g. in medical physics, the fluence that corresponds with the integrated radiance is a quantity of particular importance [12].

Definition 2.2. The fluence is defined as the integral of the radiance over the angular domain, which means

$$\Phi(x, t) := \int_{-1}^{1} \psi(x, \mu, t)\, d\mu, \quad x \in \Omega,\ t \geq 0. \tag{2.7}$$

Remark 2.3. The fluence is currently defined in a non-absorbing medium with $c = 1$. In the more general case of $\mu_a \geq 0$ and $c > 0$, we again find via scaling $ce^{-\mu_a ct}\Phi(x, ct)$.

Within radiative transfer (theory and applications), point sources are of particular importance e.g. when modelling a point light source that radiates uniformly in all directions, which we abbreviate as δ-source, or when thinking about a narrow light beam that penetrates biological tissue. These source types as well as the description of ballistic (uncollided) intensities can be conveniently handled by the Dirac delta distribution $\delta(x) := \frac{d}{dx}\Theta(x)$, with Θ being the unit step function [28, Chapter 1]. It also appears in the context of integral transforms such as Fourier, Laplace or Mellin transform, especially when discontinuous functions and their (generalized) derivatives are taken into account.

Remark 2.4. For illustration as well as for numerical considerations, the Dirac delta distribution can be approximated by several elementary functions. Two examples are

(1) $\delta(x) = \lim_{\varepsilon \to 0} \frac{e^{-x^2/(2\varepsilon)}}{\sqrt{2\pi\varepsilon}}, \quad x \in \mathbb{R},$

(2) $\delta(\phi) = \lim_{g \to 1} \frac{1}{2\pi} \frac{1 - g^2}{1 + g^2 - 2g\cos\phi}, \quad \phi \in (-\pi, \pi],$

where (2) represents a 2π-periodic Dirac delta distribution.

In this thesis, we also make use of this helpful concept without going into the theory of distributions. Instead, we refer to the textbooks [28, Chapter 1] and [29, Chapter 2], from which we adopt the following results.

Proposition 2.5. *The Dirac delta distribution considered on the entire x-axis satisfies*

(1) $f(x)\delta(x - x_0) = f(x_0)\delta(x - x_0), \quad x_0 \in \mathbb{R},$

(2) $\delta(ax) = \frac{\delta(x)}{|a|}, \quad a \in \mathbb{R},\ a \neq 0,$

(3) $\delta(g(x)) = \sum_j \frac{\delta(x - x_j)}{|g'(x_j)|}, \quad \text{where} \quad g(x_j) = 0,\ g'(x_j) \neq 0,$

(4) $\mathcal{F}(\delta)(k) = 1 \quad \forall k \in \mathbb{R},$

with $\mathcal{F}$ denoting the Fourier transform, cf. Definition 2.7.

The lowest order approximation to the RTE (in view of the angular dependence) is the classical heat or diffusion equation [5, 20]. In that case, the exact transport theory fluence (2.15) associated with the RTE (2.6) for the infinite medium caused by a δ-source reduces to the well-known heat kernel [2, p. 463]

$$\Phi(x,t) = \frac{e^{-\frac{x^2}{4\kappa t}}}{\sqrt{4\pi\kappa t}}, \quad x \in \mathbb{R},\ t > 0, \tag{2.8}$$

where $\Phi(x,0) = \delta(x)$ and $\kappa := 1/(3\mu_s)$ is the diffusion constant (or thermal conductivity). In Section 3.3, we will see that the SP_1 equation coincides with the heat equation $u_t = \kappa u_{xx}$. At this stage, it should be noted that the plane source problem treated in this thesis differs from the two-stream methodology [30]. The latter configuration, in which particles can only travel along two specific directions (e.g. particle transport in a very thin fiber), is a real one-dimensional problem that is significantly easier to solve. The idea of restricting the RTE (in view of the angular space) to a finite number of directions leads to an approximation technique known as the discrete ordinate method [23,30]. We furthermore have to address the issue of boundary conditions (BCs) that must be taken into account for modelling transport processes in finite domains. In this thesis, we take into account reflective BCs[2] according to the following definition [27].

Definition 2.6 (Reflective BC)**.** Let $\Omega \subset \mathbb{R}$ be an open domain with a reflecting boundary $\partial\Omega$, which means that a particle coming from direction $\hat{\mathbf{s}}(\theta, \varphi)$ and reaching $\partial\Omega$ will be reflected back into the medium along $\hat{\mathbf{s}}(\pi - \theta, \varphi)$. Then, the azimuthally independent radiance ψ associated with the RTE (2.6) must satisfy

$$\psi(x, \mu, t) = \psi(x, -\mu, t) \quad \forall x \in \partial\Omega,$$

and $(\mu, t) \in [-1, 1] \times [0, \infty)$.

[2] In this context, one could think of a ball before and after reaching a wall.

In the sections below, we make use of two integral transforms. One of that is the Fourier transform according to the following definition [31, p. 213].

Definition 2.7. The Fourier transform $\mathcal{F} : f \mapsto \mathcal{F}(f) = \hat{f}$ of an absolutely integrable function $f \in L_1(\mathbb{R})$ is defined as

$$\hat{f}(k) := \int_{-\infty}^{\infty} f(x)e^{-ikx}\,dx, \quad k \in \mathbb{R}.$$

Remark 2.8. For $f \in L_1(\mathbb{R})$ the Fourier transform is bounded for all $k \in \mathbb{R}$ due to

$$|\hat{f}(k)| \leq \int_{-\infty}^{\infty} |f(x)e^{-ikx}|\,dx = \int_{-\infty}^{\infty} |f(x)|\,dx < \infty. \tag{2.9}$$

Moreover, in [31, Chapter 7] it is shown by the Riemann-Lebesgue Lemma that $f \in L_1(\mathbb{R})$ implies $\hat{f} \in C_0(\mathbb{R})$ with

$$C_0(\mathbb{R}) := \{\varphi \in C(\mathbb{R}) : \lim_{|x|\to\infty} \varphi(x) = 0\}. \tag{2.10}$$

The Fourier transform has many useful properties of which we only need a few for the purposes of this work. A proof or derivation of the following results can be found, for example, in [29, Chapter 2] and [31, Chapter 7].

Proposition 2.9. *For $f \in L_1(\mathbb{R})$ with Fourier transform $\mathcal{F}(f) = \hat{f}$ we have*

(1) $f(x) = \mathcal{F}^{-1}(\hat{f})(x) = \dfrac{1}{2\pi}\displaystyle\int_{-\infty}^{\infty} \hat{f}(k)e^{ikx}\,dk, \quad x \in \mathbb{R},\ \hat{f} \in L_1(\mathbb{R}),$

(2) $\mathcal{F}(f^{(n)})(k) = (ik)^n \hat{f}(k), \ \text{if}\ f^{(0)}(x), \ldots, f^{(n-1)}(x) \to 0\ \text{as}\ |x| \to \infty,\ n \in \mathbb{N}_0,$

(3) $\mathcal{F}(f(\cdot)e^{ik_0\cdot})(k) = \hat{f}(k - k_0), \quad k_0 \in \mathbb{R},$

(4) $\displaystyle\sum_{n\in\mathbb{Z}} f(x - nT) = \frac{1}{T}\sum_{n\in\mathbb{Z}} \hat{f}(2\pi n/T)e^{2\pi inx/T}, \quad x \in \mathbb{R},\ T > 0,$

where (4) is known as the Poisson summation formula.

Besides the Fourier transform, we will also use the one-sided Laplace transform, see e.g. [28, Chapter 5] for more details on this subject.

Definition 2.10. Let $f : [0, \infty) \to \mathbb{R}$ be a continuous function with $f(t) = \mathcal{O}(e^{\sigma_0 t})$[3] as $t \to \infty$ and $\sigma_0 \in \mathbb{R}$ denoting the exponential order. Then, the one-sided Laplace transform $\mathcal{L} : f \mapsto \mathcal{L}(f) = \hat{f}$ defined by

$$\hat{f}(s) = \int_0^{\infty} f(t)e^{-st}\,dt, \quad s = \sigma + i\omega \in \mathbb{C},$$

exists in the half-plane $\{s \in \mathbb{C} : \sigma > \sigma_0\}$ with $\sigma_0 \in \mathbb{R}$ being the abscissa of convergence. The corresponding inverse relation, also known as Bromwich integral, is given by

$$f(t) = \frac{e^{\sigma t}}{2\pi}\int_{-\infty}^{\infty} \hat{f}(\sigma + i\omega)e^{i\omega t}\,d\omega \quad \forall \sigma > \sigma_0,$$

where the integration takes place along a straight line (within the region of convergence) that is parallel to the imaginary axis.

[3] Here, we use the big-$\mathcal{O}$ notation. That is, $f(t) = \mathcal{O}(g(t))$ as $t \to \infty$ means that there are constants $M > 0$ and t_0 such that $|f(t)| \leq M|g(t)|$ for all $t \geq t_0$.

Remark 2.11. If the region of convergence contains the imaginary axis, then the Bromwich integral can be evaluated for $\sigma = 0$ leading to the inverse Fourier transform, cf. Proposition 2.9. In the context of partial differential equations, the inverse Laplace transform must be in general carried out numerically. Depending on the properties of the image function $\hat{f}$, there are different approaches for reconstruction of f such as Talbot's (contour deformation) method [32, Chapter 6] or the Post-Widder inversion formula, see e.g. [32, Theorem 2.4] or Proposition 3.25.

For our purposes, we need an operational property regarding the first time derivative.

Proposition 2.12. *Let $f : [0, \infty) \to \mathbb{R}$ be a continuous function with $f(t) = \mathcal{O}(e^{\sigma_0 t})$ as $t \to \infty$. Then, the Laplace transform of f' exists for $\sigma > \sigma_0$ with*

$$\mathcal{L}(f')(s) = s\hat{f}(s) - f(0).$$

Proof. A proof of this differentiation property can be found in [28, Theorem 5.2]. □

2.2 Analytical solutions to the RTE

In general, closed-form solutions to the RTE (2.6) are very rare. Even in the simplest cases such as the infinite medium, the corresponding solution is only available in form of a quadrature that must be evaluated numerically. Nevertheless, this type of solution is also useful e.g. for verification of Monte Carlo codes and/or P_N-based methods. The purpose of this section is to provide some computable solutions to the RTE (2.6), which are needed in Section 3.5 for checking the accuracy of the derived SP_3 solutions.

2.2.1 Solution for the fluence in the infinite medium

Let us start with the derivation of an expression for the infinite-space fluence caused by an instantaneous δ-source. To this end, we consider equation (2.6) on $\Omega = \mathbb{R}$ subject to $\psi(x, \mu, 0) = \delta(x)/2$ for $(x, \mu) \in \mathbb{R} \times [-1, 1]$. The application of the Fourier transform with respect to the space and the Laplace transform in view of the time converts the RTE (2.6) into the following equation

$$(s + \mu_s + ik\mu)\hat{\psi}(k, \mu, s) = \frac{\mu_s}{2}\hat{\Phi}(k, s) + \frac{1}{2}, \tag{2.11}$$

for $k \in \mathbb{R}$, $\mu \in [-1, 1]$ and $\operatorname{Re} s = \sigma > 0$, where we have considered Proposition 2.9 and Proposition 2.12 with $\hat{\psi}(k, \mu, 0) = 1/2$ for $(k, \mu) \in \mathbb{R} \times [-1, 1]$. We note that the assumption $\sigma > 0$ is in accordance with the considerations in the work [33].

Lemma 2.13. *The fluence in Fourier-Laplace space due to an instantaneous δ-source is uniquely determined by*

$$\hat{G}(k, s) = \frac{\hat{\Phi}_0(k, s)}{1 - \mu_s \Phi_0(k, s)} \quad \text{with} \quad \hat{\Phi}_0(k, s) = \frac{1}{k} \arctan\left(\frac{k}{s + \mu_s}\right),$$

where $k \in \mathbb{R}$ and $\sigma > 0$.

Proof. By solving (2.11) for the radiance gives

$$\hat{\psi}(k,\mu,s) = \frac{1}{2}\frac{1+\mu_s\hat{\Phi}(k,s)}{s+\mu_s+ik\mu}. \tag{2.12}$$

Next, we integrate this expression over $\mu \in [-1,1]$ to obtain

$$\hat{\Phi}(k,s) = \hat{\Phi}_0(k,s)[1+\mu_s\hat{\Phi}(k,s)],$$

where we have used $\hat{\Phi}(k,s) = \int_{-1}^{1}\hat{\psi}(k,\mu,s)\,d\mu$ and $\hat{\Phi}_0$ is the uncollided fluence in the transformed space that is given by

$$\hat{\Phi}_0(k,s) := \frac{1}{2}\int_{-1}^{1}\frac{d\mu}{s+\mu_s+ik\mu} = \frac{1}{k}\arctan\left(\frac{k}{s+\mu_s}\right).$$

Therefore, the transport theory fluence in Fourier-Laplace space turns out to be

$$\hat{\Phi}(k,s) = \frac{\hat{\Phi}_0(k,s)}{1-\mu_s\hat{\Phi}_0(k,s)} =: \hat{G}(k,s). \tag{2.13}$$

□

In the next subsection, we also need the radiance in the transformed space. By inserting the expression (2.13) into (2.12) gives

$$\hat{\psi}(k,\mu,s) = \frac{1}{2}\frac{1}{s+\mu_s+ik\mu}\frac{1}{1-\mu_s\Phi_0(k,s)} =: \hat{\mathcal{G}}(k,\mu,s). \tag{2.14}$$

Theorem 2.14. *The spatially resolved fluence in time domain due to an instantaneous δ-source exhibits for $x \in \mathbb{R}$ and $t > |x|$ the following representation*

$$\begin{aligned} G(x,t) =& \frac{e^{-\mu_s t}}{2t} + \frac{1}{\pi}\int_0^{\pi\mu_s/2}\frac{e^{(k\cot(k/\mu_s)-\mu_s)t}}{\operatorname{sinc}^2(k/\mu_s)}\cos(kx)\,dk \\ &- \frac{\mu_s e^{-\mu_s t}}{4\pi t}\int_0^{|x|}\left(\frac{t-\eta}{t+\eta}\right)^{\mu_s(|x|-\eta)/2}\left[2\pi\ln\frac{t+\eta}{t-\eta}\cos\left(\mu_s\pi\frac{|x|-\eta}{2}\right)\right. \\ &\left.+\left(\pi^2-\ln^2\frac{t+\eta}{t-\eta}\right)\sin\left(\mu_s\pi\frac{|x|-\eta}{2}\right)\right]d\eta, \end{aligned} \tag{2.15}$$

where $\operatorname{sinc} x := \sin x/x$ *and* $G(x,t) = 0$ *for* $0 \le t < |x|$*, due to the finite speed of propagation.*

Proof. We have to perform $\mathcal{F}^{-1}\mathcal{L}^{-1}\hat{G} = \mathcal{L}^{-1}\mathcal{F}^{-1}\hat{G} = G$ under the use of the transformed fluence $\hat{G}$ from Lemma 2.13. This task is not easy and requires some knowledge in complex analysis. We refer at this stage to the article [33], in which the authors have proposed an appropriate contour in the complex plane in combination with the residue theorem. □

The integral representation (2.15) enables the determination of the fluence in the long-time limit. To this end, let us first investigate the contribution of

$$I(t) := \frac{1}{\pi}\int_0^{\pi\mu_s/2}\frac{e^{(k\cot(k/\mu_s)-\mu_s)t}}{\operatorname{sinc}^2(k/\mu_s)}\cos(kx)\,dk, \tag{2.16}$$

for $t \to \infty$. The particular form of this integral gives rise to the application of the Laplace formula [34, Chapter 5]

$$\int_0^b e^{-t\vartheta(k)} g(k)\, dk \approx \frac{1}{2}\sqrt{\frac{2\pi}{t\vartheta''(0)}}\, g(0) e^{-t\vartheta(0)} \quad \text{as} \quad t \to \infty. \tag{2.17}$$

This asymptotic expansion requires that $g(0) \neq 0$ and ϑ must be a monotonically increasing function on $(0, b]$ with $\vartheta'(0) = 0$ and $\vartheta''(0) > 0$. In the present case, we have $b = \pi\mu_s/2$ and $\vartheta(k) := \mu_s - k\cot(k/\mu_s)$ with $\vartheta'(0) = 0$ and $\vartheta''(0) = 2/(3\mu_s) > 0$. Moreover, the associated function g satisfies $g(0) = 1 \neq 0$ and the first derivative of ϑ is given by

$$\vartheta'(k) = \frac{k/\mu_s - \sin(2k/\mu_s)/2}{\sin^2(k/\mu_s)}, \quad 0 \leq k \leq \frac{\pi\mu_s}{2}.$$

On its domain of definition it is positive due to $\sin\xi \leq \xi$ for all $\xi \geq 0$. Hence, all requirements are fulfilled and the application of Laplace's formula (2.17) to (2.16) shows that

$$I(t) \sim \frac{1}{\sqrt{4\pi\kappa t}} =: H(t) \quad \text{as} \quad t \to \infty, \tag{2.18}$$

which coincides with the classical heat kernel (2.8) in the long-time limit. We note that the remaining terms in (2.15) decay exponentially as $t \to \infty$. Thus, expression (2.18) is the leading term of the transport theory fluence at late times. In Subsection 3.4.1, we verify the convergence of the SP_3 fluence against (2.18) when $t \to \infty$.

2.2.2 Solution of the RTE in a bounded domain

In addition to the infinite medium, it would be important to have also an exact reference solution for the bounded domain. In the case of $\Omega = (0, L)$ subject to the reflective BCs from Definition 2.6, there is the possibility to derive an expression in form of a Fourier series. Moreover, we will see that the δ-source problem can be alternatively solved by the method of images, see e.g. [35] for more details on this solution approach. Again, the starting point is the transport equation (2.6) on the whole space $\mathbb{R}$, but under consideration of the following even and $2L$-periodic source distribution

$$Q(x) = \sum_{n=0}^{\infty} \frac{2 - \delta_{n0}}{L} q_n \cos(\omega_n x), \quad q_n := \int_0^L Q(x)\cos(\omega_n x)\, dx, \tag{2.19}$$

where $\omega_n := n\pi/L$ and δ_{ij} denotes the Kronecker delta. We furthermore assume uniform convergence with $(q_n)_{n\in\mathbb{N}_0} \in \ell^1(\mathbb{N}_0)$ such that $\sum_{n=0}^{\infty} |q_n| < \infty$. As shown below, the obtained solution on $\mathbb{R}$ satisfies the intended reflective BCs according to Definition 2.6. To proceed further, we need the Fourier transform of the periodic source (2.19). It has a discrete spectrum consisting of weighted Dirac pulses, see e.g. [28, Chapter 2]. This leads to

$$\hat{Q}(k) = \frac{2\pi}{L} \sum_{n\in\mathbb{Z}} q_{|n|} \delta(k - \omega_n), \quad k \in \mathbb{R}. \tag{2.20}$$

We now can proceed in the same manner as in the previous subsection. The resulting radiance in Fourier-Laplace space is nearly the same as before and given by the product

$$\hat{\psi}(k, \mu, s) = \hat{Q}(k)\hat{\mathcal{G}}(k, \mu, s), \quad (k, \mu) \in \mathbb{R} \times [-1, 1],\ \sigma > 0.$$

Considering (2.20) and making use of the property (1) from Proposition 2.5 gives

$$\hat{\psi}(k,\mu,s) = \frac{2\pi}{L}\sum_{n\in\mathbb{Z}} \hat{\mathcal{G}}(\omega_n,\mu,s) q_{|n|}\delta(k-\omega_n), \quad (k,\mu)\in\mathbb{R}\times[-1,1],\, \sigma>0.$$

The Fourier transform can be inverted under the use of $\mathcal{F}(e^{i\omega_n \cdot})(k) = 2\pi\delta(k-\omega_n)$, yielding

$$\hat{\psi}(x,\mu,s) = \frac{1}{L}\sum_{n\in\mathbb{Z}} \hat{\mathcal{G}}(\omega_n,\mu,s) q_{|n|} e^{i\omega_n x}, \quad (x,\mu)\in\mathbb{R}\times[-1,1],\, \sigma>0. \tag{2.21}$$

At this stage, when using the symmetry property $\hat{\mathcal{G}}(k,\mu,s) = \hat{\mathcal{G}}(-k,-\mu,s)$, one can confirm the reflective BC

$$\hat{\psi}(x,\mu,s) = \hat{\psi}(x,-\mu,s) \quad \forall (x,\mu)\in\partial\Omega\times[-1,1],\, \sigma>0.$$

Thus, the radiance obtained on $\mathbb{R}$ is simultaneously a solution for the bounded domain. The fluence is found via integration under the use of $\int_{-1}^{1}\hat{\mathcal{G}}(\omega_n,\mu,s)\,d\mu = \hat{G}(\omega_n,s)$, yielding

$$\hat{\Phi}(x,s) = \frac{1}{L}\sum_{n\in\mathbb{Z}} \hat{G}(\omega_n,s) q_{|n|} e^{i\omega_n x} = \sum_{n=0}^{\infty} \frac{2-\delta_{n0}}{L}\hat{G}(\omega_n,s) q_n \cos(\omega_n x), \tag{2.22}$$

for $x\in\mathbb{R}$, $\sigma>0$ and $\hat{G}$ with property $\hat{G}(k,s) = \hat{G}(-k,s)$ is adopted from Lemma 2.13. We also see that the fluence (2.22) satisfies homogeneous Neumann BCs. Let us briefly discuss the special case $q_n = \cos(\omega_n x_0)$ with $x_0\in\Omega$. In contrast to the considerations above, the coefficients q_n do not decay towards zero and lead to the periodic δ-source distribution

$$Q(x) = \sum_{n=0}^{\infty}\frac{2-\delta_{n0}}{L}\cos(\omega_n x_0)\cos(\omega_n x) = \sum_{n\in\mathbb{Z}}[\delta(x-x_0-2nL)+\delta(x+x_0-2nL)].$$

We note that this (symbolic) relation, which represents an infinite number of δ-sources, is still consistent with the Poisson summation formula from Proposition 2.9. Regarding the fluence (2.22), a symbolic manipulation by means of the Poisson summation gives

$$\begin{aligned}\hat{\Phi}(x,s) =& \frac{1}{L}\sum_{n\in\mathbb{Z}}\hat{G}(\omega_n,s)\cos(\omega_n x_0)e^{i\omega_n x} = \frac{1}{2L}\sum_{n\in\mathbb{Z}}\hat{G}(\omega_n,s)e^{i\omega_n(x+x_0)}\\ &+\frac{1}{2L}\sum_{n\in\mathbb{Z}}\hat{G}(\omega_n,s)e^{i\omega_n(x-x_0)} = \sum_{n\in\mathbb{Z}}\hat{G}(x-x_0-2nL,s)\\ &+\sum_{n\in\mathbb{Z}}\hat{G}(x+x_0-2nL,s), \quad x\in\overline{\Omega}\setminus\{x_0\},\, \sigma>0.\end{aligned} \tag{2.23}$$

This expression represents the fluence caused by a δ-source located at $x_0\in(0,L)$. Hence, this transport theory problem (under reflective BCs) can be successfully solved by the method of images. Let us go back to the Fourier series (2.21) and (2.22) with $(q_n)_{n\in\mathbb{N}_0}\in\ell^1(\mathbb{N}_0)$. Here, the remaining inverse Laplace transform must be in general carried out numerically. An exception is the lossless medium with $\mu_s = 0$. In that case, we obtain with (2.14)

$$\hat{\mathcal{G}}(\omega_n,\mu,s) = \frac{1}{2}\frac{1}{s+i\mu\omega_n} \quad \underset{\mathcal{L}^{-1}}{\Longrightarrow} \quad \hat{\mathcal{G}}(\omega_n,\mu,t) = \frac{e^{-i\mu\omega_n t}}{2}, \quad n\in\mathbb{Z},$$

and $(\mu,t)\in[-1,1]\times[0,\infty)$. Inserting this result into (2.21) leads to the radiance

$$\psi(x,\mu,t) = \sum_{n=0}^{\infty}\frac{2-\delta_{n0}}{2L}q_n\cos\omega_n(x-\mu t),$$

for $(x,\mu,t) \in \overline{\Omega} \times [-1,1] \times [0,\infty)$. Due to $|q_n \cos\omega_n(x-\mu t)| \leq |q_n|$ and $\sum_{n=0}^{\infty} |q_n| < \infty$, this series converges according to the Weierstrass majorant criterion [2, p. 87] absolutely and uniformly to a continuous function. In view of the fluence, we note on

$$\hat{G}(\omega_n,t) = \int_{-1}^{1} \hat{\mathcal{G}}(\omega_n,\mu,t)\,d\mu = \int_{-1}^{1} \frac{e^{-i\mu\omega_n t}}{2}\,d\mu = \operatorname{sinc}(\omega_n t), \quad n \in \mathbb{Z},\ t \geq 0.$$

Inserting this into (2.22) leads to the uniformly convergent series

$$\Phi(x,t) = \sum_{n=0}^{\infty} \frac{2-\delta_{n0}}{L} q_n \operatorname{sinc}(\omega_n t)\cos(\omega_n x), \quad (x,t) \in \overline{\Omega} \times [0,\infty). \tag{2.24}$$

For the classical wave equation $u_{tt} = c^2 u_{xx}$ on $\Omega = (0,L)$ under homogeneous Dirichlet or Neumann conditions, it has been shown in the literature that the total energy according to $E(t) = \frac{1}{2}\int_\Omega (u_t^2 + c^2 u_x^2)\,dx$ (assuming sufficient regularity) is constant over time, see for example [36, Section 3.3]. Due to the hyperbolic nature of the RTE, one may expect a similar result for the radiance in a lossless medium. Let us investigate the following energy function

$$E(t) := \|\psi(\cdot,t)\|^2_{L_2(\Omega\times[-1,1])} = \int_{-1}^{1}\int_{0}^{L} \psi^2(x,\mu,t)\,dx d\mu, \quad t \geq 0. \tag{2.25}$$

The RTE (2.6) in lossless media reduces to $\psi_t + \mu\psi_x = 0$ with $\psi(x,\mu,0) = Q(x)/2$. This simple transport equation is solved by $\psi(x,\mu,t) = Q(x-\mu t)/2$. Due to the fact that Q is even and $2L$-periodic, we have $\psi(x,\mu,t) = \psi(x,-\mu,t)$ for $(x,\mu,t) \in \partial\Omega \times [-1,1] \times [0,\infty)$. In view of the energy integral (2.25), we get

$$\begin{aligned} E(t) &= \frac{1}{4}\int_{-1}^{1}\int_{0}^{L} Q^2(x-\mu t)\,dx d\mu = \frac{1}{8}\int_{-1}^{1}\int_{0}^{2L} Q^2(x-\mu t)\,dx d\mu \\ &= \frac{1}{4}\int_{-1}^{1}\int_{0}^{L} Q^2(\xi)\,d\xi d\mu = \frac{1}{2}\int_{0}^{L} Q^2(x)\,dx = E(0), \end{aligned} \tag{2.26}$$

where we again have used the symmetry and periodicity of Q. This shows that the introduced energy function (2.25) is a conserved quantity. Below, we will see that the P_N method represents in lossless media a conservative scheme. For illustration purposes, we will consider the derived Fourier series solution (2.22) within the last numerical experiment from Section 3.5. In view of the SP_3 equations discussed in Section 3.4, we will apply the Poisson's summation formula in exactly the same way as we did to obtain the fluence expression (2.23).

3 On the SP_N Equations in Time Domain

The simplified P_N equations (SP_N equations) can be derived from the P_N equations belonging to the azimuthally independent RTE (2.6). Thus, we first have to derive these equations before we can apply the remaining simplifications with respect to the time derivatives. There are different ways to proceed further. One possibility would be to start the analysis directly from the transport equation (2.6). On the other hand, to get a deeper insight into the P_N methodology and its applicability to more complicated (higher dimensional) problems, it is also possible to start from the original equation (2.1) and carry out the simplifications afterwards. Although being more extensive, we prefer to show the second option. Let us start with a short overview about the spherical harmonics and some of its basic properties.

3.1 The spherical harmonics method

Within the spherical harmonics method, in radiative transfer abbreviated as P_N method, all angle-dependent quantities such as the (unknown) radiance, the source term as well as the scattering phase function are represented in terms of spherical harmonics [4, 5]. They form an orthonormal basis of the Hilbert space of square-integrable functions. A spherical harmonic function $Y_\ell^m : \mathbb{S}^2 \to \mathbb{C}$ of degree $\ell \in \mathbb{N}_0$ and order m ($|m| \leq \ell$) can be defined as [2, p. 282]

$$Y_\ell^m(\hat{\mathbf{s}}) := \sqrt{\frac{2\ell+1}{4\pi}\frac{(\ell-m)!}{(\ell+m)!}} P_\ell^m(\cos\theta) e^{im\varphi},$$

for $\hat{\mathbf{s}} = \hat{\mathbf{s}}(\theta,\varphi) \in \mathbb{S}^2$ and P_ℓ^m are the associated Legendre functions according to [2, p. 319]

$$P_\ell^m(x) := (-1)^m (1-x^2)^{\frac{m}{2}} \frac{d^m P_\ell(x)}{dx^m}, \quad |x| \leq 1,\ 0 \leq m \leq \ell.$$

For negative values $-\ell \leq m \leq -1$, we note on the useful relation [2, p. 319]

$$P_\ell^m(x) = (-1)^m \frac{(l+m)!}{(l-m)!} P_\ell^{-m}(x), \quad |x| \leq 1,$$

yielding $Y_\ell^m = (-1)^m \overline{Y_\ell^{-m}}$.[1] The first few spherical harmonics are given

$$Y_0^0(\hat{\mathbf{s}}) = \frac{1}{\sqrt{4\pi}}, \quad Y_1^0(\hat{\mathbf{s}}) = \sqrt{\frac{3}{4\pi}}\cos\theta \quad \text{and} \quad Y_1^1(\hat{\mathbf{s}}) = -\frac{1}{2}\sqrt{\frac{3}{2\pi}}\sin\theta e^{i\varphi}.$$

With the above normalization these functions are orthonormal in the sense [2, p. 283]

$$\langle Y_\ell^m, Y_{\ell'}^{m'} \rangle_{L_2(\mathbb{S}^2)} := \int_{\mathbb{S}^2} Y_\ell^m(\hat{\mathbf{s}}) \overline{Y_{\ell'}^{m'}}(\hat{\mathbf{s}})\, d\hat{\mathbf{s}} = \delta_{\ell\ell'}\delta_{mm'}. \tag{3.1}$$

Concerning the expansion of a function $f \in L_2(\mathbb{S}^2)$ in terms of spherical harmonics, we adopt from [1] the following important result.

[1] In general, we denote by $\overline{f}$ the complex conjugate of f.

Proposition 3.1. *Every function $f \in L_2(\mathbb{S}^2)$ can be represented in terms of the spherical harmonics according to*

$$f(\hat{\mathbf{s}}) = \sum_{\ell=0}^{\infty} \sum_{m=-\ell}^{\ell} f_\ell^m Y_\ell^m(\hat{\mathbf{s}}), \quad \text{where} \quad f_\ell^m = \langle f, Y_\ell^m \rangle_{L_2(\mathbb{S}^2)}.$$

The convergence with respect to the L_2-norm $\|f\|_{L_2(\mathbb{S}^2)}^2 := \int_{\mathbb{S}^2} |f(\hat{\mathbf{s}})|^2 \, d\hat{\mathbf{s}}$ is

$$\lim_{N\to\infty} \|f - f_N\|_{L_2(\mathbb{S}^2)} = \lim_{N\to\infty} \left\| \sum_{\ell=N+1}^{\infty} \sum_{m=-\ell}^{\ell} f_\ell^m Y_\ell^m \right\|_{L_2(\mathbb{S}^2)} = 0,$$

where $f_N := \sum_{\ell=0}^{N} \sum_{m=-\ell}^{\ell} f_\ell^m Y_\ell^m$ denotes the Nth partial sum.

Remark 3.2. The Nth partial sum $f_N \in \mathcal{S}_N := \operatorname{span}\{Y_\ell^m : |m| \le \ell, 0 \le \ell \le N\}$ is the best approximation of f within the subspace $\mathcal{S}_N$ of dimension $(N+1)^2$ with respect to the L_2-norm. This means

$$\|f - f_N\|_{L_2(\mathbb{S}^2)} \le \|f - q\|_{L_2(\mathbb{S}^2)} \quad \forall q \in \mathcal{S}_N.$$

Proof. Due to the orthogonality $\langle f - f_N, p \rangle_{L_2(\mathbb{S}^2)} = 0$ for all $p \in \mathcal{S}_N$ we find for an arbitrary $q \in \mathcal{S}_N$ (Pythagorean identity)

$$\|f - q\|_{L_2(\mathbb{S}^2)}^2 = \|f - f_N + f_N - q\|_{L_2(\mathbb{S}^2)}^2 = \|f - f_N\|_{L_2(\mathbb{S}^2)}^2 + \|f_N - q\|_{L_2(\mathbb{S}^2)}^2,$$

where we have considered $f_N - q \in \mathcal{S}_N$. This is just the best approximation property. □

The scattering phase function occurring in equation (2.1) has a particular form, namely

$$f(\hat{\mathbf{s}} \cdot \hat{\mathbf{s}}') = f(\cos\theta \cos\theta' + \sin\theta \sin\theta' \cos(\varphi - \varphi')).$$

For this kind of rotationally invariant function, which means that there is no dependence on a laboratory coordinate system, the corresponding expansion coefficients can be computed more conveniently by means of the Funk-Hecke formula [3, Theorem 2.16]

$$\int_{\mathbb{S}^2} f(\hat{\mathbf{s}} \cdot \hat{\mathbf{s}}') \overline{Y_\ell^m}(\hat{\mathbf{s}}) \, d\hat{\mathbf{s}} = 2\pi \overline{Y_\ell^m}(\hat{\mathbf{s}}') \int_{-1}^{1} f(\mu) P_\ell(\mu) \, d\mu. \tag{3.2}$$

In addition, if we set $2\pi \int_{-1}^{1} f(\mu) P_\ell(\mu) \, d\mu =: f_\ell$ and making use of the addition theorem for spherical harmonics [5, p. R89]

$$P_\ell(\hat{\mathbf{s}} \cdot \hat{\mathbf{s}}') = \frac{4\pi}{2\ell + 1} \sum_{m=-\ell}^{\ell} \overline{Y_\ell^m}(\hat{\mathbf{s}}') Y_\ell^m(\hat{\mathbf{s}}),$$

we can identify with $f_\ell^m = f_\ell \overline{Y_\ell^m}(\hat{\mathbf{s}}')$ the simple Legendre series

$$f(\hat{\mathbf{s}} \cdot \hat{\mathbf{s}}') = \sum_{\ell=0}^{\infty} \sum_{m=-\ell}^{\ell} f_\ell \overline{Y_\ell^m}(\hat{\mathbf{s}}') Y_\ell^m(\hat{\mathbf{s}}) = \sum_{\ell=0}^{\infty} \frac{2\ell + 1}{4\pi} f_\ell P_\ell(\hat{\mathbf{s}} \cdot \hat{\mathbf{s}}').$$

As an example, the Henyey-Greenstein phase function is an often considered model within biomedical optics applications [20]. It has the following explicit representation [26, p. 148]

$$f_{\mathrm{HG}}(\hat{\mathbf{s}}\cdot\hat{\mathbf{s}}') = \frac{1}{4\pi}\frac{1-g^2}{(1+g^2-2g\,\hat{\mathbf{s}}\cdot\hat{\mathbf{s}}')^{3/2}} = \sum_{\ell=0}^{\infty}\frac{2\ell+1}{4\pi}g^{\ell}P_{\ell}(\hat{\mathbf{s}}\cdot\hat{\mathbf{s}}'),$$

with $g\in(-1,1)$ being the so-called anisotropy factor. This function provides also an approximation of the Dirac delta distribution on the unit sphere such as [26, p. 148]

$$\lim_{g\to 1} f_{\mathrm{HG}}(\hat{\mathbf{s}}\cdot\hat{\mathbf{s}}') = \frac{\delta(1-\hat{\mathbf{s}}\cdot\hat{\mathbf{s}}')}{2\pi} = \delta(\hat{\mathbf{s}}-\hat{\mathbf{s}}') = \delta(\cos\theta-\cos\theta')\delta(\varphi-\varphi').$$

Within the P_N method, the radiance I from (2.1) is (in view of the angular space) projected onto the finite-dimensional space $\mathcal{S}_N$ with $N\geq 1$ being the truncation parameter that is necessary for realization of the P_N method on a computer. Consequently, we have the representation [5, p. R47]

$$I(\mathbf{x},\hat{\mathbf{s}},t)\approx I_N(\mathbf{x},\hat{\mathbf{s}},t) = \sum_{\ell=0}^{N}\sum_{m=-\ell}^{\ell}\sqrt{\frac{2\ell+1}{4\pi}}\phi_{\ell}^{m}(\mathbf{x},t)Y_{\ell}^{m}(\hat{\mathbf{s}}), \tag{3.3}$$

for $(\mathbf{x},\hat{\mathbf{s}},t)\in\overline{V}\times\mathbb{S}^2\times[0,\infty)$. Here, the pre-factor $\sqrt{(2\ell+1)/(4\pi)}$ is only due to convenience for reducing the size of the coefficients within the P_N equations. Next, we insert the approximated radiance $I_N\approx I$ into (2.1) under the use of the derivatives

$$\begin{aligned}
\frac{1}{c}\frac{\partial}{\partial t}I_N(\mathbf{x},\hat{\mathbf{s}},t) &= \sum_{\ell=0}^{N}\sum_{m=-\ell}^{\ell}\sqrt{\frac{2\ell+1}{4\pi}}\frac{1}{c}\frac{\partial}{\partial t}\phi_{\ell}^{m}(\mathbf{x},t)Y_{\ell}^{m}(\hat{\mathbf{s}}),\\
\hat{\mathbf{s}}\cdot\nabla I_N(\mathbf{x},\hat{\mathbf{s}},t) &= \sum_{\ell=0}^{N}\sum_{m=-\ell}^{\ell}\sqrt{\frac{2\ell+1}{4\pi}}\,\hat{\mathbf{s}}\cdot\nabla\phi_{\ell}^{m}(\mathbf{x},t)Y_{\ell}^{m}(\hat{\mathbf{s}}),
\end{aligned}$$

where we have used the linearity of the partial derivative operator (applied to a finite series). In view of the integral term on the right-hand side of (2.1), we find with (3.2)

$$\begin{aligned}
\int_{\mathbb{S}^2} f(\hat{\mathbf{s}}\cdot\hat{\mathbf{s}}')I_N(x,\hat{\mathbf{s}}',t)\,d\hat{\mathbf{s}}' &= \sum_{\ell=0}^{N}\sum_{m=-\ell}^{\ell}\sqrt{\frac{2\ell+1}{4\pi}}\phi_{\ell}^{m}(\mathbf{x},t)\int_{\mathbb{S}^2} f(\hat{\mathbf{s}}\cdot\hat{\mathbf{s}}')Y_{\ell}^{m}(\hat{\mathbf{s}}')\,d\hat{\mathbf{s}}'\\
&= \sum_{\ell=0}^{N}\sum_{m=-\ell}^{\ell}\sqrt{\frac{2\ell+1}{4\pi}}\phi_{\ell}^{m}(\mathbf{x},t)f_{\ell}Y_{\ell}^{m}(\hat{\mathbf{s}}).
\end{aligned}$$

Collecting the provided information enables us to write

$$\sum_{\ell=0}^{N}\sum_{m=-\ell}^{\ell}\sqrt{\frac{2\ell+1}{4\pi}}\left(\frac{1}{c}\frac{\partial}{\partial t}+\sigma_{\ell}+\hat{\mathbf{s}}\cdot\nabla\right)\phi_{\ell}^{m}(\mathbf{x},t)Y_{\ell}^{m}(\hat{\mathbf{s}}) = 0, \tag{3.4}$$

for $(\mathbf{x},\hat{\mathbf{s}},t)\in V\times\mathbb{S}^2\times(0,\infty)$ and $\sigma_{\ell}:=\mu_a+\mu_s(1-f_{\ell})$. To proceed further, we use the identities $\sin\varphi=(e^{i\varphi}-e^{-i\varphi})/(2i)$ and $\cos\varphi=(e^{i\varphi}+e^{-i\varphi})/2$ to get

$$\begin{aligned}
\hat{\mathbf{s}}\cdot\nabla &= \cos\theta\partial_x+\sin\theta\cos\varphi\partial_y+\sin\theta\sin\varphi\partial_z\\
&= \cos\theta\partial_x+\frac{1}{2}\sin\theta e^{i\varphi}(\partial_y-i\partial_z)+\frac{1}{2}\sin\theta e^{-i\varphi}(\partial_y+i\partial_z).
\end{aligned}$$

Multiplying both sides of (3.4) with the test function $\sqrt{\frac{4\pi}{2\ell'+1}}\overline{Y_{\ell'}^{m'}} \in \mathcal{S}_N$ results in

$$\sum_{\ell=0}^{N}\sum_{m=-\ell}^{\ell}\sqrt{\frac{2\ell+1}{2\ell'+1}}\left[\frac{1}{c}\frac{\partial}{\partial t}+\sigma_l+\cos\theta\partial_x+\frac{1}{2}\sin\theta e^{i\varphi}(\partial_y-i\partial_z)\right.$$
$$\left.+\frac{1}{2}\sin\theta e^{-i\varphi}(\partial_y+i\partial_z)\right]\phi_\ell^m(\mathbf{x},t)Y_\ell^m(\hat{\mathbf{s}})\overline{Y_{\ell'}^{m'}}(\hat{\mathbf{s}})=0.$$

We finally have to integrate this expression over the unit sphere. For this, we can use the following recurrence relations for the spherical harmonics [5, p. R90]

$$\begin{aligned}
\cos\theta Y_\ell^m =& \sqrt{\frac{(\ell+m)(\ell-m)}{(2\ell-1)(2\ell+1)}}Y_{\ell-1}^m+\sqrt{\frac{(\ell+1+m)(\ell+1-m)}{(2\ell+1)(2\ell+3)}}Y_{\ell+1}^m,\\
\sin\theta e^{i\varphi}Y_\ell^m =& \sqrt{\frac{(\ell-m)(\ell-m-1)}{(2\ell-1)(2\ell+1)}}Y_{\ell-1}^{m+1}-\sqrt{\frac{(\ell+m+1)(\ell+m+2)}{(2\ell+1)(2\ell+3)}}Y_{\ell+1}^{m+1},\\
\sin\theta e^{-i\varphi}Y_\ell^m =& \sqrt{\frac{(\ell-m+1)(\ell-m+2)}{(2\ell+1)(2\ell+3)}}Y_{\ell+1}^{m-1}-\sqrt{\frac{(\ell+m)(\ell+m-1)}{(2\ell-1)(2\ell+1)}}Y_{\ell-1}^{m-1}.
\end{aligned}$$

With these formulae all integrals can be evaluated via the orthogonality relation (3.1). For example, we have

$$\begin{aligned}
\int_{\mathbb{S}^2}\cos\theta Y_\ell^m(\hat{\mathbf{s}})\overline{Y_{\ell'}^{m'}}(\hat{\mathbf{s}})\,d\hat{\mathbf{s}} =& \sqrt{\frac{(\ell'+m')(\ell'-m')}{(2\ell'-1)(2\ell'+1)}}\delta_{\ell,\ell'-1}\delta_{mm'}\\
+&\sqrt{\frac{(\ell'+1+m')(\ell'+1-m')}{(2\ell'+1)(2\ell'+3)}}\delta_{\ell,\ell'+1}\delta_{mm'}.
\end{aligned}\tag{3.5}$$

The remaining integrals can be evaluated in the same way. After that, we get

$$\begin{aligned}
&\partial_x\left[\frac{\sqrt{(\ell'+m')(\ell'-m')}}{2\ell'+1}\phi_{\ell'-1}^{m'}+\frac{\sqrt{(\ell'+1+m')(\ell'+1-m')}}{2\ell'+1}\phi_{\ell'+1}^{m'}\right]\\
&-\frac{1}{2}(\partial_y-i\partial_z)\left[\frac{\sqrt{(\ell'+m'-1)(\ell'+m')}}{2\ell'+1}\phi_{\ell'-1}^{m'-1}-\frac{\sqrt{(\ell'-m'+1)(\ell'-m'+2)}}{2\ell'+1}\phi_{\ell'+1}^{m'-1}\right]\\
&+\frac{1}{2}(\partial_y+i\partial_z)\left[\frac{\sqrt{(\ell'-m'-1)(\ell'-m')}}{2\ell'+1}\phi_{\ell'-1}^{m'+1}-\frac{\sqrt{(\ell'+m'+1)(\ell'+m'+2)}}{2\ell'+1}\phi_{\ell'+1}^{m'+1}\right]\\
&+\frac{1}{c}\frac{\partial\phi_{\ell'}^{m'}}{\partial t}+\sigma_{\ell'}\phi_{\ell'}^{m'}=0,\quad(\mathbf{x},t)\in V\times\mathbb{R}_+.
\end{aligned}$$

We now can summarize the resulting P_N system consisting of $(N+1)^2$ coupled partial differential equations. That is

$$\begin{aligned}
&(2\ell+1)\left(\frac{1}{c}\frac{\partial\phi_\ell^m}{\partial t}+\sigma_\ell\phi_\ell^m\right)+a_{\ell m}\frac{\partial\phi_{\ell-1}^m}{\partial x}+a_{\ell+1,m}\frac{\partial\phi_{\ell+1}^m}{\partial x}\\
&\quad-\frac{1}{2}\left(\frac{\partial}{\partial y}-i\frac{\partial}{\partial z}\right)\left(b_{\ell-1,m}\phi_{\ell-1}^{m-1}-c_{\ell+1,m}\phi_{\ell+1}^{m-1}\right)\\
&\quad+\frac{1}{2}\left(\frac{\partial}{\partial y}+i\frac{\partial}{\partial z}\right)\left(c_{\ell-1,m}\phi_{\ell-1}^{m+1}-b_{\ell+1,m}\phi_{\ell+1}^{m+1}\right)=0,\quad(\mathbf{x},t)\in V\times\mathbb{R}_+,
\end{aligned}\tag{3.6}$$

for $\ell = 0, 1, \ldots, N$, $|m| \leq \ell$ and moments of the form $\phi_\ell^m = \phi_\ell^m(\mathbf{x}, t)$. The corresponding coefficients are given by

$$a_{\ell m} := \sqrt{\ell^2 - m^2}, \quad b_{\ell m} := \sqrt{(\ell + m)(\ell + m + 1)}, \quad c_{\ell m} := b_{\ell,-m}.$$

We note that our obtained system (3.6) differs slightly from that found in [5] due to the differences in the parametrization of the direction variable (2.2). It remains to provide the associated initial condition. This can be done via comparison such as

$$I(\mathbf{x}, \hat{\mathbf{s}}, 0) \approx I_N(\mathbf{x}, \hat{\mathbf{s}}, 0) = \sum_{\ell=0}^{N} \sum_{m=-\ell}^{\ell} \sqrt{\frac{2\ell+1}{4\pi}} \phi_\ell^m(\mathbf{x}, 0) Y_\ell^m(\hat{\mathbf{s}}) \stackrel{!}{=} c\frac{Q(\mathbf{x})}{4\pi}$$

$$= \sum_{\ell=0}^{N} \sum_{m=-\ell}^{\ell} \sqrt{\frac{2\ell+1}{4\pi}} cQ(\mathbf{x}) \delta_{\ell 0} \delta_{m0} Y_\ell^m(\hat{\mathbf{s}}) \quad \Longrightarrow \quad \phi_\ell^m(\mathbf{x}, 0) = cQ(\mathbf{x}) \delta_{\ell 0} \delta_{m0},$$

for $\mathbf{x} \in V$. We leave the discussion about the three-dimensional P_N equations at this stage. In the next section, we derive the intended P_N equations for the plane symmetric medium based on the three-dimensional P_N equations (3.6) just derived.

3.2 The P_N equations under plane symmetry

We now apply the simplifications from Section 2.1 to the system (3.6) in order to obtain the P_N equations associated with the azimuthally independent transport equation (2.6). The separation of the absorption at the beginning allows us to consider (3.6) for $\mu_a = 0$. We also recall the convention $c = 1$ for the speed of light. The isotropic (constant) scattering phase function corresponds with $f_\ell = \delta_{\ell 0}$, yielding $\sigma_\ell = \mu_a + \mu_s(1 - f_\ell) = \mu_s(1 - \delta_{\ell 0})$. Due to the infinitely extended plane source Q, we know from Section 2.1 that the problem is independent of y and z and governed by the equation (2.4). Hence, (3.6) simplifies at this stage to the following block-diagonal system

$$\frac{\partial \phi_\ell^m}{\partial t} + \sigma_\ell \phi_\ell^m + \frac{a_{\ell m}}{2\ell + 1} \frac{\partial \phi_{\ell-1}^m}{\partial x} + \frac{a_{\ell+1,m}}{2\ell + 1} \frac{\partial \phi_{\ell+1}^m}{\partial x} = 0, \tag{3.7}$$

for $(x, t) \in \Omega \times \mathbb{R}_+$ and $\phi_\ell^m(x, 0) = Q(x)\delta_{\ell 0}\delta_{m0}$ with $Q \in C^1(\Omega)$. These P_N equations belong to the transport equation (2.4). The corresponding radiance $\Psi_N \approx \Psi$ has the form

$$\Psi_N(x, \mu, \varphi, t) = \sum_{\ell=0}^{N} \sum_{m=-\ell}^{\ell} \sqrt{\frac{2\ell+1}{4\pi}} \phi_\ell^m(x, t) Y_\ell^m(\hat{\mathbf{s}}), \tag{3.8}$$

where the coefficients ϕ_ℓ^m now depend only on two instead of four variables. The integrated radiance from (2.5) is found via integration of (3.8) using

$$\int_0^{2\pi} Y_\ell^m(\hat{\mathbf{s}})\, d\varphi = 2\pi \sqrt{\frac{2\ell+1}{4\pi}} P_\ell^0(\mu) \delta_{m0},$$

where we note on $\int_0^{2\pi} e^{im\varphi}\, d\varphi = 2\pi\delta_{m0}$. Hence, we arrive at the Legendre series

$$\psi_N(x, \mu, t) = \sum_{\ell=0}^{N} \frac{2\ell+1}{2} \phi_\ell(x, t) P_\ell(\mu) \approx \psi(x, \mu, t), \tag{3.9}$$

which only considers the moments $\phi_\ell^0 = \phi_\ell$ for $m = 0$. This means that the P_N equations we are looking for correspond to the block for $m = 0$ of system (3.7). The resulting equations considered on $\Omega \times \mathbb{R}_+$ can be given as

$$\begin{aligned} &\frac{\partial \phi_0}{\partial t} + \frac{\partial \phi_1}{\partial x} = 0, \\ &\frac{\partial \phi_\ell}{\partial t} + \frac{\ell}{2\ell+1}\frac{\partial \phi_{\ell-1}}{\partial x} + \frac{\ell+1}{2\ell+1}\frac{\partial \phi_{\ell+1}}{\partial x} + \mu_s \phi_\ell = 0, \quad \ell = 1, 2, \ldots, N, \end{aligned} \tag{3.10}$$

for the moments $\phi_\ell \in C^1(\Omega \times \mathbb{R}_+)$ with $\phi_\ell(x, 0) = Q(x)\delta_{\ell 0}$ for $x \in \Omega$ and $\phi_{N+1} = 0$. These are the desired P_N equations associated with the transport equation (2.6).[2] From now on, when we refer to the P_N equations, we always mean (3.10) respective (3.11). The truncation parameter $N \geq 1$ is typically an odd number. One reason for this convention can be reviewed in [10]. The Legendre polynomials occurring in (3.9) satisfy the orthogonality relation $\int_{-1}^{1} P_\ell(x) P_m(x)\, dx = \frac{2\delta_{\ell m}}{2\ell+1}$, see for example [2, p. 310].

Remark 3.3. The fluence from Definition 2.2 corresponds with the zero order moment ϕ_0, due to

$$\Phi(x, t) \approx \int_{-1}^{1} \psi_N(x, \mu, t)\, d\mu = \sum_{\ell=0}^{N} \frac{2\ell+1}{2} \phi_\ell(x, t) \int_{-1}^{1} P_\ell(\mu)\, d\mu = \phi_0(x, t).$$

The P_N equations (3.10) can be conveniently written in matrix notation. For this, we introduce the vector-valued function

$$\boldsymbol{\phi} : \overline{\Omega} \times [0, \infty) \to \mathbb{R}^{N+1} \quad \text{with} \quad \boldsymbol{\phi} = \begin{pmatrix} \phi_0 \\ \phi_1 \\ \vdots \\ \phi_N \end{pmatrix},$$

together with the diagonal matrix $\Sigma := \operatorname{diag}(0, \mu_s, \mu_s, \ldots, \mu_s) \in \mathbb{R}^{N+1,N+1}$ and

$$A := \begin{pmatrix} 0 & 1 & 0 & 0 & \cdots & 0 \\ \frac{1}{3} & 0 & \frac{2}{3} & 0 & \cdots & \vdots \\ 0 & \frac{2}{5} & \ddots & \ddots & \cdots & 0 \\ 0 & 0 & \ddots & \ddots & \ddots & 0 \\ \vdots & \cdots & \cdots & \ddots & \ddots & \frac{N}{2N-1} \\ 0 & \cdots & 0 & 0 & \frac{N}{2N+1} & 0 \end{pmatrix} \in \mathbb{R}^{N+1,N+1}.$$

Then, system (3.10) becomes

$$\boldsymbol{\phi}_t + A\boldsymbol{\phi}_x + \Sigma\boldsymbol{\phi} = 0, \quad x \in \Omega,\ t > 0, \tag{3.11}$$

subject to $\boldsymbol{\phi}(x, 0) = Q(x)e_0$ for $x \in \Omega$ with $e_0 := (1, 0, \ldots, 0)^T \in \mathbb{R}^{N+1}$. It remains to transfer the BC from Definition 2.6 into the frame of the P_N methodology. Let $x_b \in \partial\Omega$ be an element of the boundary. By requiring $\psi_N(x_b, \mu, t) = \psi_N(x_b, -\mu, t)$ for all $(\mu, t) \in [-1, 1] \times [0, \infty)$, one obtains

$$\sum_{\ell=0}^{N} \frac{2\ell+1}{2} [1 - (-1)^\ell] \phi_\ell(x_b, t) P_\ell(\mu) \overset{!}{=} 0 \quad \forall (\mu, t) \in [-1, 1] \times [0, \infty),$$

[2] As already mentioned, the system (3.10) can be derived more conveniently if one starts from (2.6). Then, the unknown radiance can be directly expressed in Legendre polynomials according to (3.9)

where we have used $P_\ell(-\mu) = (-1)^\ell P_\ell(\mu)$, see e.g. [2, p. 304] for more details on the Legendre polynomials. Due to the linear independence of these polynomials, the reflective BC from Definition 2.6 translates into the zero BC

$$\phi_\ell(x,t) = 0 \quad \forall (x,t) \in \partial\Omega \times [0,\infty),\ \ell = 1,3,\dots,N. \tag{3.12}$$

Example 3.4. Let us consider the lowest order approximation on $\Omega = (0,L)$ for the $2L$-periodic source distribution (2.19). From (3.10) we get for $N = 1$ the time-dependent P_1 equations

$$\begin{aligned} \frac{\partial \phi_0}{\partial t} + \frac{\partial \phi_1}{\partial x} &= 0, \\ \frac{\partial \phi_0}{\partial x} + 3\frac{\partial \phi_1}{\partial t} + 3\mu_s \phi_1 &= 0, \end{aligned} \tag{3.13}$$

with initial conditions $\phi_0(x,0) = Q(x)$ and $\phi_1(x,0) = 0$ for $x \in \Omega$. The corresponding zero BCs are $\phi_1(0,t) = \phi_1(L,t) = 0$ for $t \geq 0$, cf. (3.12). A computable solution to this problem is given by the Fourier series (3.33) for $N = 1$.

The P_1 equations (3.13) represent the Telegrapher equation. This can be seen as follows. The first equation $\partial_t \phi_0 + \partial_x \phi_1 = 0$ gives $\partial_t^2 \phi_0 = -\partial_t \partial_x \phi_1$. From the second equation, we find $\partial_x^2 \phi_0 + 3\mu_s \partial_x \phi_1 + 3\partial_x \partial_t \phi_1 = 0$. The combination of these results and the assumption that Schwarz's theorem can be applied leads to the Telegrapher equation

$$\frac{\partial^2 \phi_0}{\partial t^2} + \mu_s \frac{\partial \phi_0}{\partial t} = \frac{1}{3}\frac{\partial^2 \phi_0}{\partial x^2}, \quad x \in \Omega,\ t > 0, \tag{3.14}$$

subject to $\phi_0(x,0) = Q(x)$ and $\partial_t \phi_0(x,0) = 0$ for $x \in \Omega$. Moreover, for $x \in \partial\Omega$, we obtain from the second equation of the system (3.13) the condition $\partial_x \phi_0(x,t) = 0$ for all $t \geq 0$, because $\phi_1(x,t) = 0 = \partial_t \phi_1(x,t)$. Thus, the BCs belonging to the Telegrapher equation (3.14) are given by the homogeneous Neumann conditions $\partial_x \phi_0(0,t) = \partial_x \phi_0(L,t) = 0$ for $t \geq 0$. We also note on the particular case $\mu_s = 0$. Then, the Telegrapher equation (3.14) reduces to a classical wave equation with propagation speed $1/\sqrt{3}$. In some cases, equation (3.14) admits a closed-form solution.

Theorem 3.5. *The Telegrapher equation on $\Omega = \mathbb{R}$ subject to the initial conditions $\phi_0(x,0) = \delta(x)$ and $\partial_t \phi_0(x,0) = 0$ for $x \in \mathbb{R}$ admits an explicit solution of the form*

$$\begin{aligned} \phi_0(x,t) =& \frac{\sqrt{3}}{2} e^{-\mu_s t/2} \delta(t - \sqrt{3}|x|) + \mu_s \frac{\sqrt{3}}{4} e^{-\mu_s t/2} \Theta(t^2 - 3x^2) \\ &\times \left[I_0\Big(\frac{\mu_s}{2}\sqrt{t^2 - 3x^2}\Big) + \frac{t}{\sqrt{t^2 - 3x^2}} I_1\Big(\frac{\mu_s}{2}\sqrt{t^2 - 3x^2}\Big) \right], \end{aligned} \tag{3.15}$$

with I_n for $n = 0, 1$ being the modified Bessel function of the first kind.

Proof. In the literature, fundamental solutions to the Telegrapher equation are often derived by means of integral transforms [37]. While it is not difficult to recover the solution in the transformed space, the required inversion leads often to complicated integrals that must be looked up in tables. In the following, we propose an elementary proof with reference to the theory for the classical wave equation. We first introduce $\phi_0(x,t) := e^{-\mu_s t/2} u(x,t)$. In view of the initial values, we note on $u(x,0) = \phi_0(x,0)$ and (by the product rule) $\partial_t u(x,0) = (\mu_s/2)\phi_0(x,0)$. Inserting this ansatz into (3.14) leads to the new initial value problem

$$\begin{cases} u_{tt} - \dfrac{1}{3} u_{xx} = \Big(\dfrac{\mu_s}{2}\Big)^2 u, & x \in \mathbb{R},\ t > 0, \\ u(x,0) = \delta(x), & x \in \mathbb{R}, \\ u_t(x,0) = \dfrac{\mu_s}{2}\delta(x), & x \in \mathbb{R}. \end{cases} \tag{3.16}$$

Next, we seek a solution in form of the function series

$$u(x,t) = \sum_{n=0}^{\infty} \left(\frac{\mu_s}{2}\right)^{2n} u_n(x,t), \quad x \in \mathbb{R},\, t \geq 0, \tag{3.17}$$

where the convergence is shown at the end of the proof. Inserting this into (3.16) leads to the following system of recursively defined wave equations

$$\begin{aligned} \partial_t^2 u_0 - \frac{1}{3}\partial_x^2 u_0 &= 0, \\ \partial_t^2 u_n - \frac{1}{3}\partial_x^2 u_n &= u_{n-1}, \quad n \geq 1, \end{aligned}$$

subject to $u_n(x,0) = \delta(x)\delta_{n0}$ and $\partial_t u_n(x,0) = (\mu_s/2)\delta(x)\delta_{n0}$. Thus, starting from u_0, we can successively determine all elements $u_{n\geq 1}$. In this context, we need the complete solution of the classical wave equation on $\mathbb{R}$, see for example [2, p. 477]. The first equation is just a homogeneous wave equation that can be solved by the d'Alembert formula, yielding

$$u_0(x,t) = \frac{\sqrt{3}}{2}\delta(t - \sqrt{3}|x|) + \mu_s \frac{\sqrt{3}}{4}\Theta(t^2 - 3x^2). \tag{3.18}$$

The second inhomogeneous wave equation under zero initial values is formally solved via integration of the right-hand side over the characteristic triangle in the xt-plane with corners $(x - t/\sqrt{3}, 0)$, $(x + t/\sqrt{3}, 0)$ and (x,t). This results in

$$u_n(x,t) = \frac{\sqrt{3}}{2}\int_\Delta u_{n-1}\, dS = \frac{\sqrt{3}}{2}\int_0^t \int_{x-\frac{t-s}{\sqrt{3}}}^{x+\frac{t-s}{\sqrt{3}}} u_{n-1}(y,s)\, dyds.$$

The computation of u_n for several $n = 1, 2, \ldots$ gives rise to the assumption

$$u_n(x,t) = \frac{\sqrt{3}}{2^{2n+1}(n!)^2}\left[\frac{\mu_s}{2}(t^2 - 3x^2)^n + 2nt(t^2 - 3x^2)^{n-1}\right]\Theta(t^2 - 3x^2), \tag{3.19}$$

for an arbitrary $n \in \mathbb{N}$. We want to confirm this formula by induction. We begin with $n = 1$, which requires the computation of $\frac{\sqrt{3}}{2}\int_\Delta u_0\, dS$. In this context, we rewrite the Dirac delta distribution occurring in (3.18) under consideration of Proposition 2.5, yielding

$$\begin{aligned} &\delta(t - \sqrt{3}|x|) = \delta(\sqrt{3}|x| - t) = \frac{1}{\sqrt{3}}\delta(|x| - t/\sqrt{3}) \\ =&\frac{\delta(x - t/\sqrt{3}) + \delta(x + t/\sqrt{3})}{\sqrt{3}} = \frac{d}{dx}\frac{\Theta(x - t/\sqrt{3}) + \Theta(x + t/\sqrt{3})}{\sqrt{3}}. \end{aligned}$$

With this and under the use of $\int \Theta(\lambda)\, d\lambda = \lambda\Theta(\lambda) + C$, we find regarding the Dirac delta distribution

$$I_1(x,t) := \int_0^t \int_{x-\frac{t-s}{\sqrt{3}}}^{x+\frac{t-s}{\sqrt{3}}} \frac{d}{dy}\frac{\Theta(y - s/\sqrt{3}) + \Theta(y + s/\sqrt{3})}{\sqrt{3}}\, dyds = \frac{t}{\sqrt{3}}\Theta(t^2 - 3x^2).$$

For the second double integral, we perform a linear coordinate transformation according to

$$\begin{cases} y = \dfrac{\xi + \eta}{2}, \\ s = \sqrt{3}\dfrac{\xi - \eta}{2}, \end{cases} \quad \Longrightarrow \quad \left|\frac{\partial(y,s)}{\partial(\xi,\eta)}\right| = \frac{\sqrt{3}}{2}, \tag{3.20}$$

which is also used for the induction step. Under this transformation, the characteristic triangle becomes a right one with corners $(x-t/\sqrt{3}, x-t/\sqrt{3})$, $(x+t/\sqrt{3}, x+t/\sqrt{3})$ and $(x+t/\sqrt{3}, x-t/\sqrt{3})$ in the $\xi\eta$-plane. The application of the transformation formula for multiple integrals leads to

$$I_2(x,t) := \int_0^t \int_{x-\frac{t-s}{\sqrt{3}}}^{x+\frac{t-s}{\sqrt{3}}} \Theta(s^2-3y^2)\,dyds = \frac{\sqrt{3}}{2}\int_{x-t/\sqrt{3}}^{x+t/\sqrt{3}} \int_{x-t/\sqrt{3}}^{\xi} \Theta(-3\xi\eta)\,d\eta d\xi$$
$$= \Theta(t^2-3x^2)\frac{\sqrt{3}}{2}\int_0^{x+t/\sqrt{3}} \int_{x-t/\sqrt{3}}^{0} d\eta d\xi = \frac{t^2-3x^2}{2\sqrt{3}}\Theta(t^2-3x^2).$$

We now can combine both integral contributions to obtain

$$\frac{\sqrt{3}}{2}\int_\Delta u_0\,dS = \frac{\sqrt{3}}{2}\left[\frac{\sqrt{3}}{2}I_1(x,t) + \mu_s\frac{\sqrt{3}}{4}I_2(x,t)\right] = u_1(x,t),$$

which agrees with formula (3.19) for $n=1$. We assume the correctness of (3.19) for a natural number $n \geq 1$. For the induction step, we have to evaluate $\frac{\sqrt{3}}{2}\int_\Delta u_n\,dS$ with u_n from (3.19). In doing so, we again use the coordinate transformation (3.20) to obtain

$$\begin{aligned}
\frac{\sqrt{3}}{2}\int_\Delta u_n\,dS =& \frac{3\sqrt{3}}{2^{2n+3}(n!)^2}\int_{x-t/\sqrt{3}}^{x+t/\sqrt{3}} \int_{x-t/\sqrt{3}}^{\xi} \Big[\frac{\mu_s}{2}(-3\xi\eta)^n \\
&+ \sqrt{3}n(\xi-\eta)(-3\xi\eta)^{n-1}\Big]\,\Theta(-3\xi\eta)\,d\eta d\xi \\
=& \frac{3\sqrt{3}}{2^{2n+3}(n!)^2}\int_0^{x+t/\sqrt{3}} \int_{x-t/\sqrt{3}}^{0} \Big[\frac{\mu_s}{2}(-3\xi\eta)^n \\
&+ \sqrt{3}n(\xi-\eta)(-3\xi\eta)^{n-1}\Big]\,d\eta d\xi\cdot\Theta(t^2-3x^2) \\
=& \frac{\sqrt{3}\cdot\Theta(t^2-3x^2)}{2^{2(n+1)+1}((n+1)!)^2}\Big[\frac{\mu_s}{2}(t^2-3x^2)^{n+1} + 2(n+1)t(t^2-3x^2)^n\Big],
\end{aligned}$$

which agrees with u_{n+1} from (3.19) and hence the induction is completed. The last step consists in the evaluation of the series (3.17). For $x \in \mathbb{R}$ and $t \geq \sqrt{3}|x|$ we get

$$\begin{aligned}
u(x,t) =& \frac{\sqrt{3}}{2}\delta(t-\sqrt{3}|x|) + \mu_s\frac{\sqrt{3}}{4}\sum_{n=0}^{\infty}\Big(\frac{\mu_s}{2}\Big)^{2n}\frac{(t^2-3x^2)^n}{2^{2n}(n!)^2} \\
&+ t\sqrt{3}\sum_{n=1}^{\infty}\Big(\frac{\mu_s}{4}\Big)^{2n}\frac{(t^2-3x^2)^{n-1}}{(n-1)!n!} = \frac{\sqrt{3}}{2}\delta(t-\sqrt{3}|x|) \\
&+ \mu_s\frac{\sqrt{3}}{4}\left[I_0\Big(\frac{\mu_s}{2}\sqrt{t^2-3x^2}\Big) + \frac{t}{\sqrt{t^2-3x^2}}I_1\Big(\frac{\mu_s}{2}\sqrt{t^2-3x^2}\Big)\right],
\end{aligned}$$

where we have incorporated the modified Bessel function of the first kind according to the definition [2, p. 246]

$$I_m(x) := \Big(\frac{x}{2}\Big)^m\sum_{n=0}^{\infty}\frac{(x/2)^{2n}}{n!(n+m)!}, \quad x\in\mathbb{R},\ m\in\mathbb{N}_0,$$

which is known to be an absolute convergent series. The proof of Theorem 3.5 is completed after setting $\phi_0(x,t) = e^{-\mu_s t/2}u(x,t)$. □

As we have just seen, the Telegrapher equation could be solved with recourse to the general solution to the classical wave equation $\partial_t^2\phi_0 = \frac{1}{3}\partial_x^2\phi_0$. The latter one is a second order formulation of the P_1 equations (3.13) in the non-scattering (lossless) medium. This concept is also applicable to higher order P_N equations by seeking for a solution $\boldsymbol{\phi} = \sum_{n=0}^{\infty}\boldsymbol{\xi}_n$, which leads to the following recursively defined first order systems

$$\begin{aligned} &\partial_t\boldsymbol{\xi}_0 + A\partial_x\boldsymbol{\xi}_0 = 0, \\ &\partial_t\boldsymbol{\xi}_n + A\partial_x\boldsymbol{\xi}_n = -\Sigma\boldsymbol{\xi}_{n-1}, \quad n \geq 1, \end{aligned} \tag{3.21}$$

subject to $\boldsymbol{\xi}_n(x,0) = Q(x)e_0\delta_{n0}$ for $x \in \mathbb{R}$. Looking at the left-hand side, we see that it makes sense to give a closer look at the P_N equations in lossless media. After that, we will focus entirely on the time-dependent SP_N equations.

3.2.1 The P_N equations in lossless media

In general, it is not easy to solve the P_N equations in closed form. For lossless media, when $\mu_s = 0$, there is the possibility to derive an analytical solution that is also useful for verification of numerical approaches. Furthermore, as shown above, it can be used to construct solutions for the lossy medium. We remind on the convention $N \geq 1$ and N odd.

Theorem 3.6. *Let $Q \in C^1(\mathbb{R})$ be the spatial distribution of particles that are initially emitted into the unbounded domain $\Omega = \mathbb{R}$. Then, the Cauchy problem*

$$\begin{cases} \boldsymbol{\phi}_t + A\boldsymbol{\phi}_x = 0, \quad (x,t) \in \mathbb{R} \times \mathbb{R}_+, \\ \boldsymbol{\phi}(x,0) = Q(x)e_0, \quad x \in \mathbb{R}, \end{cases} \tag{3.22}$$

has a classical solution of the form

$$\boldsymbol{\phi}(x,t) = D^{-1}U \begin{pmatrix} Q(x-\lambda_0 t) & 0 & \cdots & 0 \\ 0 & Q(x-\lambda_1 t) & \ddots & \vdots \\ \vdots & \ddots & \ddots & 0 \\ 0 & \cdots & 0 & Q(x-\lambda_N t) \end{pmatrix} U^T e_0, \tag{3.23}$$

for $(x,t) \in \mathbb{R} \times [0,\infty)$. It can be written more explicitly in terms of the moments

$$\phi_\ell(x,t) = \frac{1}{\sqrt{2\ell+1}} \sum_{j=0}^{\frac{N-1}{2}} \left[Q(x-\lambda_j t) + (-1)^\ell Q(x+\lambda_j t) \right] u_j^{(0)} u_j^{(\ell)}, \tag{3.24}$$

where $D := \operatorname{diag}\left(\sqrt{1}, \sqrt{3}, \ldots, \sqrt{2N+1}\right)$ and (λ_j, u_j) for $j = 0, 1, \ldots, N$ are the eigenpairs of the associated Jacobi matrix

$$J_{N+1} = \begin{pmatrix} 0 & \frac{1}{\sqrt{3}} & 0 & 0 & \cdots & 0 \\ \frac{1}{\sqrt{3}} & 0 & \frac{2}{\sqrt{15}} & 0 & \cdots & \vdots \\ 0 & \frac{2}{\sqrt{15}} & \ddots & \ddots & \cdots & 0 \\ 0 & 0 & \ddots & \ddots & \ddots & 0 \\ \vdots & \cdots & \cdots & \ddots & \ddots & \frac{N}{\sqrt{4N^2-1}} \\ 0 & \cdots & 0 & 0 & \frac{N}{\sqrt{4N^2-1}} & 0 \end{pmatrix} \in \mathbb{R}^{N+1,N+1}.$$

Proof. First, we notice that the matrix A is similar to the Jacobi matrix due to the factorization $DAD^{-1} = J_{N+1}$. The Jacobi matrix itself is a symmetric tridiagonal matrix which admits the decomposition $J_{N+1} = U\Lambda U^T$, where $\Lambda = \mathrm{diag}(\lambda_j)_{0\le j\le N}$ contains the real-valued eigenvalues. With the current entries of J_{N+1}, they coincide with the roots of the Legendre polynomial P_{N+1}, see for example [38, Chapter 2]. The orthogonal matrix U is the eigenvector matrix with property $U^TU = I$, where $I \in \mathbb{R}^{N+1,N+1}$ denotes the identity matrix. We therefore have the decomposition $A = D^{-1}U\Lambda U^TD$ so that the system of P_N equations decouples into the following $N+1$ transport equations

$$\mathbf{w}_t + \Lambda \mathbf{w}_x = 0, \quad \mathbf{w}(x,0) = Q(x)U^T e_0, \tag{3.25}$$

where we have introduced the function $\mathbf{w} := U^T D\,\boldsymbol{\phi}$. The general solution to the jth equation of (3.25) is given by $w_j(x,t) = C_j(x-\lambda_j t)$ with C_j being an arbitrary continuously differentiable function. The incorporation of the initial condition (component-wise) gives

$$w_j(x,0) = e_j^T\mathbf{w}(x,0) = Q(x)u_j^Te_0 \overset{!}{=} C_j(x) \quad \Longrightarrow \quad w_j(x,t) = Q(x-\lambda_j t)u_j^Te_0.$$

With this result, we get for the original solution

$$\boldsymbol{\phi}(x,t) = D^{-1}U\,\mathbf{w}(x,t) = D^{-1}U\begin{pmatrix} Q(x-\lambda_0 t)u_0^Te_0 \\ Q(x-\lambda_1 t)u_1^Te_0 \\ \vdots \\ Q(x-\lambda_N t)u_N^Te_0 \end{pmatrix}, \quad x\in\mathbb{R},\, t\ge 0,$$

which is the same as given in (3.23). The more explicit representation (3.24) is found by considering the symmetry of the eigenpairs. That is, for N odd, the spectrum of A is of the form $\sigma(A) = \{\pm\lambda_j : 0 \le j \le (N-1)/2\}$. Furthermore, if $u_j \in \mathbb{R}^{N+1}$ is an eigenvector with components $u_j^{(\ell)}$ $(\ell = 0,\dots,N)$ belonging to the eigenvalue λ_j, then $(-1)^\ell u_j^{(\ell)}$ are the components associated with $-\lambda_j$. □

Expression (3.24) displays the hyperbolic nature of the P_N equations. There is no change/improvement of the initial regularity and the domain of dependence regarding the value $\boldsymbol{\phi}(x_0,t_0)$ is given by the finite set $\{(x_0 \pm \lambda_j t_0, 0) : 0 \le j \le (N-1)/2\}$. The corresponding characteristics can be found without the prior determination of an explicit solution by making use of the following definition (see e.g. [36, p. 55] or [39, pp. 142–143]).

Definition 3.7 (Characteristics of a first order system)**.** Characteristics are curves along which it is not possible to determine the first order derivatives of the unknown solution using only the information provided by the Cauchy data and the first order system.

Based on this definition, we are able to state the following result, which also applies to lossy media.

Proposition 3.8. *The characteristics of the P_N equations* (3.11) *are given by the lines $x \pm \lambda_j t = $ const., where λ_j are the positive roots of the equation $P_{N+1}(\lambda) = 0$.*

Proof. Let $(x, t(x))^T \in \mathbb{R}^2$ be a continuously differentiable curve for $x \in J \subset \mathbb{R}$ on which we would like to prescribe Cauchy data according to

$$\boldsymbol{\phi}(x,t(x)) = \boldsymbol{\gamma}(x) = (\gamma_0(x), \gamma_1(x), \dots, \gamma_N(x))^T. \tag{3.26}$$

Taking the first derivative with respect to the curve parameter leads to

$$\boldsymbol{\phi}_x(x,t(x)) + t'(x)\,\boldsymbol{\phi}_t(x,t(x)) = \boldsymbol{\gamma}'(x). \tag{3.27}$$

On the other hand, the P_N equations (3.11) must also be satisfied along the selected curve, yielding the following second set on conditions

$$\boldsymbol{\phi}_t(x,t(x)) + A\boldsymbol{\phi}_x(x,t(x)) = -\Sigma\,\boldsymbol{\gamma}(x). \tag{3.28}$$

From (3.27), we find $\boldsymbol{\phi}_x(x,t(x)) = \boldsymbol{\gamma}'(x) - t'(x)\boldsymbol{\phi}_t(x,t(x))$. Inserting this into (3.28) results in the system of linear equations

$$(t'(x)A - I)\boldsymbol{\phi}_t(x,t(x)) = A\boldsymbol{\gamma}'(x) + \Sigma\,\boldsymbol{\gamma}(x). \tag{3.29}$$

This system is, in general, not solvable if

$$\det(t'(x)A - I) = \det(t'(x)\Lambda - I) = \prod_{j=0}^{\frac{N-1}{2}} \left[1 - \left(t'(x)\lambda_j\right)^2\right] = 0.$$

Thus, given $\boldsymbol{\phi}(x,t(x)) = \boldsymbol{\gamma}(x)$ with $t'(x)\lambda_j = \pm 1$ and $j \in \{0,\dots,(N-1)/2\}$, we cannot find the first order derivatives of $\boldsymbol{\phi}$ along $x \pm \lambda_j t = \text{const.}$ under the use of the P_N equations. □

Example 3.9. The zero order moment (fluence) belonging to the P_3 equations can be found from (3.24) and summarized as

$$\begin{aligned}\phi_0(x,t) =& \frac{18+\sqrt{30}}{72}[Q(x-\lambda_0 t) + Q(x+\lambda_0 t)] \\ &+ \frac{18-\sqrt{30}}{72}[Q(x-\lambda_1 t) + Q(x+\lambda_1 t)], \quad x \in \mathbb{R},\ t \geq 0,\end{aligned} \tag{3.30}$$

where the wave velocities $\lambda_0 = \sqrt{\frac{3}{7} - \frac{2}{7}\sqrt{\frac{6}{5}}}$ and $\lambda_1 = \sqrt{\frac{3}{7} + \frac{2}{7}\sqrt{\frac{6}{5}}}$ are the positive roots of $P_4(\lambda) = 0$. For illustration purposes, Figure 3.1 shows the time evolution of the fluence (3.30) for the Gaussian wave packet $Q(x) = e^{-\frac{x^2}{2\varepsilon}}/\sqrt{2\pi\varepsilon}$ with $\varepsilon = 0.1$.

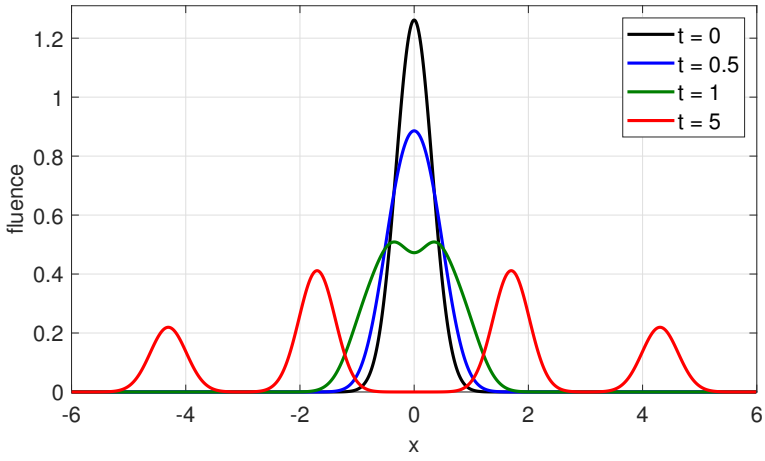

Figure 3.1: Time evolution of the fluence in the infinite medium obtained from the P_3 equations.

In Section 3.5, we also consider within the numerical experiments solutions to the P_3 equations in order to highlight differences to the derived SP_3 equations. In contrast to the system (3.11), the P_N equations in Fourier space

$$\hat{\boldsymbol{\phi}}_t + (\Sigma + ikA)\hat{\boldsymbol{\phi}} = 0, \quad k \in \mathbb{R},\, t > 0, \tag{3.31}$$

with $\hat{\boldsymbol{\phi}}(k,0) = \hat{Q}(k)e_0$ for $k \in \mathbb{R}$ are solvable with relatively little effort, even for the lossy medium. The corresponding solution leads to the matrix exponential with property $\frac{d}{dt}e^{Mt} = Me^{Mt} = e^{Mt}M$. Further details on this matrix-valued function can be found, for example, in [40, Chapter 1]. Hence, the initial value problem (3.31) is solved by

$$\hat{\boldsymbol{\phi}}(k,t) = \hat{Q}(k)e^{-(\Sigma+ikA)t}e_0, \quad k \in \mathbb{R},\, t \geq 0. \tag{3.32}$$

For an even source distribution $\hat{Q}(-k) = \hat{Q}(k)$, one can deduce from the (tridiagonal) system (3.31) the symmetry relation $\hat{\phi}_\ell(-k,t) = (-1)^\ell \hat{\phi}_\ell(k,t)$ for $\ell = 0, 1, \ldots, N$. The usefulness of this property becomes apparent when considering the even and $2L$-periodic source distribution (2.19) together with its Dirac-like spectrum (2.20). Then, as shown in Subsection 2.2.2, we can invert (3.32) to get in space-time domain

$$\boldsymbol{\phi}(x,t) = \frac{1}{L}\sum_{n\in\mathbb{Z}} q_{|n|}e^{i\omega_n x}e^{-(\Sigma+i\omega_n A)t}e_0, \quad x \in \mathbb{R},\, t \geq 0. \tag{3.33}$$

For ℓ odd, we deduce $\phi_\ell(0,t) = \phi_\ell(L,t) = 0$ for $t \geq 0$, which is due to the mentioned symmetry in Fourier space. More concretely, for $x = 0$ and ℓ odd, we have

$$\phi_\ell(0,t) = e_\ell^T \boldsymbol{\phi}(0,t) = \frac{q_0}{L}\delta_{\ell 0} + \frac{1+(-1)^\ell}{L}\sum_{n\geq 1} q_n e_\ell^T e^{-(\Sigma+i\omega_n A)t}e_0 = 0 \quad \forall t \geq 0.$$

The same result can be confirmed for the boundary point $x = L$. Thus, the obtained expression (3.33) is simultaneously a solution for the bounded domain $\Omega = (0,L)$, because it satisfies the required BC (3.12). For the lossless medium, it can be directly seen that if Q is even and $2L$-periodic, the odd moments from (3.24) vanish at $\partial\Omega = \{0, L\}$. In contrast to the solution from Theorem 3.6, the series (3.33) is also valid in lossy media. It will be used later in Section 3.5. For illustration purposes, let us perform a comparison between the transport theory fluence (2.24) and the zero order moment from (3.24). To get the bounded domain $\Omega = (0,L)$, we employ the Poisson kernel

$$P(x) := \frac{1}{L}\frac{1-\varrho^2}{1+\varrho^2-2\varrho\cos(\pi x/L)}, \quad x \in \mathbb{R},$$

where $|\varrho| < 1$ and set in view of the initial source distribution

$$Q(x) := \frac{P(x-x_0)+P(x+x_0)}{2} = \sum_{n=0}^{\infty}\frac{2-\delta_{n0}}{L}q_n\cos(\omega_n x). \tag{3.34}$$

Here, $q_n = \varrho^n\cos(\omega_n x_0)$ are the corresponding Fourier coefficients with $x_0 \in \Omega$. This source is even, $2L$-periodic and normalized according to $\int_\Omega Q(x)\,dx = 1$. Figure 3.2 displays the fluence in a bounded domain with $L = 3$ caused by the Poisson-like distribution (3.34) with $\varrho = 0.6$ and $x_0 = 2$. The P_N-based solution (3.24) was evaluated for the order $N = 7$ and the Fourier series (2.24) was truncated at $n_{max} = 20$. As can be seen, the zero order moment of the P_7 equations (black dashed lines) provides a reasonable approximation of the transport theory fluence (red and green line). We also note on the equilibrium state $\lim_{t\to\infty}\Phi(x,t) = 1/L = 1/3$ for all $x \in \overline{\Omega}$.

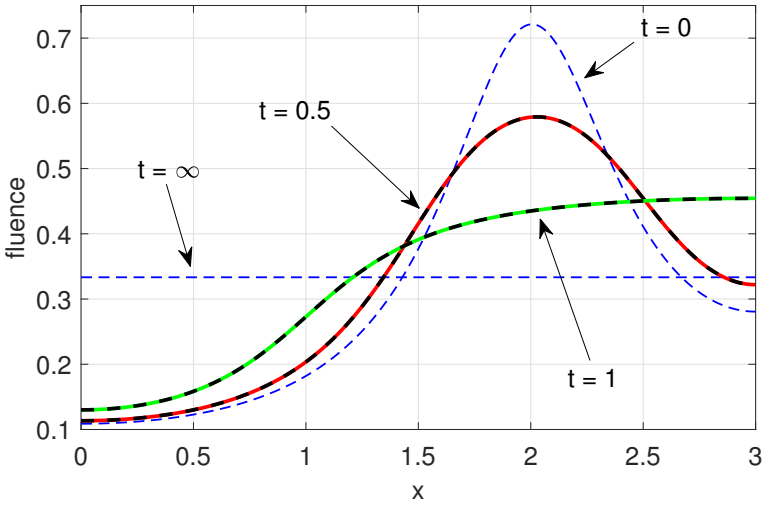

Figure 3.2: Time evolution of the fluence in a lossless and bounded domain due to a Poisson-like initial condition.

As a consequence of Theorem 3.6, we additionally can show the following well-posedness result.

Corollary 3.10. *The Cauchy problem* (3.22) *has a unique solution that depends continuously on the initial data.*

Proof. In view of the existence, we note that $\boldsymbol{\phi}$ from (3.23) is of class C^1 because $Q \in C^1(\mathbb{R})$. Furthermore, we have $\boldsymbol{\phi}(x,0) = Q(x)D^{-1}UU^T e_0 = Q(x)e_0$ and

$$\boldsymbol{\phi}_t = D^{-1}U\mathbf{w}_t = D^{-1}U(-\Lambda \mathbf{w}_x) = -D^{-1}U\Lambda U^T D\boldsymbol{\phi}_x = -A\boldsymbol{\phi}_x,$$

where we have used $A = D^{-1}U\Lambda U^T D$. Thus, we have $\boldsymbol{\phi}_t + A\boldsymbol{\phi}_x = 0$ and hence the existence of a solution. Regarding the uniqueness, we have decoupled in the proof of Theorem 3.6 the original P_N system into $N+1$ simple transport equations of the form $w_{j,t} + \lambda_j w_{j,x} = 0$ with $w_j(x,0) = Q(x)u_j^T e_0$ for $x \in \mathbb{R}$. Let w_j be a solution of class C^1 and $(x,t) \in \mathbb{R} \times [0,\infty)$ an arbitrary point. Then, w_j is constant along the line $(x + \lambda_j(s-t), s)^T$ for $s \geq 0$ that passes through the point (x,t). We therefore obtain

$$w_j(x + \lambda_j(s-t), s) = w_j(x,t) = w_j(x - \lambda_j t, 0) = Q(x - \lambda_j t)u_j^T e_0 \quad \forall s \geq 0.$$

Thus, the value $w_j(x,t)$ is uniquely determined by the initial condition. Hence, $\boldsymbol{\phi} = D^{-1}U\mathbf{w}$ is also unique. To show the continuous dependence, we take into account the induced matrix norm $\|\cdot\| : \mathbb{R}^{n,n} \to \mathbb{R}$ defined by

$$\|M\|_p := \sup_{x \neq 0} \frac{\|Mx\|_p}{\|x\|_p}, \quad p \geq 1,\ M \in \mathbb{R}^{n,n},$$

with the vector norm $\|x\|_p^p := \sum_{i=1}^n |x_i|^p$. This matrix norm is compatible in the sense $\|Mx\|_p \leq \|M\|_p \|x\|_p$ for all $M \in \mathbb{R}^{n,n}, x \in \mathbb{R}^n$ and sub-multiplicative according to $\|MN\|_p \leq \|M\|_p \|N\|_p$ for all $M, N \in \mathbb{R}^{n,n}$. We then obtain under the assumption $\|Q\|_{L_\infty(\mathbb{R})} < \delta$ the

uniform estimate

$$\begin{aligned}\|\boldsymbol{\phi}(x,t)\|_\infty &= \left\|D^{-1}D\boldsymbol{\phi}(x,t)\right\|_\infty \\ &\le \left\|D^{-1}\right\|_\infty \left\|U\operatorname{diag}(Q(x-\lambda_j t))_{0\le j\le N}U^T e_0\right\|_\infty \\ &\le \left\|U\operatorname{diag}(Q(x-\lambda_j t))_{0\le j\le N}U^T e_0\right\|_2 \\ &\le \left\|U\operatorname{diag}(Q(x-\lambda_j t))_{0\le j\le N}U^T\right\|_2 \|e_0\|_2 \\ &= \|\operatorname{diag}(Q(x-\lambda_j t))_{0\le j\le N}\|_2 = \max_{0\le j\le N}|Q(x-\lambda_j t)| < \delta,\end{aligned}$$

where we have used $\|D^{-1}\|_\infty = 1$, $\|x\|_\infty \le \|x\|_2$ and the invariance of the spectral norm under orthogonal transformations. For a given $\varepsilon > 0$ and under the assumption $\boldsymbol{\psi}(x,0) = Q(x)e_0$ and $\boldsymbol{\varphi}(x,0) = P(x)e_0$, we can choose $\delta = \varepsilon$ to ensure

$$\|Q-P\|_{L_\infty(\mathbb{R})} < \delta \implies \|\boldsymbol{\psi}(\cdot,t) - \boldsymbol{\varphi}(\cdot,t)\|_{L_\infty(\mathbb{R})} < \varepsilon \quad \forall t \ge 0.$$

□

To conclude this subsection, we want to show that the P_N method preserves the initially entered energy. We first have to translate the energy definition (2.25) into the frame of the P_N method. In doing so, we evaluate (2.25) for the projected radiance $\psi_N \approx \psi$. This gives

$$\begin{aligned}\|\psi_N(\cdot,t)\|^2_{L_2(\Omega\times[-1,1])} &= \int_\Omega \int_{-1}^1 \psi_N^2(x,\mu,t)\,d\mu dx = \int_\Omega \sum_{\ell=0}^N \frac{2\ell+1}{2}\phi_\ell^2(x,t)\,dx \\ &= \frac{1}{2}\int_\Omega \|D\boldsymbol{\phi}(x,t)\|_2^2\,dx = \frac{1}{2}\|D\boldsymbol{\phi}(\cdot,t)\|^2_{L_2(\Omega)}, \quad t \ge 0,\end{aligned}$$

with D being the diagonal matrix from Theorem 3.6. Concerning the integration over $\mu \in [-1,1]$, we have considered the Parseval-like relation

$$\|f_N\|^2_{L_2(-1,1)} = \langle f_N, f_N\rangle_{L_2(-1,1)} = \sum_{\ell=0}^N \frac{2\ell+1}{2} f_\ell^2.$$

Hence, in the light of the P_N method, we introduce the following energy function

$$E(t) := \frac{1}{2}\|D\boldsymbol{\phi}(\cdot,t)\|^2_{L_2(\Omega)} = \frac{1}{2}\|\mathbf{w}(\cdot,t)\|^2_{L_2(\Omega)}, \quad t \ge 0. \tag{3.35}$$

To incorporate this quantity, we multiply both sides of (3.25) with $\mathbf{w}^T$ (which is also of class C^1) followed by an integration over Ω, which results in

$$E'(t) = -\int_\Omega \mathbf{w}^T\Lambda\mathbf{w}_x\,dx = -\frac{1}{2}\int_\Omega \partial_x(\mathbf{w}^T\Lambda\mathbf{w})\,dx = 0.$$

The last conclusion is due to the zero BC (3.12). That is, for all $x \in \partial\Omega$, we have

$$(\mathbf{w}^T\Lambda\mathbf{w})(x,t) = (\boldsymbol{\phi}^T D J_{N+1} D\boldsymbol{\phi})(x,t) = 0 \quad \forall t \ge 0,$$

where $DJ_{N+1}D$ has the same structure as J_{N+1} from Theorem 3.6. Therefore, the P_N method under the zero BCs (3.12) is a conservative scheme with

$$E(t) = E(0) = \frac{1}{2}\|D\boldsymbol{\phi}(\cdot,0)\|^2_{L_2(\Omega)} = \frac{1}{2}\int_\Omega Q^2(x)\,dx \quad \forall t \ge 0,$$

which agrees (for all orders $N \ge 1$) with the exact transport theory value (2.26). At this stage, we also note on the article [27], dealing with the convergence of the P_N method to the solution of the RTE (2.6) under reflective BCs. After this excursus on the P_N equations in lossless media, we continue with the derivation of the SP_N equations.

3.3 Derivation of the time-dependent SP_N equations

The SP_N equations in time-domain are obtained from the P_N equations (3.10) by neglecting the time derivatives applied to the odd moments [9, 13, 14]. It is important to note that this does not insinuate odd moments of the form $\phi_\ell(x,t) = \phi_\ell(x)$. The main motivation for this simplification is due to the difficulty in solving the hyperbolic P_N equations and the breakdown of the classical diffusion approximation in several situations of high practical importance. Thus, the SP_N method yields a compromise between accuracy and computational effort [15]. There are also physical reasons for neglecting the time derivatives of the odd moments. For example, in the field of biomedical optics, there is the assumption that the (relative) change of the odd moments within a characteristic time is very small [9]. For reactor core analysis, it is assumed that the time variation of the odd moments is much smaller than the spatial variation of the even moments, see for example [13]. In the case of the classical diffusion approximation, we get under the assumption $\partial_t \phi_1 \approx 0$ from the second P_1 equation of the system (3.13) the well-known Fick's law

$$-\kappa \partial_x \phi_0(x,t) = \phi_1(x,t) + \frac{1}{\mu_s}\partial_t \phi_1(x,t) \approx \phi_1(x,t), \tag{3.36}$$

where the first moment $\phi_1(x,t) = \int_{-1}^{1} \psi(x,\mu,t)\mu \, d\mu$ represents the diffuse flux. In this context, we also refer to [20, Chapter 3] for some historical aspects on Fick's law. The neglect of the time derivative regarding the odd moments can therefore be seen as a generalization of the assumption made in (3.36). Of course, the removal of certain time derivatives does not remain without consequences, especially at short times. However, when the data at early times are negligible, this does not represent a serious limitation. In the publication [9], the authors mentioned the parabolic nature of the SP_N equations without any concrete verification. Let us continue with the classification of the SP_N equations in the sense of the characteristics and with finding out the consequences of the missing time derivatives.

Proposition 3.11. *The characteristics of the SP_N equations are given by the lines $t =$ const. in the xt-plane.*

Proof. We can start as in the proof of Proposition 3.8. In view of the Cauchy data, we adopt equations (3.26) and (3.27). To enable a smooth transition from the hyperbolic P_N equations to the desired simplified system, we replace (3.28) by the following ϵ-dependent P_N equations

$$I_\epsilon \boldsymbol{\phi}_t(x,t(x)) + A\boldsymbol{\phi}_x(x,t(x)) = -\Sigma\,\boldsymbol{\gamma}(x), \quad x \in J, \tag{3.37}$$

where $I_\epsilon := \operatorname{diag}(1,\epsilon,1,\epsilon,\ldots,1,\epsilon) \in \mathbb{R}^{N+1,N+1}$. Thus, we have scaled the time derivative of the odd moments with the parameter $\epsilon \in [0,1]$. The resulting system of linear equations becomes

$$(t'(x)A - I_\epsilon)\boldsymbol{\phi}_t(x,t(x)) = A\boldsymbol{\gamma}'(x) + \Sigma\,\boldsymbol{\gamma}(x),$$

which looks nearly like (3.29). As before, the characteristics are found by setting the determinant equal to zero. The use of the product rule for determinants leads to[3]

$$\det(t'(x)A - I_\epsilon) = \det(t'(x)A - \sqrt{\epsilon}I) = \prod_{j=0}^{\frac{N-1}{2}} \left[\epsilon - \left(t'(x)\lambda_j\right)^2\right] = 0.$$

[3] In this context, we note on the factorization

$$t'A - I_\epsilon = \frac{1}{\sqrt{\epsilon}} I_{\sqrt{\epsilon}}(t'A - \sqrt{\epsilon}I)I_{\sqrt{\epsilon}} \quad \forall \epsilon \in (0,1].$$

The characteristics to the scaled P_N equations (3.37) turn out to be

$$t(x) = \frac{\pm\sqrt{\epsilon}}{\lambda_j} x + \text{const.} \quad \text{for} \quad j = 0, \ldots, \frac{N-1}{2}.$$

Thus, for $\epsilon \to 0$, we arrive at the SP_N equations that exhibit horizontal characteristics. □

We see that the removal of the time derivatives applied to the odd moments transfers the hyperbolic P_N equations (3.11) into a parabolic system. The SP_N equations in first order form, that is $I_0\boldsymbol{\phi}_t + A\boldsymbol{\phi}_x + \Sigma\boldsymbol{\phi} = 0$ ($\epsilon = 0$), are typically converted into a system of $(N+1)/2$ coupled diffusion-like equations. This reformulation can be done as follows. By selecting an arbitrary equation from (3.10) for ℓ odd and the neglect of $\partial_t \phi_\ell$ gives

$$\frac{\ell}{2\ell+1}\frac{\partial \phi_{\ell-1}}{\partial x} + \frac{\ell+1}{2\ell+1}\frac{\partial \phi_{\ell+1}}{\partial x} + \mu_s \phi_\ell = 0.$$

Solving this equation for the odd moment ϕ_ℓ results in

$$\phi_\ell = -\frac{1}{\mu_s}\left(\frac{\ell}{2\ell+1}\frac{\partial \phi_{\ell-1}}{\partial x} + \frac{\ell+1}{2\ell+1}\frac{\partial \phi_{\ell+1}}{\partial x}\right). \tag{3.38}$$

Next, we replace all odd moments occurring in the ℓth P_N equation (ℓ even) of the system (3.10) by the expression (3.38). The resulting second order form becomes

$$\begin{aligned}
\frac{\partial \phi_0}{\partial t} =& \frac{1}{3\mu_s}\frac{\partial^2 \phi_0}{\partial x^2} + \frac{2}{3\mu_s}\frac{\partial^2 \phi_2}{\partial x^2} \\
\frac{\partial \phi_\ell}{\partial t} =& \frac{1}{\mu_s}\frac{\ell(\ell-1)}{(2\ell+1)(2\ell-1)}\frac{\partial^2 \phi_{\ell-2}}{\partial x^2} + \frac{1}{\mu_s}\frac{1}{2\ell+1}\left(\frac{\ell^2}{2\ell-1} + \frac{(\ell+1)^2}{2\ell+3}\right)\frac{\partial^2 \phi_\ell}{\partial x^2} \\
&+ \frac{1}{\mu_s}\frac{(\ell+1)(\ell+2)}{(2\ell+1)(2\ell+3)}\frac{\partial^2 \phi_{\ell+2}}{\partial x^2} - \mu_s \phi_\ell \quad \text{for} \quad \ell = 2, 4, \ldots, N-1
\end{aligned} \tag{3.39}$$

for $(x,t) \in \Omega \times \mathbb{R}_+$ and the moments $\phi_\ell \in C^{2,1}(\Omega \times \mathbb{R}_+)$ with $\phi_{N+1} = 0$. In view of the initial condition, we have $\phi_\ell(x,0) = Q(x)\delta_{\ell 0}$ for $x \in \Omega$ and $\ell = 0, 2, \ldots, N-1$. By defining the vector-valued function $\boldsymbol{\psi} := (\phi_0, \phi_2, \ldots, \phi_{N-1})^T$, we can write (3.39) schematically as vectorial diffusion equation

$$\boldsymbol{\psi}_t + S\boldsymbol{\psi} = \mathcal{D}\boldsymbol{\psi}_{xx}, \quad x \in \Omega,\ t > 0. \tag{3.40}$$

Remark 3.12. The characteristics to the SP_N equations can also be obtained from the second order form (3.40). In that case, we have to look for curves on which the determination of the second order derivatives becomes impossible. Suppose that $\boldsymbol{\psi}$ and its first derivatives have already been fixed by the prescribed Cauchy data and available in the form

$$\boldsymbol{\psi}(x, t(x)) = \boldsymbol{\alpha}(x), \quad \boldsymbol{\psi}_x(x, t(x)) = \boldsymbol{\beta}(x) \quad \text{and} \quad \boldsymbol{\psi}_t(x, t(x)) = \boldsymbol{\gamma}(x).$$

By differentiating the latter two conditions with respect to the curve parameter and incorporating equation (3.40) results in the linear system

$$\begin{pmatrix} \mathcal{D} & 0 & 0 \\ I & t'(x)I & 0 \\ 0 & I & t'(x)I \end{pmatrix} \begin{pmatrix} \boldsymbol{\psi}_{xx}(x, t(x)) \\ \boldsymbol{\psi}_{xt}(x, t(x)) \\ \boldsymbol{\psi}_{tt}(x, t(x)) \end{pmatrix} = \begin{pmatrix} S\boldsymbol{\alpha}(x) + \boldsymbol{\gamma}(x) \\ \boldsymbol{\beta}'(x) \\ \boldsymbol{\gamma}'(x) \end{pmatrix}.$$

Suppose that $\det \mathcal{D} \neq 0$. Then, the second order derivatives can be determined in all cases if $t' \neq 0$. On the other side, if $t' = 0$, we see that $\boldsymbol{\psi}_{tt}$ remains completely undetermined. All in all we again find $t = \text{const.}$ as characteristics.

The BCs to the derived SP_N equations (3.39) respective (3.40) can be found under the use of the condition (3.12) in combination with the relation (3.38). That is, for $x \in \partial\Omega$, the left-hand side of (3.38) becomes zero. The resulting homogeneous system (with an upper bidiagonal matrix) has only the trivial solution, yielding the Neumann-type condition

$$\boldsymbol{\psi}_x(x,t) = 0 \quad \forall (x,t) \in \partial\Omega \times [0,\infty), \tag{3.41}$$

that belongs to the system (3.40).

Example 3.13. Let us consider the SP_1 equation[4] on $\Omega = (0,L)$ for the $2L$-periodic source distribution (2.19) with $Q'(0) = Q'(L) = 0$. From (3.39) we get for $N = 1$

$$\frac{\partial \phi_0}{\partial t} = \kappa \frac{\partial^2 \phi_0}{\partial x^2}, \quad x \in \Omega,\ t > 0, \tag{3.42}$$

subject to $\phi_0(x,0) = Q(x)$ for $x \in \Omega$ and $\kappa = 1/(3\mu_s)$. The corresponding Neumann BCs are given by $\partial_x \phi_0(0,t) = \partial_x \phi_0(L,t) = 0$ for all $t \geq 0$. This problem has a unique solution, see for example [31, pp. 48–51], with representation

$$\phi_0(x,t) = \sum_{n=0}^{\infty} \frac{2-\delta_{n0}}{L} q_n e^{-\kappa\omega_n^2 t} \cos(\omega_n x), \quad x \in \overline{\Omega},\ t \geq 0, \tag{3.43}$$

where $\omega_n := n\pi/L$. It belongs to $C^\infty(\overline{\Omega} \times (0,\infty)) \cap C(\overline{\Omega} \times [0,\infty))$. We also recall the fundamental solution to (3.42) on $\Omega = \mathbb{R}$ that is given by the heat kernel (2.8).

Now we turn our attention to the SP_3 equations, which represent the next higher approximation over the standard heat (SP_1) equation. The following Section 3.4 contains the main results of this thesis.

3.4 The time-dependent SP_3 equations

We now consider the time-dependent SP_N equations for the order $N = 3$. That is

$$\boldsymbol{\psi}_t + S\boldsymbol{\psi} = \mathcal{D}\boldsymbol{\psi}_{xx}, \quad x \in \Omega,\ t > 0, \tag{3.44}$$

where $\boldsymbol{\psi} = (\phi_0, \phi_2)^T$ and the matrices associated with this system are given by

$$\mathcal{D} = \begin{pmatrix} d_{11} & d_{12} \\ d_{21} & d_{22} \end{pmatrix} = \begin{pmatrix} \dfrac{1}{3\mu_s} & \dfrac{2}{3\mu_s} \\ \dfrac{2}{15\mu_s} & \dfrac{11}{21\mu_s} \end{pmatrix} \quad \text{and} \quad S = \begin{pmatrix} 0 & 0 \\ 0 & \mu_s \end{pmatrix}. \tag{3.45}$$

We furthermore assume $\mu_s > 0$ and the corresponding initial condition reads

$$\boldsymbol{\psi}(x,0) = \begin{pmatrix} Q(x) \\ 0 \end{pmatrix}, \quad x \in \Omega. \tag{3.46}$$

We consider both the infinite medium $\Omega = \mathbb{R}$ and the finite domain $\Omega = (0,L)$ under the Neumann-type condition (3.41). A vector-valued function $\boldsymbol{\psi} \in C^{2,1}(\Omega \times \mathbb{R}_+, \mathbb{R}^2)$ that satisfies (3.44) and (3.46) can be considered as a classical solution to the time-dependent SP_3 equations. We also remind at this stage on the absorption and the speed of light in the medium. Both can be readily incorporated afterwards according to $ce^{-\mu_a ct}\boldsymbol{\psi}(x,ct)$.

[4] This is nothing other than the well-known heat equation (diffusion equation without absorption).

3.4.1 Considerations in the infinite medium

This subsection is primarily intended as preparation for the next Subsection 3.4.2, in which we will incorporate some of the results obtained for the infinite medium. In the present case of an unbounded domain, some caution is required when it comes to the question of well-posedness. Without a boundedness condition on the solution, the classical heat equation $u_t = u_{xx}$ on $\Omega = \mathbb{R}$ is solved by $u = 0$ and also by the (unbounded) candidate

$$u(x,t) = \sum_{k=0}^{\infty} \frac{g^{(k)}(t)}{(2k)!} x^{2k} \quad \text{with} \quad g(t) = \begin{cases} e^{-1/t^2} & \text{for } t > 0, \\ 0 & \text{for } t = 0, \end{cases}$$

which we have adopted from [36, p. 145]. Moreover, in both cases we have $u(x,0) = 0$ for $x \in \mathbb{R}$. Thus, there are (at least) two possible solutions to the same initial value problem. According to the textbook [41, Section 3.4], uniqueness can be guaranteed by requiring additionally an exponential boundedness condition. It can be expected that the same sort of solutions will also be present when dealing with the SP_3 equations on $\Omega = \mathbb{R}$. We therefore omit the well-posedness issue in the case of the infinite medium. Regarding the more realistic case of a bounded domain (cf. Subsection 3.4.2), we verify in detail the existence of a classical solution, its uniqueness as well as the continuous dependence on the initial data. Let us continue with the derivation of a formal solution to the SP_3 equations (3.44) by making use of the Fourier transform formalism. In doing so, we multiply both sides of (3.44) and (3.46) with e^{-ikx}, followed by an integration over $\mathbb{R}$. In this context, we assume $Q \in L_1(\mathbb{R})$ which implies $\hat{Q} = \mathcal{F}(Q) \in C_0(\mathbb{R})$, cf. Remark 2.8. The consideration of the differentiation property (2) from Proposition 2.9 leads in Fourier space to the Cauchy problem

$$\hat{\boldsymbol{\psi}}_t + A\hat{\boldsymbol{\psi}} = 0, \quad k \in \mathbb{R},\, t > 0, \tag{3.47}$$

where $\hat{\boldsymbol{\psi}} = (\hat{\phi}_0, \hat{\phi}_2)^T = \mathcal{F}(\boldsymbol{\psi})$ and $\hat{\boldsymbol{\psi}}(k,0) = (\hat{Q}(k), 0)^T$ for $k \in \mathbb{R}$. The time-independent coefficient matrix is given by

$$A(k) := S + k^2\mathcal{D} = \begin{pmatrix} d_{11}k^2 & d_{12}k^2 \\ d_{21}k^2 & d_{22}k^2 + \mu_s \end{pmatrix} \in \mathbb{R}^{2,2}. \tag{3.48}$$

Thus, we have converted the SP_3 equations (3.44) into a first order system with constant coefficients. From the theory of ordinary differential equations, it is known that (3.47) admits a unique solution. It can be given in terms of the matrix exponential, similar as in the case of the Cauchy problem (3.31). Setting $A = U\mathrm{diag}(\lambda_1, \lambda_2)U^{-1}$ enables us to write

$$\hat{\boldsymbol{\psi}}(k,t) = e^{-At}\begin{pmatrix} \hat{Q} \\ 0 \end{pmatrix} = U\begin{pmatrix} e^{-\lambda_1 t} & 0 \\ 0 & e^{-\lambda_2 t} \end{pmatrix} U^{-1}\begin{pmatrix} \hat{Q} \\ 0 \end{pmatrix}, \quad k \in \mathbb{R},\, t \geq 0. \tag{3.49}$$

The required eigenvalues and eigenvectors can be given explicitly by starting with the roots of the characteristic polynomial

$$\det(A - \lambda I) = \lambda^2 - \left(\mu_s + \frac{6k^2}{7\mu_s}\right)\lambda + \frac{3k^4}{35\mu_s^2} + \frac{k^2}{3} = 0.$$

This quadratic equation exhibits real-valued solutions of the form $\lambda_1 = p + q$ and $\lambda_2 = p - q$ with

$$p(k) := \frac{3k^2}{7\mu_s} + \frac{\mu_s}{2} \quad \text{and} \quad q(k) := \sqrt{\frac{24k^4}{245\mu_s^2} + \frac{2k^2}{21} + \frac{\mu_s^2}{4}}.$$

Concerning the asymptotic stability, it is worth to mention that both eigenvalues are non-negative. Otherwise, the moments in Fourier space would grow exponentially as $t \to \infty$.

The positivity of λ_1 is evident because p and q are both positive real numbers. In view of λ_2, Vieta's formula gives

$$\lambda_1\lambda_2 = \frac{3k^4}{35\mu_s^2} + \frac{k^2}{3} \geq 0 \quad \Longrightarrow \quad \lambda_2 \geq 0.$$

The eigenvectors follow as solution of $(A - \lambda_j I)u_j = 0$ $(j = 1, 2)$, which leads to

$$u_1 = \begin{pmatrix} d_{12}k^2 \\ \lambda_1 - d_{11}k^2 \end{pmatrix}, \qquad u_2 = \begin{pmatrix} d_{12}k^2 \\ \lambda_2 - d_{11}k^2 \end{pmatrix}.$$

The moments (3.49) can be given in the form $\hat{\boldsymbol{\psi}}(k,t) = \hat{Q}(k)\hat{\mathbf{G}}(k,t)$, with

$$\begin{aligned} \hat{G}_0(k,t) &= \frac{1+h(k)}{2}e^{-\lambda_2(k)t} + \frac{1-h(k)}{2}e^{-\lambda_1(k)t}, \\ \hat{G}_2(k,t) &= \frac{k^2}{15\mu_s}\frac{e^{-\lambda_1(k)t} - e^{-\lambda_2(k)t}}{q(k)}, \end{aligned} \tag{3.50}$$

and $h(k) := \left(\frac{2k^2}{21\mu_s} + \frac{\mu_s}{2}\right)/q(k)$. We note that the moments $\hat{G}_j$ correspond to the source $\hat{Q} = 1 = \mathcal{F}(\delta)$. As a composition of elementary functions, they are smooth. Let us derive at this stage two useful estimates. In view of $\hat{G}_0$, we have introduced in (3.50) the even function h, which takes the values $h(0) = 1$ and $h(\pm\infty) = \sqrt{30}/18 \approx 0.304 < 1$. The first derivative satisfies

$$h'(k) = -\frac{4}{45\mu_s}\frac{k^3}{(q(k))^3} \leq 0 \quad \forall k \geq 0.$$

We therefore obtain $h(\mathbb{R}) = (\sqrt{30}/18, 1]$ and the upper bound

$$\hat{G}_0(k,t) \leq e^{-\lambda_2(k)t}\left(\frac{1+h(k)}{2} + \frac{1-h(k)}{2}\right) = e^{-\lambda_2(k)t}, \tag{3.51}$$

for all $k \in \mathbb{R}$ and $t \geq 0$, where we have used $e^{-\lambda_1(k)t} \leq e^{-\lambda_2(k)t}$. The eigenvalue λ_2 can be estimated under the use $\sqrt{\frac{24}{245}} > \frac{2}{21}$, yielding

$$\left(\sqrt{\frac{24}{245}}\frac{k^2}{\mu_s} + \frac{\mu_s}{2}\right)^2 = \frac{24k^4}{245\mu_s^2} + \frac{2}{7}\sqrt{\frac{6}{5}}k^2 + \frac{\mu_s^2}{4} \geq (q(k))^2 \quad \forall k \in \mathbb{R}.$$

With this result, we deduce for all $k \in \mathbb{R}$

$$\lambda_2(k) = p(k) - q(k) \geq p(k) - \left(\frac{2}{7}\sqrt{\frac{6}{5}}\frac{k^2}{\mu_s} + \frac{\mu_s}{2}\right) = ak^2,$$

where $a := \left(\frac{3}{7} - \frac{2}{7}\sqrt{\frac{6}{5}}\right)/\mu_s \approx 0.116/\mu_s$ has the meaning of a diffusion constant. Notice that $a \in \sigma(\mathcal{D})$ is just the smaller eigenvalue of the diffusion matrix $\mathcal{D}$ from (3.45). Hence, (3.51) becomes

$$\hat{G}_0(k,t) \leq e^{-\lambda_2(k)t} \leq e^{-ak^2t} \quad \forall (k,t) \in \mathbb{R} \times [0,\infty), \tag{3.52}$$

where equality arises for $k = 0$ or $t = 0$. In view of the second moment $\hat{G}_2$, we note on

$$0 \leq \frac{1}{15\mu_s}\frac{k^2}{q(k)} < \frac{7}{6\sqrt{30}} \quad \forall k \in \mathbb{R}.$$

Thus, we get for $k \in \mathbb{R}$ and $t \geq 0$ the upper bound

$$|\hat{G}_2(k,t)| = \frac{k^2}{15\mu_s} \frac{e^{-\lambda_2(k)t} - e^{-\lambda_1(k)t}}{q(k)} \leq \frac{7}{6\sqrt{30}} e^{-ak^2 t}. \tag{3.53}$$

With these relations on hand we can show two things. Concerning the zero order moment (fluence) in space domain, we have (notice that $\hat{G}_0$ is non-negative)

$$|G_0(x,t)| \leq \frac{1}{2\pi} \int_{\mathbb{R}} \hat{G}_0(k,t) |e^{ikx}| \, dk = G_0(0,t) \leq \frac{1}{\pi} \int_0^\infty e^{-ak^2 t} \, dk = \frac{1}{\sqrt{4\pi a t}}, \tag{3.54}$$

for all $x \in \mathbb{R}$ and $t > 0$. Thus, the fluence in SP_3 approximation due to a δ-source can be uniformly bounded by a square root function, similar as the classical heat kernel (2.8). Secondly, we have for all $t > 0$ and $m \in \mathbb{N}_0$

$$\int_{\mathbb{R}} |\hat{G}_j(k,t) k^m| \, dk \leq 2 \int_0^\infty k^m e^{-\lambda_2(k)t} \, dk \leq 2 \int_0^\infty k^m e^{-ak^2 t} \, dk = \frac{\Gamma\left(\frac{m+1}{2}\right)}{(at)^{\frac{m+1}{2}}},$$

with Γ denoting the gamma function [2, p. 242]. This result has a direct consequence on the smoothness in real space. It can be shown that $k^m \hat{f}(k) \in L_1(\mathbb{R})$ implies $f^{(r)} \in C_0(\mathbb{R})$ for $r = 0, 1, \ldots, m$, see for example [42, Theorem 9.2.13]. The moments in real space can be (formally) reconstructed by means of the inverse Fourier transform

$$\boldsymbol{\psi}(x,t) = \frac{1}{2\pi} \int_{-\infty}^{\infty} \hat{\boldsymbol{\psi}}(k,t) e^{ikx} \, dk, \quad x \in \mathbb{R}, \, t \geq 0. \tag{3.55}$$

For an even source distribution $\hat{Q}(-k) = \hat{Q}(k)$, the inverse (3.55) reduces to a Fourier cosine transform. In particular, in the case of a δ-source when $\hat{Q} = 1$, we get for $x \in \mathbb{R}$ and $t > 0$

$$G_j(x,t) = \frac{1}{\pi} \int_0^\infty \hat{G}_j(k,t) \cos(kx) \, dk, \quad j = 0, 2. \tag{3.56}$$

Notice that $\hat{G}_j$ $(j = 0, 2)$ are the moments from (3.50). There is an interesting result on the SP_N equations, which coincides with the famous Einstein formula $\langle x^2 \rangle(t) = 2\kappa t$ for the mean-square displacement in the theory of Brownian motion. For more information on this topic, we refer to the textbook [43].

Proposition 3.14. *The second-order moment $\langle x^2 \rangle(t) = \int_{\mathbb{R}} x^2 G_0(x,t) \, dx$ for $t \geq 0$ of the fluence to the SP_N equations on $\Omega = \mathbb{R}$ caused by a δ-source agrees for all orders $N \geq 1$ with Einstein's formula for the mean-square displacement.*

Proof. Based on the differentiation property (2) from Proposition 2.9, it is not difficult to deduce the relation $\mathcal{F}(x^n f(x))(k) = i^n \frac{d^n}{dk^n} \hat{f}(k)$. Using this for $n = 2$ and setting $k = 0$ gives for the second order moment $\langle x^2 \rangle(t) = -\partial_k^2 \hat{G}_0(0,t)$ for $t \geq 0$. To find the required derivative at $k = 0$, we consider the SP_N equations (3.40) in Fourier space

$$\hat{\mathbf{G}}_t + (S + k^2 \mathcal{D}) \hat{\mathbf{G}} = 0, \quad \hat{\mathbf{G}}(k,0) = e_0 = (1, 0, \ldots, 0) \in \mathbb{R}^{\frac{N+1}{2}},$$

for $(k,t) \in \mathbb{R} \times \mathbb{R}_+$ and $\hat{\mathbf{G}} = (\hat{G}_0, \hat{G}_2, \ldots, \hat{G}_{N-1})^T$. The corresponding solution can be again given in terms of the matrix exponential. In particular, the zero order moment becomes

$$\hat{G}_0(k,t) = e_0^T \hat{\mathbf{G}}(k,t) = e_0^T e^{-(S + k^2 \mathcal{D})t} e_0, \quad k \in \mathbb{R}, \, t \geq 0.$$

Next, we use the (convergent) Taylor series for the matrix exponential and remind on the diagonal matrix $S = \operatorname{diag}(0, \mu_s, \dots, \mu_s)$. We then obtain the expression

$$\hat{G}_0(k,t) = 1 - \frac{k^2 t}{3\mu_s} + k^4 e_0^T \mathcal{D} \sum_{n=0}^{\infty} (-1)^n t^{n+2} \frac{(S + k^2\mathcal{D})^n}{(n+2)!} \mathcal{D} e_0. \tag{3.57}$$

The use of the difference formula for the second derivative gives

$$\frac{\hat{G}_0(\varepsilon,t) - 2\hat{G}_0(0,t) + \hat{G}_0(-\varepsilon,t)}{\varepsilon^2} = -2\kappa t + 2\varepsilon^2 e_0^T \mathcal{D} \sum_{n=0}^{\infty} (-1)^n t^{n+2} \frac{(S + \varepsilon^2\mathcal{D})^n}{(n+2)!} \mathcal{D} e_0,$$

for a small number $\varepsilon > 0$ and $\kappa = 1/(3\mu_s)$. In the limit $\varepsilon \to 0$, we arrive at Einstein's formula[5]

$$\langle x^2 \rangle(t) = -\partial_k^2 \hat{G}_0(k,t)\Big|_{k=0} = 2\kappa t \quad \forall t \geq 0.$$

□

Remark 3.15. In accordance with the classical heat kernel (2.8), the fluence to the SP_N equations on $\Omega = \mathbb{R}$ caused by a δ-source is normalized according

$$\int_{\mathbb{R}} G_0(x,t)\, dx = \hat{G}_0(0,t) = 1 \quad \forall t \geq 0,$$

for all orders $N \geq 1$. This can be readily verified by setting $k = 0$ in (3.57).

We furthermore want to find the SP_3 fluence (caused by a δ-source) in the long-time limit. It can be found under the use of the Laplace formula (2.17) for $b = \infty$. In this context, we write the zero order moment from (3.56) according to

$$\begin{aligned} G_0(x,t) =& \frac{1}{\pi} \int_0^\infty e^{-\lambda_2(k)t} \frac{1 + h(k)}{2} \cos(kx)\, dk \\ &+ \frac{1}{2\pi} \int_0^\infty e^{-\lambda_1(k)t} \cos(kx)\, dk - \frac{1}{2\pi} \int_0^\infty e^{-\lambda_1(k)t} h(k) \cos(kx)\, dk. \end{aligned}$$

The main contribution for $t \to \infty$ arises from a small environment around $k = 0$, due to the rapid decay of the exponentials. Let us verify the requirements. We have $\lambda_1'(0) = \lambda_2'(0) = 0$, $\lambda_1''(0) = 22/(21\mu_s) > 0$ and $\lambda_2''(0) = 2/(3\mu_s) > 0$. Moreover, λ_1 and λ_2 are both monotonically increasing on $(0,\infty)$ and in all cases the associated function g satisfies $g(0) \neq 0$. Therefore, using formula (2.17), we see that the fluence in SP_3 approximation behaves like

$$G_0(x,t) \sim \frac{1}{\sqrt{4\pi\kappa t}} = H(t) \quad \text{as} \quad t \to \infty, \tag{3.58}$$

which coincides with the exact transport theory fluence at late times, see (2.18). To transmit this exact asymptotic behavior from transport theory to the SP_3 fluence, it was necessary to separate the absorption before neglecting the time derivatives applied to the odd moments. Otherwise, the SP_3 equations would still look like (3.44), but the diffusion matrix (3.45) would depend on absorption, which prevents the convergence to the exact asymptotic value. We note that this is principally the same problematic as in the case of the classical diffusion

[5] Einstein's result approaches the exact transport theory value at late times, see e.g. [44]

$$\frac{2}{3} \frac{\mu_s t - 1 + e^{-\mu_s t}}{\mu_s^2} \Big/ 2\kappa t \sim 1 \quad \text{as} \quad t \to \infty.$$

equation. Here, there is a discussion about the correct treatment of the absorption for almost thirty years, see e.g. [45–48]. We also want to confirm (3.58) by a numerical experiment. For this, we have evaluated G_0 from (3.56) for the time values $t_1 = 10^6$ and $t_2 = 10^9$. Moreover, we have set $x = 1$ and the scattering coefficient is assumed to be $\mu_s = 0.5$. As a result, we find the numerical values

$$\frac{G_0(1,t_1)}{H(t_1)} = 1.000000825000392 \quad \text{and} \quad \frac{G_0(1,t_2)}{H(t_2)} = 1.000000000824997.$$

We note that these ratios are independent of the absorption, because the exponential factor $e^{-\mu_a t}$ cancels out. We finally want to provide a fourth order formulation to the SP_3 equations. It can found from system (3.44) by eliminating the moment ϕ_2 and by adding a second initial condition. The latter requirement follows directly from the first equation of (3.44) and reads

$$\partial_t \phi_0(x,0) = \frac{1}{3\mu_s}\partial_x^2 \phi_0(x,0) + \frac{2}{3\mu_s}\partial_x^2 \phi_2(x,0) = \frac{Q''(x)}{3\mu_s},$$

for $x \in \mathbb{R}$. The resulting fourth order formulation for the fluence $\phi_0 \in C^{4,2}(\mathbb{R} \times \mathbb{R}_+)$ can then be written in the form

$$\frac{\partial^2 \phi_0}{\partial t^2} + \mu_s \frac{\partial \phi_0}{\partial t} = \frac{1}{3}\frac{\partial^2 \phi_0}{\partial x^2} + \frac{6}{7\mu_s}\frac{\partial^3 \phi_0}{\partial t \partial x^2} - \frac{3}{35\mu_s^2}\frac{\partial^4 \phi_0}{\partial x^4}, \quad x \in \mathbb{R},\, t > 0, \tag{3.59}$$

subject to $\phi_0(x,0) = Q(x)$ and $\partial_t \phi_0(x,0) = Q''(x)/(3\mu_s)$ for $x \in \mathbb{R}$. Compared with the classical heat equation, this higher order model contains a coupling between the space and time variable in form of a mixed partial derivative. If we assume for a moment that integration and differentiation would be interchangeable, then it can be verified that ϕ_0 from (3.55) satisfies equation (3.59). In the next subsection, we will apply the finite cosine transform (FCT) in order to solve the SP_3 equations on a bounded domain.

3.4.2 Solution for a bounded domain via the FCT

We now employ the SP_3 equations (3.44) as a simplified transport model on the finite domain $\Omega = (0, L)$ with reflecting boundaries. As shown above, reflective BCs correspond in the frame of the SP_N methodology with the Neumann-type conditions (3.41). Hence, we consider the SP_3 equations (3.44) subject to

$$\boldsymbol{\psi}_x(0,t) = \boldsymbol{\psi}_x(L,t) = 0 \quad \forall t \geq 0. \tag{3.60}$$

In view oft the initial condition (3.46), we assume throughout this subsection the compatibility condition $Q'(0) = Q'(L) = 0$ and that Q is representable on $\overline{\Omega}$ in form of the uniformly convergent cosine series (2.19). Considered on the entire space, Q represents an even and $2L$-periodic function. Similar as for the classical heat equation, it would be possible to seek for separable solutions. Let us briefly discuss this method on hand of the separation ansatz $\phi_j(x,t) := X_j(x)T_j(t)$ $(j = 0, 2)$. Inserting this into the SP_3 equations (3.44) results in

$$\begin{pmatrix} X_0 T_0' \\ X_2 T_2' \end{pmatrix} + S \begin{pmatrix} X_0 T_0 \\ X_2 T_2 \end{pmatrix} = \mathcal{D} \begin{pmatrix} X_0'' T_0 \\ X_2'' T_2 \end{pmatrix}, \quad x \in \Omega,\, t > 0. \tag{3.61}$$

In contrast to the classical heat equation, we are not able to perform the separation directly. We therefore divide the first equation by T_2 and the second one by T_0. After that, we

additionally apply on the obtained equations the partial derivative with respect to t. We then get the following separated equations

$$\begin{aligned} 3\mu_s \frac{(T_0'/T_2)'}{(T_0/T_2)'} &= \frac{X_0''}{X_0} = -\omega^2, \\ \frac{21\mu_s}{11} \frac{((T_2' + \mu_s T_2)/T_0)'}{(T_2/T_0)'} &= \frac{X_2''}{X_2} = -\eta^2. \end{aligned} \tag{3.62}$$

By the homogeneous Neumann conditions (3.60), we find for the unknown separation constants the discrete values $\omega_k = \eta_k = k\pi/L$ with $k \in \mathbb{N}_0$. Furthermore, the appropriate eigenfunctions have the form $X_{j,k}(x) = \alpha_{j,k} \cos(\omega_k x)$ $(j = 0, 2)$. To find the corresponding time-dependent factors $T_{j,k}$, we insert the obtained eigenfunctions into (3.61) and get for each $k \in \mathbb{N}_0$ a condition of the form

$$\frac{d}{dt} \begin{pmatrix} \alpha_{0,k} T_{0,k} \\ \alpha_{2,k} T_{2,k} \end{pmatrix} + A_k \begin{pmatrix} \alpha_{0,k} T_{0,k} \\ \alpha_{2,k} T_{2,k} \end{pmatrix} = \begin{pmatrix} 0 \\ 0 \end{pmatrix}, \quad t > 0, \tag{3.63}$$

where $A_k := A(\omega_k)$ is the matrix from (3.48). The general solution to (3.63) is given by

$$\begin{pmatrix} \alpha_{0,k} T_{0,k}(t) \\ \alpha_{2,k} T_{2,k}(t) \end{pmatrix} = e^{-A_k t} \boldsymbol{\beta}_k, \quad k \in \mathbb{N}_0,\ t \geq 0,$$

with $\boldsymbol{\beta}_k = (\beta_{0,k}, \beta_{2,k})^T$ being an arbitrary constant vector. Multiplying both sides of this expression by $\cos(\omega_k x)$ results in the eigensolutions

$$\boldsymbol{\psi}_k(x,t) = \begin{pmatrix} T_{0,k}(t) X_{0,k}(x) \\ T_{2,k}(t) X_{2,k}(x) \end{pmatrix} = e^{-A_k t} \boldsymbol{\beta}_k \cos(\omega_k x), \quad k \in \mathbb{N}_0,\ t \geq 0.$$

The general solution to our problem is then obtained via superposition

$$\boldsymbol{\psi}(x,t) = \sum_{k=0}^{\infty} \boldsymbol{\psi}_k(x,t), \quad x \in \overline{\Omega},\ t \geq 0. \tag{3.64}$$

If we consider the cosine series (2.19) as initial condition, we can fix the unknown vector according to

$$\boldsymbol{\beta}_k \overset{!}{=} \frac{2 - \delta_{k0}}{L} \begin{pmatrix} s_k \\ 0 \end{pmatrix}, \quad s_k = \int_0^L Q(x) \cos(\omega x)\, dx, \quad k \in \mathbb{N}_0. \tag{3.65}$$

We omit at this stage the justification of the obtained series solution, because we will do this shortly after we have confirmed (3.64) via the FCT. In the present case of homogeneous Neumann conditions, we will see that using the FCT is a little more convenient than seeking for separable solutions. At the same time, we can use some of the results prepared in the previous subsection. The FCT we are going to consider is defined as follows [29, Definition 10.2.2].

Definition 3.16. The FCT of a piecewise smooth[6] function $f : [0, L] \to \mathbb{R}$ is the sequence $(a_k)_{k \in \mathbb{N}_0} \in \ell^1(\mathbb{N}_0)$ with elements

$$a_k = \int_0^L f(x) \cos(\omega_k x)\, dx, \quad \omega_k = k\pi/L,\ k \in \mathbb{N}_0. \tag{3.66}$$

The inverse relation corresponds with the uniformly convergent cosine series

$$f(x) = \sum_{k=0}^{\infty} \frac{2 - \delta_{k0}}{L} a_k \cos(\omega_k x), \quad x \in [0, L]. \tag{3.67}$$

[6] We denote a function $f \in C(\overline{\Omega})$ as piecewise smooth if it has a piecewise continuous first derivative, see for example [2, pp. 19–20].

As is typical for finite transforms, the FCT exhibits a discrete spectrum. For our purposes, we need the following relations concerning the FCT.

Proposition 3.17. *Let $(a_k)_{k\in\mathbb{N}_0} \in \ell^1(\mathbb{N}_0)$ be the FCT according to (3.66) of a sufficiently smooth function f defined on $[0, L]$. Then, we have*

$$(1) \quad \int_0^L f''(x)\cos(\omega_k x)\,dx = -\omega_k^2 a_k, \quad f'(0) = f'(L) = 0,\ f \in C^2[0, L],$$

$$(2) \quad \int_0^L f^2(x)\,dx = \sum_{k=0}^{\infty} \frac{2-\delta_{k0}}{L} a_k^2, \quad f \text{ piecewise smooth.}$$

Proof. The differentiation property (1) results from integration by parts. The Parseval relation (2) can be obtained by multiplying both sides of (3.67) with $f(x)$ followed by an integration over $(0, L)$, which leads to

$$\int_0^L f^2(x)\,dx = \sum_{k=0}^{\infty} \frac{2-\delta_{k0}}{L} a_k \int_0^L f(x)\cos(\omega_k x)\,dx = \sum_{k=0}^{\infty} \frac{2-\delta_{k0}}{L} a_k^2.$$

We note that term-by-term integration is allowed due to the uniform convergence. □

We now can proceed as for the unbounded domain. That is, we multiply both sides of the system (3.44) by $\cos(\omega_k x)$ ($k \in \mathbb{N}_0$), followed by an integration over Ω. At the same time, we make use of the differentiation property (1) from Proposition 3.17 under consideration of the homogeneous BCs (3.60). As a result, we obtain the Cauchy problem

$$\boldsymbol{\psi}_k'(t) + A_k \boldsymbol{\psi}_k(t) = 0, \quad k \in \mathbb{N}_0,\ t > 0, \tag{3.68}$$

with $\boldsymbol{\psi}_k(0) = (s_k, 0)^T$ for $k \in \mathbb{N}_0$. Thus, we have obtained practically the same initial value problem as in (3.47). Hence, the corresponding solution can be given in the form

$$\boldsymbol{\psi}_k(t) = \begin{pmatrix} \phi_{0,k}(t) \\ \phi_{2,k}(t) \end{pmatrix} = s_k \begin{pmatrix} G_{0,k}(t) \\ G_{2,k}(t) \end{pmatrix} = s_k \mathbf{G}_k(t), \quad k \in \mathbb{N}_0,\ t \geq 0, \tag{3.69}$$

where $G_{j,k}(t) := \hat{G}_j(\omega_k, t)$ and $\hat{G}_j$ ($j = 0, 2$) are adopted from (3.50). The inverse FCT (3.67) applied to the function sequence $(\boldsymbol{\psi}_k)_{k\in\mathbb{N}_0}$ is then in agreement with the eigenfunction expansion (3.64). Now it is time to address the well-posedness of the recovered (formal) solution to the SP_3 equations. In doing so, we start with an energy analysis.

Lemma 3.18. *Let $(\boldsymbol{\psi}_k)_{k\in\mathbb{N}_0}$ be the function sequence with elements from (3.69). Then, the energy function $E : [0, \infty) \to [0, \infty)$ defined by*

$$E(t) := \sum_{k=0}^{\infty} \frac{2-\delta_{k0}}{2L} \|D_e \boldsymbol{\psi}_k(t)\|_2^2 = \frac{1}{2} \|D_e \boldsymbol{\psi}(\cdot, t)\|_{L_2(\Omega)}^2, \tag{3.70}$$

with $D_e := \operatorname{diag}(1, \sqrt{5})$ and $E(0) = \frac{1}{2}\int_0^L (Q(x))^2\,dx$ belongs to $C^1([0, \infty))$ and satisfies the relation $0 \leq E(t) \leq E(0)$ for all $t \geq 0$. In addition, there holds the energy inequality

$$E(t) - E(\infty) \leq (E(0) - E(\infty)) e^{-2\lambda_2(\omega_1)t}, \quad t \geq 0, \tag{3.71}$$

where $E(\infty) = \lim_{t\to\infty} E(t) = s_0^2/(2L)$ and $\omega_1 = \pi/L$.

Proof. We first note that the scaling of the (even) moments with D_e is used to hold a certain similarity to the energy definition (3.35) for the P_N equations. The integral representation on the right-hand side of (3.70) results from the Parseval relation (2) from Proposition 3.17. The function series (3.70) converges uniformly on $[0, \infty)$ due to

$$\|D_e \boldsymbol{\psi}_k(t)\|_2^2 \leq \frac{265}{216} s_k^2 e^{-2a\omega_k^2 t} \leq \frac{265}{216} s_k^2 \quad \forall k \in \mathbb{N}_0,$$

where we have used the estimates (3.52) and (3.53). The series obtained after termwise differentiation still converges uniformly up to $t = 0$. To show this, we consider

$$\frac{1}{2}\frac{d}{dt}\|D_e \boldsymbol{\psi}_k(t)\|_2^2 = -\boldsymbol{\psi}_k(t)^T \tilde{A}_k \boldsymbol{\psi}_k(t), \quad k \in \mathbb{N}_0,\ t \geq 0,$$

where we have used $\boldsymbol{\psi}_k'(t) = -A_k \boldsymbol{\psi}_k(t)$. The matrix $\tilde{A}_k$ is symmetric and looks like

$$\tilde{A}_k := D_e^2 A_k = \begin{pmatrix} \dfrac{\omega_k^2}{3\mu_s} & \dfrac{2\omega_k^2}{3\mu_s} \\ \dfrac{2\omega_k^2}{3\mu_s} & \dfrac{55\omega_k^2}{21\mu_s} + 5\mu_s \end{pmatrix}, \quad k \in \mathbb{N}_0. \tag{3.72}$$

The Cauchy–Schwarz inequality enables for $k \in \mathbb{N}_0$ and $t \geq 0$ the estimate

$$|\boldsymbol{\psi}_k(t)^T \tilde{A}_k \boldsymbol{\psi}_k(t)| \leq \|\tilde{A}_k \boldsymbol{\psi}_k(t)\|_2 \, \|\boldsymbol{\psi}_k(t)\|_2 \leq \|\tilde{A}_k\|_2 \, \|\boldsymbol{\psi}_k(t)\|_2^2 \,. \tag{3.73}$$

The spectral norm of the symmetric matrix $\tilde{A}_k$ equals its spectral radius $\varrho(\tilde{A}_k) = \|\tilde{A}_k\|_2$. The spectral radius itself can be bounded by any compatible matrix norm such as $\varrho(\tilde{A}_k) \leq \|\tilde{A}_k\|_\infty = 5\mu_s + 23\omega_k^2/(7\mu_s)$. Hence, (3.73) becomes for all $k \in \mathbb{N}_0$ and $t \geq 0$

$$|\boldsymbol{\psi}_k(t)^T \tilde{A}_k \boldsymbol{\psi}_k(t)| \leq \frac{1129}{1080}\left(5\mu_s + \frac{23}{7}\frac{\omega_k^2}{\mu_s}\right) s_k^2 e^{-2a\omega_k^2 t} \leq (c_1 + c_2\omega_k^2) s_k^2.$$

It remains to show the convergence of $\sum_{k=1}^{\infty} (\omega_k s_k)^2$. By assumption, Q' is piecewise continuous and the Fourier coefficients of $Q \in C(\overline{\Omega})$ can be reformulated via integration by parts. That is

$$s_k = -\frac{1}{\omega_k}\int_0^L Q'(x)\sin(\omega_k x)\,dx = -\frac{\beta_k}{\omega_k} \quad \forall k \in \mathbb{N}.$$

The coefficients of a piecewise continuous function satisfy Bessel's inequality [2, p. 56]. Hence, in view of $\beta_k := \int_0^L Q'(x)\sin(\omega_k x)\,dx$, we get

$$\sum_{k=1}^{M} \beta_k^2 \leq \frac{L}{2}\int_0^L (Q'(x))^2\,dx < \infty \quad \forall M \in \mathbb{N}.$$

Due to $|\beta_k| = |\omega_k s_k|$, we deduce $\sum_{k=1}^{\infty}(\omega_k s_k)^2 = \sum_{k=1}^{\infty}\beta_k^2 < \infty$. Thus, term-by-term differentiation of the energy series (3.70) is permissible and leads to the continuous function

$$E'(t) = -\frac{2}{L}\sum_{k=1}^{\infty} \boldsymbol{\psi}_k(t)^T \tilde{A}_k \boldsymbol{\psi}_k(t), \quad t \geq 0. \tag{3.74}$$

The leading principal minors of $\tilde{A}_k$ for $k \in \mathbb{N}$ satisfy $\omega_k^2/(3\mu_s) > 0$ and

$$\det \tilde{A}_k = \frac{\omega_k^2}{3\mu_s}\left(\frac{55\omega_k^2}{21\mu_s} + 5\mu_s\right) - \frac{4\omega_k^4}{9\mu_s^2} = \frac{3}{7}\frac{\omega_k^4}{\mu_s^2} + \frac{5\omega_k^2}{3} > 0, \tag{3.75}$$

which means that (3.72) is a positive definite matrix. In view of (3.74), this in turn shows that $E'(t) \leq 0$ and hence $0 \leq E(t) \leq E(0)$ for all $t \geq 0$. The second part, namely the energy inequality (3.71), can be derived from the series (3.74) as follows. We first note on

$$\boldsymbol{\psi}_k(t)^T \tilde{A}_k \boldsymbol{\psi}_k(t) \geq \boldsymbol{\psi}_k(t)^T \tilde{A}_1 \boldsymbol{\psi}_k(t), \quad k \in \mathbb{N},\, t \geq 0.$$

Moreover, we perform the manipulation

$$\tilde{A}_1 = D_e^2 A_1 = D_e^2 [A_1 - \lambda_2(\omega_1) I + \lambda_2(\omega_1) I], \quad \omega_1 = \pi/L,$$

with $\lambda_2(\omega_1) = p(\omega_1) - q(\omega_1)$ being the smaller eigenvalue of the matrix $A_1 = A(\omega_1)$ from (3.48) with property $\lambda_2(\omega_1) \leq \lambda_2(\omega_k)$ for all $k \in \mathbb{N}$. With these relations on hand, we deduce from (3.74) after some smaller rearrangements the following differential inequality

$$E'(t) + 2\lambda_2(\omega_1) E(t) \leq 2\lambda_2(\omega_1) E(\infty) - \frac{2}{L} \sum_{k=1}^{\infty} \boldsymbol{\psi}_k(t)^T [\tilde{A}_1 - \lambda_2(\omega_1) D_e^2] \boldsymbol{\psi}_k(t).$$

Note that $E(\infty) = s_0^2/(2L)$ is the first (time-independent) term in the energy series (3.70). The symmetric matrix $\tilde{A}_1 - \lambda_2(\omega_1) D_e^2 = D_e^2 [A_1 - \lambda_2(\omega_1) I]$ has the eigenvalues 0 and

$$\operatorname{trace}(\tilde{A}_1 - \lambda_2(\omega_1) D_e^2) = 2\mu_s + \frac{8}{21} \frac{\omega_1^2}{\mu_s} + 6q(\omega_1) > 0,$$

which means that it is positive semidefinite. This leads to the inequality

$$\frac{d}{dt} \left(E(t) e^{2\lambda_2(\omega_1) t} \right) \leq 2\lambda_2(\omega_1) E(\infty) e^{2\lambda_2(\omega_1) t}, \quad t \geq 0.$$

By the monotonicity of the integral, we find after integration over $[0, t]$ the inequality (3.71). □

Remark 3.19. The energy inequality (3.71) could also be derived as in the case of the heat equation $u_t = \kappa u_{xx}$. That is, we can multiply the SP_3 system (3.44) with $\boldsymbol{\psi}^T D_e^2$ followed by an integration over Ω. Moreover, after integration by parts under the use of the homogeneous Neumann BCs (3.60), we can incorporate the following Poincaré-like inequality[7]

$$\int_\Omega \boldsymbol{\psi}^T D_e^2 \mathcal{D}\, \boldsymbol{\psi}\, dx - L\, \boldsymbol{\psi}_m^T D_e^2 \mathcal{D}\, \boldsymbol{\psi}_m \leq C^2 \int_\Omega \boldsymbol{\psi}_x^T D_e^2 \mathcal{D}\, \boldsymbol{\psi}_x\, dx,$$

with $C := L/\pi = 1/\omega_1$ and the mean value $\boldsymbol{\psi}_m := \frac{1}{L} \int_0^L \boldsymbol{\psi}(x,t)\, dx = (s_0/L, 0)^T$. Note that the matrix $D_e^2 \mathcal{D}$ is symmetric and positive definite.

We are now in position to verify the existence and uniqueness of a solution to the SP_3 equations in a bounded domain.

Theorem 3.20. *Let $Q \in C(\overline{\Omega})$ be a piecewise smooth source distribution with $Q'(0) = Q'(L) = 0$. Then, the SP_3 equations* (3.44) *on $\Omega = (0, L)$ subject to the Neumann-type BCs* (3.60) *and the initial condition* (3.46) *admit a unique solution in form of the uniformly convergent cosine series*

$$\boldsymbol{\psi}(x,t) = \sum_{k=0}^{\infty} \frac{2 - \delta_{k0}}{L} \boldsymbol{\psi}_k(t) \cos(\omega_k x), \quad x \in \overline{\Omega},\, t \geq 0, \tag{3.76}$$

[7] This relation can be obtained e.g. under the use of the cosine series (3.76).

with $\boldsymbol{\psi}_k$ being the time-dependent Fourier coefficients from (3.69)*. In addition, if we consider the defining equation for the source coefficients s_k, we additionally have*

$$\boldsymbol{\psi}(x,t) = \int_0^L \boldsymbol{\mathcal{K}}(x,\eta,t)Q(\eta)\,d\eta, \quad x \in \overline{\Omega},\, t > 0, \tag{3.77}$$

where the corresponding integral kernel $\boldsymbol{\mathcal{K}} = (\mathcal{K}_0, \mathcal{K}_2)^T$ is defined as

$$\boldsymbol{\mathcal{K}}(x,\eta,t) := \sum_{k=0}^{\infty} \frac{2-\delta_{k0}}{L} \mathbf{G}_k(t)\cos(\omega_k\eta)\cos(\omega_k x). \tag{3.78}$$

Proof. We begin with verifying the existence of a solution. In view of the series (3.76), we define $\boldsymbol{\Psi}_k(x,t) := \boldsymbol{\psi}_k(t)\cos(\omega_k x)$. Note that each $\boldsymbol{\Psi}_k$ is an eigensolution of the SP_3 equations (3.44). The derived estimates (3.52) and (3.53) can be used to provide the uniform upper bound

$$\|\boldsymbol{\Psi}_k(x,t)\|_\infty \leq \|\boldsymbol{\psi}_k(t)\|_\infty = |s_k|\,\|\mathbf{G}_k(t)\|_\infty \leq Me^{-a\omega_k^2 t_0} \quad \forall k \in \mathbb{N}_0,$$

for an arbitrary $t_0 > 0$. We furthermore have used $|s_k| \leq \int_0^L |Q(x)|\,dx = M$. The application of the ratio test shows that $\sum_{k=0}^{\infty} e^{-a\omega_k^2 t_0} < \infty$. Thus, according to the Weierstrass majorant criterion [2, p. 87], the series (3.76) converges on $\overline{\Omega} \times [t_0, \infty)$ absolutely and uniformly to a continuous vector-field. Next, we investigate the partial derivatives

$$\partial_x \boldsymbol{\Psi}_k(x,t) = -\omega_k \boldsymbol{\psi}_k(t)\sin(\omega_k x) \quad \text{and} \quad \partial_t \boldsymbol{\Psi}_t(x,t) = -A_k\boldsymbol{\psi}_k(t)\cos(\omega_k x),$$

that exist everywhere and vanish for $k = 0$. They can also be uniformly bounded on the domain $\overline{\Omega} \times [t_0, \infty)$ for each $k \in \mathbb{N}$ according to

$$\|\partial_x \boldsymbol{\Psi}_k(x,t)\|_\infty \leq M\omega_k e^{-a\omega_k^2 t_0} \quad \text{and} \quad \|\partial_t \boldsymbol{\Psi}_k(x,t)\|_\infty \leq M(\mu_s + \omega_k^2/\mu_s)e^{-a\omega_k^2 t_0},$$

where we have used $\|A_k\|_\infty \leq \mu_s + \omega_k^2/\mu_s$. Again, by the ratio test, both upper bounds can be summed up. Consequently, the series obtained after termwise differentiation of (3.76) converge uniformly and yield (continuous) representations for $\boldsymbol{\psi}_x$ and $\boldsymbol{\psi}_t$. Regarding the necessary conditions for termwise differentiation of a function series, we refer to [2, p. 92]. Moreover, we have on $\overline{\Omega} \times [t_0, \infty)$ the uniform estimate

$$\|\partial_x^m \partial_t^n \boldsymbol{\Psi}_k(x,t)\|_\infty \leq M\omega_k^m(\mu_s + \omega_k^2/\mu_s)^n e^{-a\omega_k^2 t_0} \quad \forall k \in \mathbb{N}.$$

Due to $\sum_{k=1}^{\infty} \omega_k^m(\mu_s + \omega_k^2/\mu_s)^n e^{-a\omega_k^2 t_0} < \infty$ (ratio test), we successively come to the same conclusion for higher order derivatives. In particular, the series solution (3.76) satisfies on $\overline{\Omega} \times [t_0, \infty)$ the SP_3 equations (3.44), due to (termwise differentiation)

$$\begin{aligned}\boldsymbol{\psi}_t + S\boldsymbol{\psi} - \mathcal{D}\boldsymbol{\psi}_{xx} &= \sum_{k=0}^{\infty} \frac{2-\delta_{k0}}{L}(\partial_t \boldsymbol{\Psi}_k + S\boldsymbol{\Psi}_k - \mathcal{D}\partial_x^2 \boldsymbol{\Psi}_k) \\ &= \sum_{k=0}^{\infty} \frac{2-\delta_{k0}}{L}(-A_k + S + \omega_k^2\mathcal{D})\boldsymbol{\Psi}_k = 0.\end{aligned}$$

For $t > 0$, we can differentiate the series (3.76) to confirm $\boldsymbol{\psi}_x(0,t) = \boldsymbol{\psi}_x(L,t) = 0$. When $t = 0$, we remind on the compatibility condition $Q'(0) = Q'(L) = 0$. This means that the BCs are satisfied for $t \geq 0$. In view of the initial condition, we have the alternative estimate

$$\|\boldsymbol{\Psi}_k(x,t)\|_\infty \leq |s_k|\,\|\mathbf{G}_k(t)\|_\infty \leq |s_k| \quad \forall k \in \mathbb{N}_0,$$

which holds true on $\overline{\Omega} \times [0,\infty)$. Due to $(s_k)_{k\in\mathbb{N}_0} \in \ell^1(\mathbb{N}_0)$, we can interchange limit with summation (due to the uniform convergence) which results in

$$\lim_{t\to 0} \boldsymbol{\psi}(x,t) = \sum_{k=0}^{\infty} \frac{2-\delta_{k0}}{L} \lim_{t\to 0} \boldsymbol{\Psi}_k(x,t) = \begin{pmatrix} Q(x) \\ 0 \end{pmatrix} \quad \forall x \in \Omega,$$

where we have used $\boldsymbol{\Psi}_k(x,0) = (s_k,0)^T \cos(\omega_k x)$. Thus, we in fact have found a solution to our problem with regularity $\phi_j \in C^\infty(\overline{\Omega}\times(0,\infty)) \cap C(\overline{\Omega}\times[0,\infty))$ for $j = 0,2$. As typical for parabolic systems, solutions to the SP_3 equations undergo smoothing as soon as $t > 0$. The integral representation (3.77) follows by replacing s_k by $\int_0^L Q(\eta)\cos(\omega_k\eta)\,d\eta$ in the series (3.76). Then, the exchange of summation and integration, which is allowed due to the uniform convergence on $\overline{\Omega}\times(0,\infty)$, yields the integral representation (3.77). To show the uniqueness, let $\boldsymbol{\psi}$ and $\boldsymbol{\varphi}$ be two classical solutions to the same problem. Then, by Lemma 3.18, we find $0 \le \|\boldsymbol{\psi}(\cdot,t) - \boldsymbol{\varphi}(\cdot,t)\|_{L_2(\Omega)} \le 0$ for all $t \ge 0$ and hence $\boldsymbol{\psi} = \boldsymbol{\varphi}$. □

A direct consequence of Lemma 3.18 is the following result on the stability and the long-time behavior.

Corollary 3.21. *The solution to the SP_3 equations from Theorem 3.20 depends continuously on the initial data and converges exponentially in time to the equilibrium state $\boldsymbol{\psi}_m = \lim_{t\to\infty} \boldsymbol{\psi}(x,t) = (s_0/L,0)^T$.*

Proof. Under the assumption $\|Q\|_{L_2(\Omega)} < \delta$, we obtain from Lemma 3.18 the estimate

$$\|\boldsymbol{\psi}(\cdot,t)\|_{L_2(\Omega)} \le \|D_e\boldsymbol{\psi}(\cdot,t)\|_{L_2(\Omega)} \le \|Q\|_{L_2(\Omega)} < \delta \quad \forall t \ge 0.$$

This means that for every $\varepsilon > 0$, we can choose $\delta = \varepsilon$ to ensure

$$\|\boldsymbol{\psi}(\cdot,0) - \boldsymbol{\varphi}(\cdot,0)\|_{L_2(\Omega)} < \delta \implies \|\boldsymbol{\psi}(\cdot,t) - \boldsymbol{\varphi}(\cdot,t)\|_{L_2(\Omega)} < \varepsilon \quad \forall t \ge 0. \tag{3.79}$$

Thus, small perturbations in the initial data yield small deviations in the solution. In addition, we can measure the stability in the maximum norm. For this, we consider the integral representation (3.77) under $\|Q\|_{L_\infty(\Omega)} < \delta$ and $|\mathcal{K}_j(x,\eta,t)| \le \frac{1}{L}\sum_{k\in\mathbb{Z}} e^{-a\omega_k^2 t_0}$ for $t \ge t_0 > 0$. The last series can be bounded by the Poisson summation formula (cf. Proposition 2.9) according to[8]

$$\frac{1}{L}\sum_{k\in\mathbb{Z}} e^{-a\omega_k^2 t_0} = \frac{1}{\sqrt{\pi a t_0}} \sum_{k\in\mathbb{Z}} \exp\left(-\frac{k^2L^2}{at_0}\right) \le \frac{1}{\sqrt{\pi a t_0}} \sum_{k\in\mathbb{Z}} \frac{1}{1+k^2L^2/(at_0)}.$$

For the last step, we have used $1+x \le e^x$ for all $x \in \mathbb{R}$. Under consideration of $\sum_{k\in\mathbb{Z}} \frac{1}{1+(\beta k)^2} = \frac{\pi}{\beta}\coth(\pi/\beta)$, we find with Hölder's inequality on $\overline{\Omega}\times[t_0,\infty)$ the upper bound

$$|\phi_j(x,t)| \le \|Q\|_{L_\infty(\Omega)} \int_0^L |\mathcal{K}_j(x,\eta,t)|\,d\eta < \delta\sqrt{\pi}\coth(\pi\sqrt{at_0}/L).$$

Hence, for an arbitrary $\varepsilon > 0$, we find with $\delta = \varepsilon\tanh(\pi\sqrt{at_0}/L)/\sqrt{\pi}$ the implication

$$\|\boldsymbol{\psi}(\cdot,0)\|_{L_\infty(\Omega)} < \delta \implies \|\boldsymbol{\psi}(\cdot,t)\|_{L_\infty(\Omega)} < \varepsilon \quad \forall t \ge t_0.$$

[8] In this context, we note on the required transform pair, see for example [31, p. 223]

$$\mathcal{F}^{-1}(e^{-\alpha k^2})(x) = \exp[-x^2/(4\alpha)]/\sqrt{4\pi\alpha}, \quad \alpha > 0.$$

The convergence to the equilibrium state follows directly from the energy inequality (3.71) by making use of

$$\frac{1}{2}\,\|\boldsymbol{\psi}(\cdot,t)-\boldsymbol{\psi}_m\|^2_{L_2(\Omega)}=\frac{1}{2}\,\|\boldsymbol{\psi}(\cdot,t)\|^2_{L_2(\Omega)}-E(\infty)\leq E(t)-E(\infty),$$

where we again have considered $\|\boldsymbol{\psi}(\cdot,t)\|_{L_2(\Omega)}\leq\|D_e\boldsymbol{\psi}(\cdot,t)\|_{L_2(\Omega)}$. Consequently, we get

$$\|\boldsymbol{\psi}(\cdot,t)-\boldsymbol{\psi}_m\|_{L_2(\Omega)}\leq\|\boldsymbol{\psi}(\cdot,0)-\boldsymbol{\psi}_m\|_{L_2(\Omega)}\,e^{-\lambda_2(\omega_1)t},\quad t\geq 0,$$

where we note on $E(0)=\frac{1}{2}\|\boldsymbol{\psi}(\cdot,0)\|^2_{L_2(\Omega)}$. For media with $L\mu_s\gg 1$ we have $\omega_1/\mu_s\ll 1$. Then, the rate of decay approaches that for the heat (SP_1) equation, due to

$$\lambda_2(\omega_1)=\frac{3\omega_1^2}{7\mu_s}+\frac{\mu_s}{2}-\sqrt{\frac{24\omega_1^4}{245\mu_s^2}+\frac{2\omega_1^2}{21}+\frac{\mu_s^2}{4}}\approx\frac{\omega_1^2}{3\mu_s}=\kappa/C^2,$$

with $C=1/\omega_1=L/\pi$ being the Poincaré constant. □

The kernel (3.78) has the meaning of a fundamental solution on a bounded domain.[9] In accordance with Subsection 2.2.2, we can apply the Poisson summation formula to both components, which results in

$$\mathcal{K}_j(x,\eta,t)=\sum_{k\in\mathbb{Z}}[G_j(x-\eta-2kL,t)+G_j(x+\eta-2kL,t)],\tag{3.80}$$

for $(x,\eta,t)\in[0,L]^2\times\mathbb{R}_+$ and G_j are the moments for the infinite medium. This means that the point source problem for the SP_3 equations on a bounded domain can also be solved by the method of images. In the next subsection, we derive closed-form expressions for the kernels (3.80) in Laplace space. The subsequent inversion of the Laplace transform enables us to verify the series representation (3.78) by a numerical experiment.

3.4.3 Solution for a bounded domain via the Laplace transform

In Subsection 3.4.1, we have used the Fourier transform in order to reduce the SP_3 equations to an ordinary first order system. The transformed moments $\hat{G}_j$ ($j=0,2$) could be found in explicit form, cf. (3.50). In this subsection, we apply also the one-sided Laplace transform (cf. Definition 2.10) with respect to time. As a consequence, the SP_3 equations (3.44) are reduced to a system of linear equations in Fourier-Laplace space. If we invert only the Fourier transform, we get moments of the form $\hat{G}_j(x,s)$. Then, by the method of images, we can construct the desired kernels for the bounded domain according to

$$\hat{\mathcal{K}}_j(x,\eta,s)=\sum_{k\in\mathbb{Z}}[\hat{G}_j(x-\eta-2kL,s)+\hat{G}_j(x+\eta-2kL,s)],\tag{3.81}$$

where $x,\eta\in[0,L]$ and $s\in\mathbb{R}_+$. The reason for restricting the complex Laplace variable to the positive real axis is due to the Post-Widder inversion formula, see Proposition 3.25. We will see that the series for $\hat{\mathcal{K}}_j$ can be summarized in closed form. It should be noted that the Laplace transform approach offers the possibility to incorporate much more complicated BCs than the Neumann-type conditions currently considered. However, the required inverse transform must be in general carried out numerically.

[9] This kernel function satisfies the initial condition $\boldsymbol{\mathcal{K}}(x,\eta,0)=(\delta(x-\eta),0)^T$ for $x,\eta\in\Omega$.

Proposition 3.22. *The moments of the fundamental solution to the SP_3 equations on $\Omega = \mathbb{R}$ in Laplace space are given by*

$$\hat{G}_j(x,s) = \frac{A_j}{2}\frac{e^{-\kappa_1|x|}}{\kappa_1} + \frac{B_j}{2}\frac{e^{-\kappa_2|x|}}{\kappa_2}, \quad x \in \mathbb{R},\ s \in \mathbb{R}_+, \tag{3.82}$$

for $j = 0, 2$. The corresponding parameters are defined as

$$\begin{aligned} A_0 &= \frac{1}{9}\frac{105\mu_s^2(s+\mu_s) - 55\kappa_1^2\mu_s}{\kappa_2^2 - \kappa_1^2}, \quad A_2 = \frac{1}{9}\frac{14\kappa_1^2\mu_s}{\kappa_2^2 - \kappa_1^2}, \\ B_0 &= \frac{1}{9}\frac{105\mu_s^2(s+\mu_s) - 55\kappa_2^2\mu_s}{\kappa_1^2 - \kappa_2^2}, \quad B_2 = \frac{1}{9}\frac{14\kappa_2^2\mu_s}{\kappa_1^2 - \kappa_2^2}, \\ \kappa_{1/2} &= \sqrt{5\mu_s s + \frac{35}{18}\mu_s^2 \pm \mu_s\sqrt{\frac{40}{3}s^2 + \frac{70}{9}\mu_s s + \frac{1225}{324}\mu_s^2}}. \end{aligned} \tag{3.83}$$

Proof. We start with the SP_3 equations in Fourier space, see (3.47), under consideration of the initial condition $\hat{\mathbf{G}}(k,0) = (1,0)^T$ for $k \in \mathbb{R}$. The application of the Laplace transform leads to the following system of linear equations

$$[sI + A(k)]\hat{\mathbf{G}}(k,s) = (1,0)^T, \quad k \in \mathbb{R},\ s \in \mathbb{R}_+, \tag{3.84}$$

where we have used the differentiation property for the first derivative, cf. Proposition 2.12. The corresponding solution is given by

$$\begin{aligned} \hat{G}_0(k,s) &= \frac{55k^2\mu_s + 105\mu_s^2(s+\mu_s)}{9k^4 + (90s+35\mu_s)k^2\mu_s + 105\mu_s^2 s(s+\mu_s)}, \\ \hat{G}_2(k,s) &= \frac{-14k^2\mu_s}{9k^4 + (90s+35\mu_s)k^2\mu_s + 105\mu_s^2 s(s+\mu_s)}. \end{aligned} \tag{3.85}$$

These expressions can be written in form of the following partial fractions

$$\hat{G}_j(k,s) = \frac{A_j}{k^2+\kappa_1^2} + \frac{B_j}{k^2+\kappa_2^2}, \quad k \in \mathbb{R},\ s \in \mathbb{R}_+.$$

We note that the coefficients belonging to these decompositions do not depend on $k \in \mathbb{R}$, see (3.83). Hence, the inverse Fourier transform[10] can be carried out analytically, which results in the moments from Proposition 3.22. □

Remark 3.23. The moments (3.82) can also be derived by solving $s\hat{\boldsymbol{\psi}} + S\hat{\boldsymbol{\psi}} = \mathcal{D}\hat{\boldsymbol{\psi}}_{xx}$ in Laplace space. More concretely, we then seek for a function that satisfies

$$\hat{\boldsymbol{\psi}}_{xx} = M\hat{\boldsymbol{\psi}}, \quad x \in \mathbb{R}\setminus\{0\},\ s \in \mathbb{R}_+, \tag{3.86}$$

with $M := \mathcal{D}^{-1}\mathrm{diag}(s, s+\mu_s)$ including the following continuity and jump condition

$$\begin{aligned} &\hat{\boldsymbol{\psi}}(0^+,s) = \hat{\boldsymbol{\psi}}(0^-,s), \\ &\hat{\boldsymbol{\psi}}_x(0^+,s) - \hat{\boldsymbol{\psi}}_x(0^-,s) = -\mathcal{D}^{-1}\begin{pmatrix}1\\0\end{pmatrix}, \end{aligned}$$

[10] In this context, we make use of the transform pair

$$\mathcal{F}(e^{-a|x|})(k) = \int_{-\infty}^{\infty} e^{-a|x|}e^{-ikx}\,dx = \frac{2a}{k^2+a^2}, \quad a > 0.$$

for all $s \in \mathbb{R}_+$. The general solution to (3.86) can be formally written in the form

$$\hat{\boldsymbol{\psi}}(x,s) = e^{\sqrt{M}x}\mathbf{c} + e^{-\sqrt{M}x}\mathbf{d},$$

with arbitrary constant vectors $\mathbf{c}$ and $\mathbf{d}$. In the present case, when $s \in \mathbb{R}_+$, the matrix M is diagonalizable with real-valued and positive eigenvalues κ_1^2 and κ_2^2, which are exactly those from (3.83). This means that the square root $\sqrt{M}$ is similar to $\operatorname{diag}(\kappa_1, \kappa_2)$. Hence, we find the following more compact alternative to (3.82)

$$\hat{\mathbf{G}}(x,s) = \frac{1}{2} e^{-\sqrt{M}|x|} \left(\mathcal{D}\sqrt{M}\right)^{-1} \begin{pmatrix} 1 \\ 0 \end{pmatrix}, \quad x \in \mathbb{R},\, s \in \mathbb{R}_+. \tag{3.87}$$

This expression can be conveniently evaluated in Matlab using the functions `expm` and `sqrtm` for the exponential and the square root of a matrix. The vector-valued function (3.87) has a certain similarity to Green's function of the classical heat equation in Laplace space, namely

$$\hat{G}_0(x,s) = \mathcal{L}\left(\frac{e^{-\frac{x^2}{4\kappa t}}}{\sqrt{4\pi\kappa t}}\right)(s) = \frac{1}{2} e^{-\sqrt{m}|x|} \left(\kappa\sqrt{m}\right)^{-1}, \tag{3.88}$$

for $(x,s) \in \mathbb{R} \times \mathbb{R}_+$ and $m := \kappa^{-1}s$.

Based on Proposition 3.22, we can give the desired kernels for the bounded domain.

Corollary 3.24. *The kernels* (3.81) *in Laplace space that satisfy the Neumann conditions* $\partial_x \hat{\boldsymbol{\mathcal{K}}}(0,\eta,s) = \partial_x \hat{\boldsymbol{\mathcal{K}}}(L,\eta,s) = 0$ *for* $(\eta,s) \in \Omega \times \mathbb{R}_+$ *are explicitly given by*

$$\begin{aligned} \hat{\mathcal{K}}_j(x,\eta,s) =& \frac{A_j}{2} \frac{\cosh\kappa_1(|x-\eta|-L) + \cosh\kappa_1(x+\eta-L)}{\kappa_1 \sinh(\kappa_1 L)} \\ &+ \frac{B_j}{2} \frac{\cosh\kappa_2(|x-\eta|-L) + \cosh\kappa_2(x+\eta-L)}{\kappa_2 \sinh(\kappa_2 L)}, \end{aligned} \tag{3.89}$$

where $x, \eta \in [0,L]$ *and* $s \in \mathbb{R}_+$. *The coefficients* A_j, B_j *and* κ_j *for* $j = 0, 2$ *are adopted from* (3.83). *In addition, the kernels written as vector-valued function become*

$$\begin{aligned} \hat{\boldsymbol{\mathcal{K}}}(x,\eta,s) =& \frac{1}{2} \Big[\cosh\sqrt{M}(|x-\eta|-L) \\ &+ \cosh\sqrt{M}(x+\eta-L)\Big] \left(\mathcal{D}\sqrt{M}\sinh(\sqrt{M}L)\right)^{-1} \begin{pmatrix} 1 \\ 0 \end{pmatrix}. \end{aligned}$$

Proof. We only have to evaluate the series (3.81) under consideration of the moments from Proposition 3.22. This can be done under the use of

$$\sum_{k\in\mathbb{Z}} e^{-\kappa|x-\eta-2kL|} = \frac{\cosh\kappa(|x-\eta|-L)}{\sinh(\kappa L)}, \quad \kappa > 0, \tag{3.90}$$

where $|x-\eta| \le L$. The vector-valued kernel function follows via summation of (3.87). □

For the last step, we need to apply the inverse Laplace transform to the kernels (3.89). In this way, we have the possibility to verify the derived Fourier series expansion (3.78). This is done in Subsection 3.5.2. Concerning the numerical inversion of the Laplace transform, it is advantageous to have some information about the function to be inverted. In the present case, if we consider the kernels (3.89) as function of the real variable $s \in \mathbb{R}_+$, we see that they are non-oscillating and continuously differentiable up to any order. In this situation, instead of evaluating the (complex) Bromwich contour integral, the inversion of the Laplace transform can also be carried out along the positive real axis by means of the Post-Widder inversion formula.

Proposition 3.25. *Let $f : [0, \infty) \to \mathbb{R}$ be a continuous function of exponential order $\alpha_0 \in \mathbb{R}$ and $\hat{f} = \mathcal{L}(f)$ the corresponding Laplace transform that exists for all $\sigma > \sigma_0$. Then, $f = \mathcal{L}^{-1}(\hat{f})$ can be reconstructed according to*

$$f(t) = \lim_{n\to\infty} \frac{(-1)^n}{n!} \left(\frac{n}{t}\right)^{n+1} \hat{f}^{(n)}\left(\frac{n}{t}\right), \quad t > 0. \tag{3.91}$$

Proof. A possible proof of this result can be found e.g. in [32, Theorem 2.4]. □

The direct application of the Post-Widder formula is difficult due to the required high order derivatives, which are in general not available. In Subsection 3.5.2, we make use of a discrete version of (3.91), the so-called Gaver-Stehfest formula [32, p. 144].

3.4.4 The time-harmonic SP_3 equations

Time-harmonic (monochromatic) light sources of the form $e^{-i\omega t}$, with $\omega \in \mathbb{R}$ being the angular modulation frequency, are often considered in diffuse optical tomography [9, 49, 50]. Here, the modulation frequency $f = \omega/(2\pi)$ typically lies between 25 MHz and 1 GHz [50]. It is important to note that this source type is formally defined for $t \in \mathbb{R}$ and hence a two-sided signal. Besides optical imaging, time-harmonic fields are also of importance in the context of Maxwell's equations, see e.g. the textbook [3]. Until now, we have considered the homogeneous (source-free) SP_3 equations (3.44) under a given initial condition at time zero. The same result can be obtained from the inhomogeneous system

$$\boldsymbol{\psi}_t(x,t) + S\boldsymbol{\psi}(x,t) = \mathcal{D}\boldsymbol{\psi}_{xx}(x,t) + \mathbf{Q}(x)\delta(t), \quad x \in \Omega,\, t \in \mathbb{R},$$

under $\boldsymbol{\psi}(\cdot, t) = 0$ for $t < 0$ and $\mathbf{Q} = (Q, 0)^T$. Thus, in view of the time variable, we have recovered a causal impulse response that vanishes for $t < 0$. In this case, the convolution theorem enables us to get the response to an extended source. More concretely, we have[11]

$$(\boldsymbol{\psi}(x,\cdot)e^{-\mu_a \cdot} * e^{-i\omega\cdot})(t) = e^{-i\omega t} \int_0^\infty \boldsymbol{\psi}(x,\tau) e^{-(\mu_a - i\omega)\tau}\, d\tau = e^{-i\omega t}\hat{\boldsymbol{\psi}}(x, \mu_a - i\omega), \tag{3.92}$$

for $(x,t) \in \Omega \times \mathbb{R}$. The amplitude $\hat{\boldsymbol{\psi}}$ satisfies the SP_3 equations in Laplace space

$$(sI + S)\hat{\boldsymbol{\psi}}(x,s) = \mathcal{D}\hat{\boldsymbol{\psi}}_{xx}(x,s) + \mathbf{Q}(x), \quad x \in \Omega,$$

for $s = \mu_a - i\omega$. In the time-harmonic case, we can set $\boldsymbol{\psi}(x,t) := \boldsymbol{\psi}(x)e^{-i\omega t}$ for $(x,t) \in \Omega \times \mathbb{R}$ with $\boldsymbol{\psi} : \Omega \to \mathbb{C}^2$ being the time-independent part that satisfies

$$\boldsymbol{\psi}_{xx}(x) + \mathcal{M}\boldsymbol{\psi}(x) = -\mathcal{D}^{-1}\mathbf{Q}(x), \quad x \in \Omega, \tag{3.93}$$

where $\mathcal{M} := \mathcal{D}^{-1}\mathrm{diag}(i\omega - \mu_a, i\omega - \mu_a - \mu_s) \in \mathbb{C}^{2,2}$. The time-harmonic system (3.93), which consists of two coupled Helmholtz equations, already contains the absorption. For a point source of the form $\delta(x)e^{-i\omega t}$ in the infinite medium, equation (3.93) exhibits the closed-form solution $\boldsymbol{\psi}(x) = \hat{\mathbf{G}}(x, \mu_a - i\omega)$ with $\hat{\mathbf{G}} = (\hat{G}_0, \hat{G}_2)^T$ being the moments from (3.82). Moreover, if the point source $\delta(x - x_0)e^{-i\omega t}$ is located in the finite domain $\Omega = (0, L)$, we have $\boldsymbol{\psi}(x) = \hat{\boldsymbol{\mathcal{K}}}(x, x_0, \mu_a - i\omega)$, where $\hat{\boldsymbol{\mathcal{K}}} = (\hat{\mathcal{K}}_0, \hat{\mathcal{K}}_2)^T$ are adopted from (3.89). Apart from δ-sources, we can also solve (3.93) for the more general case of $Q(x)e^{-i\omega t}$.

[11] We remind on the factor $e^{-\mu_a t}$ due to the absorption.

Proposition 3.26. *Let $Q \in C(\overline{\Omega})$ be a piecewise smooth source distribution with representation (2.19). Then, the time-harmonic SP_3 equations (3.93) on $\Omega = (0, L)$ subject to $\boldsymbol{\psi}_x(0) = \boldsymbol{\psi}_x(L) = 0$ exhibits a solution of the form*

$$\boldsymbol{\psi}(x) = \sum_{k=0}^{\infty} \frac{2 - \delta_{k0}}{L} \hat{\mathbf{G}}(\omega_k, \mu_a - i\omega) q_k \cos(\omega_k x), \quad x \in \overline{\Omega}, \tag{3.94}$$

where $\mu_a \geq 0$ and $\mu_a - i\omega \neq 0$. Moreover, $\hat{\mathbf{G}} = (\hat{G}_0, \hat{G}_2)^T$ are the moments from (3.85).

Proof. The application of the FCT to (3.93) under consideration of Proposition 3.17 leads to the system $[(\mu_a - i\omega)I + A_k]\hat{\psi}_k = (q_k, 0)^T$, which is practically the same as (3.84). It would also be possible to show the well-posedness, due to $(q_k)_{k\in\mathbb{N}_0} \in \ell^1(\mathbb{N}_0)$. □

For the modulation frequency $\omega = 0$, one obtains the solution of the SP_3 equations in the steady-state domain. On the other hand, if we consider (3.93) for variable modulation frequencies, we get solutions of the form $\boldsymbol{\psi} = \boldsymbol{\psi}(x, \omega)$. We then can reconstruct the time-dependent moments for $x \in \Omega$ and $t \geq 0$ according to

$$\int_{\mathbb{R}} \boldsymbol{\psi}(x, \omega) e^{-i\omega t}\, d\omega = \int_{\mathbb{R}} \hat{\boldsymbol{\psi}}(x, \mu_a + i\omega) e^{i\omega t}\, d\omega = 2\pi e^{-\mu_a t} \boldsymbol{\psi}(x, t). \tag{3.95}$$

Note that the second integral can be seen as a Bromwich integral, see Definition 2.10. This means also that, instead of solving the SP_3 equations directly in time domain, we alternatively could solve (3.93). However, the remaining (numerical) integration in frequency domain can become a quite challenging task especially in the neighbourhood of δ-sources, caused by the slowly decaying and oscillating integrand. Due to the causality in time domain, the real and imaginary part of $\boldsymbol{\psi}$ associated with (3.93) are connected by the Hilbert transform [28, Chapter 7]

$$\operatorname{Im} \boldsymbol{\psi}(x, \omega) = \frac{1}{\pi} \int_{\mathbb{R}} \frac{\operatorname{Re} \boldsymbol{\psi}(x, \tau)}{\omega - \tau}\, d\tau \quad \text{and} \quad \operatorname{Re} \boldsymbol{\psi}(x, \omega) = -\frac{1}{\pi} \int_{\mathbb{R}} \frac{\operatorname{Im} \boldsymbol{\psi}(x, \tau)}{\omega - \tau}\, d\tau,$$

for $(x, \omega) \in \Omega \times \mathbb{R}$ and the integrals are considered as Cauchy principal values. By taking into account $\operatorname{Re} \boldsymbol{\psi}(\cdot, -\omega) = \operatorname{Re} \boldsymbol{\psi}(\cdot, \omega)$ and $\operatorname{Im} \boldsymbol{\psi}(\cdot, -\omega) = -\operatorname{Im} \boldsymbol{\psi}(\cdot, \omega)$, we can restrict the integration to positive frequencies which leads then to the classical Kramers–Kronig relations [28, Chapter 7]. If one part is known, the other one can be computed. This is consistent with the fact that a one-sided signal is completely determined by its even or odd part.[12] Hence, as an alternative to (3.95), we can reconstruct the solution to the time-dependent SP_3 equations according to

$$e^{-\mu_a t} \boldsymbol{\psi}(x, t) = \frac{2}{\pi} \int_0^{\infty} \operatorname{Re} \boldsymbol{\psi}(x, \omega) \cos(\omega t)\, d\omega = \frac{2}{\pi} \int_0^{\infty} \operatorname{Im} \boldsymbol{\psi}(x, \omega) \sin(\omega t)\, d\omega.$$

Remark 3.27. The time-harmonic SP_3 equations (3.93) already contain the absorption, but the speed of light is missing. We can incorporate this quantity by a simple modification of (3.92) according to

$$(c\boldsymbol{\psi}(x, c\cdot) e^{-\mu_a c \cdot} * e^{-i\omega \cdot})(t) = e^{-i\omega t} \hat{\boldsymbol{\psi}}(x, \mu_a - i\omega/c), \quad x \in \Omega,\ t \in \mathbb{R}. \tag{3.96}$$

Thus, we only have to replace $i\omega$ by $i\omega/c$ in the matrix $\mathcal{M}$ occurring in (3.93).

[12] We note on

$$f_{\text{even}}(t) = \frac{f(t) + f(-t)}{2} \quad \text{and} \quad f_{\text{odd}}(t) = \frac{f(t) - f(-t)}{2}.$$

In the next section, the last numerical experiment is carried out in the frequency domain under consideration of realistic optical properties. The relevant quantities in view of experimental activities are the modulation M and the phase shift θ [50]. In the case of fluence measurements these quantities are defined as

$$M(x,\omega) := \left| \frac{\phi_0(x,\omega)}{\phi_0(x,0)} \right| \quad \text{and} \quad \theta(x,\omega) := \arg \phi_0(x,\omega), \quad (x,\omega) \in \Omega \times \mathbb{R}. \tag{3.97}$$

3.5 Numerical experiments

The derived solutions to the SP_3 equations were implemented in Matlab for comparison purposes. We show in this section the result of different numerical experiments for both the infinite medium and the bounded domain $\Omega = (0, L)$ under the Neumann-type conditions (3.60). In general, except for two examples, we restrict our attention to non-absorbing media, because the solutions to the derived SP_N equations exhibit the same exact dependence on absorption[13] as the solutions to the RTE and the P_N equations. We recall at this point that the presented results for the SP_1 equation correspond to those of the classical heat equation. We also note that the figures shown below were generated with Matlab.

3.5.1 Simulations for the infinite medium

The first comparison is for an infinite medium with scattering coefficient $\mu_s = 0.9$ that is illuminated by an instantaneous δ-source. Figure 3.3 displays the fluence for the time value $t = 2$ predicted by different theories. We see that only the exact transport theory fluence (2.15) exhibit the correct causality principle. For small distances, the SP_3 fluence according to (3.56) performs better than the classical heat kernel (2.8).

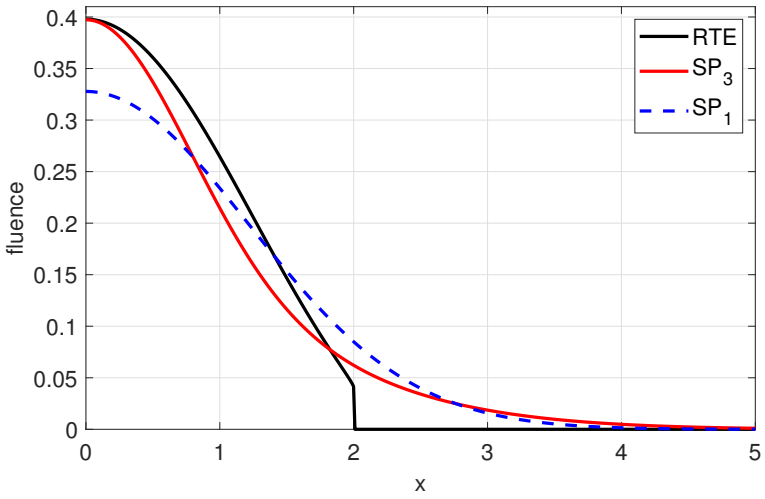

Figure 3.3: Fundamental solution in the infinite medium for $t = 2$ predicted by different theories.

We reconsider the infinite medium from the first comparison, but we replace the δ-source by the more realistic Gaussian distribution $Q(x) = e^{-\frac{x^2}{2\varepsilon}}/\sqrt{2\pi\varepsilon}$ with parameter $\varepsilon = 0.05$. In this case, the data for the transport theory fluence can be generated numerically by means

[13] That is given by a simple multiplication with the exponential $e^{-\mu_a t}$.

of the convolution. In addition, we have included the fluence predicted by the (hyperbolic) P_3 equations, which can be computed by the formulae (3.99) for $\varepsilon = 1$. Figure 3.4 shows a snapshot for the time value $t = 3$. Interestingly, in this case, the fluence belonging to the more exact and complicated P_3 equations performs not really better than the SP_3 fluence. The deviations disappear completely when increasing the P_N approximation order N.

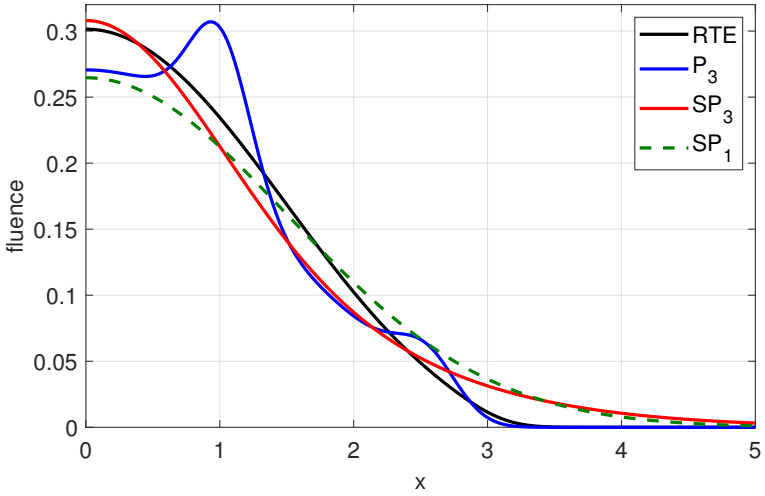

Figure 3.4: Fluence in the infinite medium for the time value $t = 3$ caused by a Gaussian distribution with $\varepsilon = 0.05$.

As mentioned at the beginning of this section, we consider in two cases also an absorbing medium. Figure 3.5 displays the time-resolved fluence G_0 from (3.56) due to a δ-source located in an infinitely extended scattering and absorbing medium with properties $\mu_s = 1$ and $\mu_a = 0.03$. As expected, the fluence predicted by the (parabolic) SP_3 equations (red solid lines) fails at short times, but converges to the exact transport theory (black dashed lines) as $t \to \infty$.

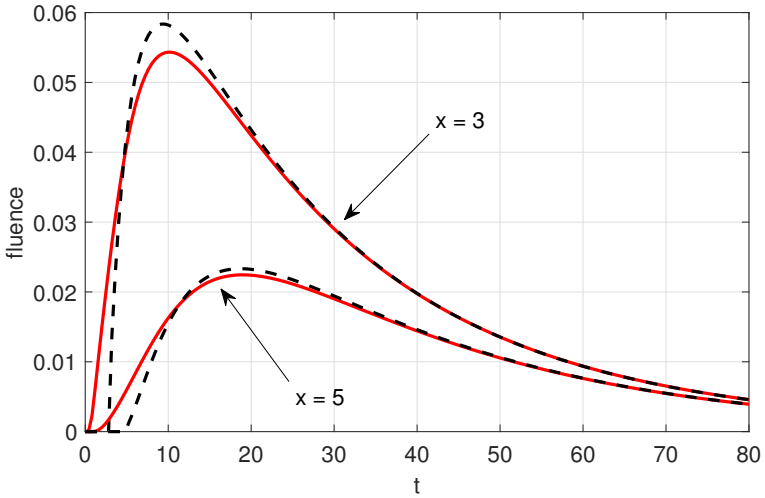

Figure 3.5: Time-resolved fluence in an infinitely extended scattering and absorbing medium evaluated at the positions $x = 3$ and $x = 5$.

For the last experiment in the infinite medium, we want to reconstruct the derived SP_3 solution (3.55) by solving the ϵ-dependent P_3 equations numerically. They are explicitly

given by

$$\frac{\partial}{\partial t}\begin{pmatrix}\phi_0\\ \epsilon\phi_1\\ \phi_2\\ \epsilon\phi_3\end{pmatrix} + A\boldsymbol{\phi}_x + \Sigma\,\boldsymbol{\phi} = 0, \quad x \in \mathbb{R},\, t > 0, \tag{3.98}$$

subject to $\boldsymbol{\phi}(x,0) = Q(x)e_0$ for $x \in \mathbb{R}$, where $e_0 = (1,0,0,0)^T$. Note that the matrices A and Σ are those from (3.11). The parameter $\epsilon \in [0,1]$ allows us to make a smooth transition from the hyperbolic P_3 equations ($\epsilon = 1$) to the parabolic SP_3 equations ($\epsilon = 0$). The P_3 equations (3.98) in Fourier space become $I_\varepsilon \hat{\boldsymbol{\phi}}_t + (\Sigma + ikA)\hat{\boldsymbol{\phi}} = 0$ with $\hat{\boldsymbol{\phi}}(k,0) = \hat{Q}(k)e_0$ and $I_\varepsilon = \operatorname{diag}(1,\epsilon,1,\epsilon)$. The corresponding solution can be again given in terms of the matrix exponential, namely $\hat{\boldsymbol{\phi}}(k,t) = \hat{Q}(k)\exp\left(-I_\varepsilon^{-1}(\Sigma + ikA)t\right)e_0$. The application of the inverse Fourier transform leads then to the moments

$$\boldsymbol{\phi}(x,t) = \frac{1}{2\pi}\int_{-\infty}^{\infty} \hat{Q}(k)\exp\left(-I_\varepsilon^{-1}(\Sigma + ikA)t\right)e_0 e^{ikx}\,dk, \quad (x,t) \in \mathbb{R}\times[0,\infty). \tag{3.99}$$

Figure 3.6 shows the zero order moment ϕ_0 (left figure) and the second order moment ϕ_2 (right figure) for different values of the parameter ϵ. The considered time value is $t = 2$. The infinite medium is characterized by the scattering coefficient $\mu_s = 0.9$. In view of the initial condition, we consider the Gaussian pulse from the second experiment. The derived solution to the SP_3 equations $\boldsymbol{\psi} = (\phi_0, \phi_2)^T$ from (3.55) is shown by the black lines. As can be seen, when ϵ goes to zero, the even moments (3.99) predicted by the ϵ-dependent P_3 equations tend to the SP_3 moments (3.55).

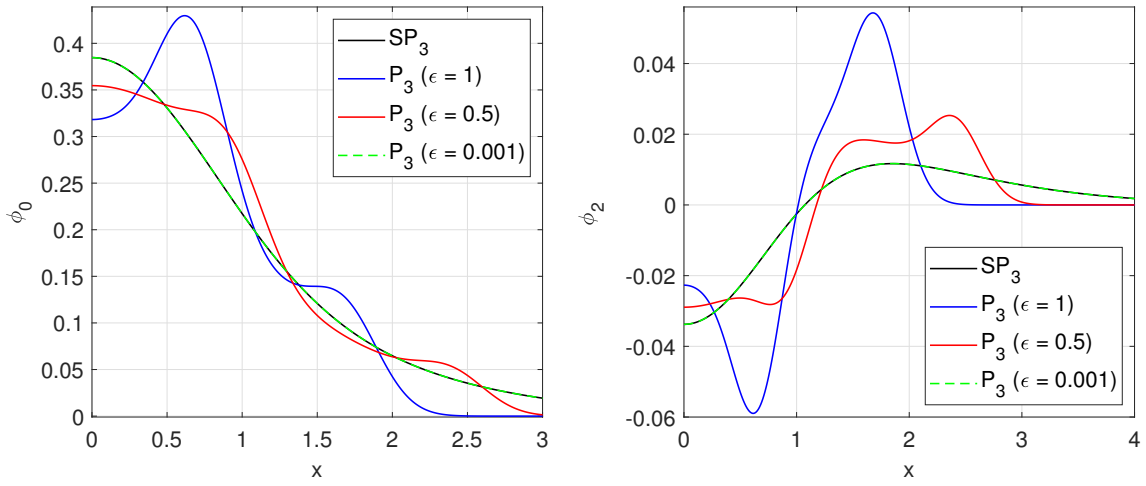

Figure 3.6: Reconstruction of the SP_3 moments via numerical solution of the ϵ-dependent P_3 equations for different values of the parameter ϵ.

3.5.2 Simulations for the bounded domain

We now perform comparisons in a bounded domain under consideration of Neumann-type conditions. The kernel function (3.78) plays a key role in solving the SP_3 equations on $\Omega = (0,L)$. The first experiment concerns with the verification of $\mathcal{K}_0$ from (3.78) by applying the Post-Widder inversion formula (3.91) to the image function $\hat{\mathcal{K}}_0$ from (3.89). The direct evaluation of the Post-Widder formula is difficult due to the required high-order derivatives in Laplace space. We therefore have implemented a computable representation for the formula

(3.91), namely the so-called Gaver-Stehfest formula. That is [32, p. 144]

$$f(t) \approx \frac{\ln 2}{t} \sum_{k=1}^{2M} V_k \hat{f}(s_k), \quad t > 0, \tag{3.100}$$

where $s_k := k \ln(2)/t$ are the discrete values on the positive real axis on which the image function $\hat{f}$ is evaluated. Moreover, the corresponding weights V_k are given by [32, p. 144]

$$V_k := (-1)^{k+M} \sum_j \frac{j^M (2j)!}{(M-j)!j!(j-1)!(k-j)!(2j-k)!},$$

where $\lfloor (k+1)/2 \rfloor \leq j \leq \min(k, M)$ and $\lfloor \cdot \rfloor$ is the floor function. Figure 3.7 shows the kernel function $\mathcal{K}_0$ for $\eta = 2$ in a bounded domain of thickness $L = 3$ and $\mu_s = 1$. Physically, it represents the fluence in a bounded domain caused by a δ-source located at $\eta = 2$. The solid colored lines correspond with the Fourier series expansion (3.78), whereas the black dashed lines are the numerical inversion of $\hat{\mathcal{K}}_0$ from (3.89) by means of the Gaver-Stehfest formula (3.100) for the value $M = 8$. We see that the numerically inverted kernel function is in good agreement with the data generated by the Fourier series (3.78).

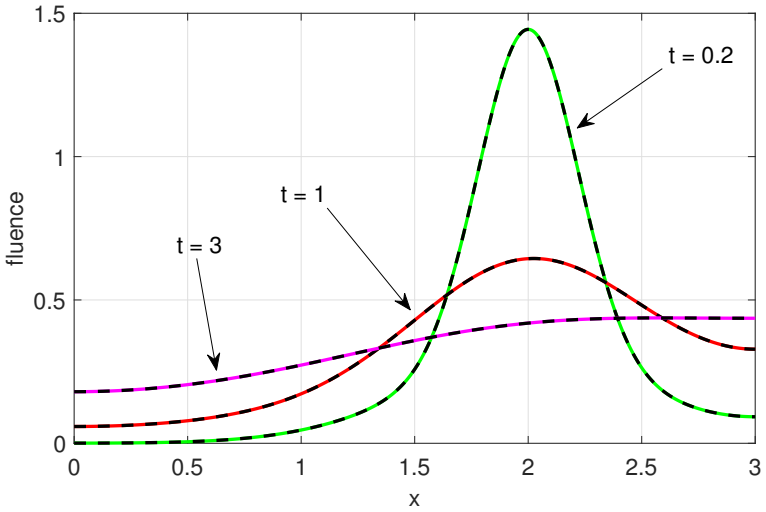

Figure 3.7: Comparison between $\mathcal{K}_0$ in Fourier series representation (3.78) and the numerical inversion of the image function $\hat{\mathcal{K}}_0$ from (3.89) by means of the Gaver-Stehfest formula (3.100).

Similar as done for the infinite space, we compare the fluence in the bounded medium $\Omega = (0, 4)$ with $\mu_s = 0.9$ predicted by different theories. In view of the initial condition, we take into account the Poisson-like distribution (3.34) for $x_0 = 3$ and $\varrho = 0.95$. This distribution satisfies also the compatibility condition $Q'(0) = Q'(L) = 0$. We additionally note that for $\varrho = 1$ we would recover the kernel function (3.78) for the bounded domain with $\eta = x_0$. The Poisson-like distribution becomes in this case a Dirac comb. Thus, we simulate in the present case a kind of damped kernel function. In view of the SP_3 equations we have to consider the Fourier series (3.76). We also incorporate the fluence belonging to the P_3 equations, which can be computed by the derived expression (3.33). Figure 3.8 displays the fluence for two time values predicted by different theories. Again, the fluence obtained from the hyperbolic P_3 equations exhibits an interesting behavior. For the smaller time value $t = 0.3$ (left figure), it agrees at least for $|x - 3| > 0.5$ with the exact transport theory. By

contrast, large deviations from the expected values are observed in the case $t = 1$ (right figure). These deviations can be removed by increasing the P_N approximation order N.

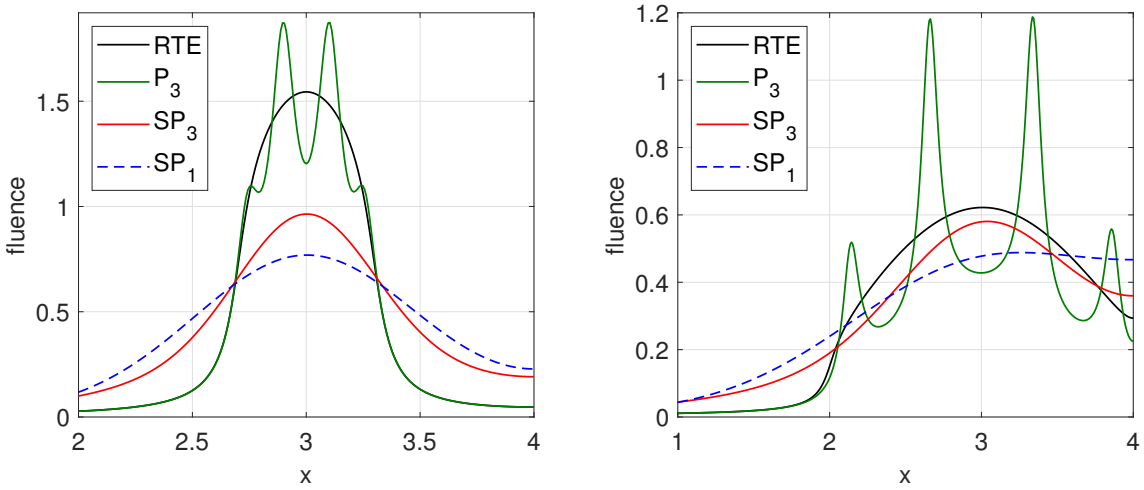

Figure 3.8: Comparison of the fluence in a bounded domain caused by a Poisson-like distribution with parameters $\varrho = 0.95$ and $x_0 = 3$. The left figure shows the case $t = 0.3$, whereas the right one corresponds with $t = 1$.

To address the question of uniqueness and stability, we have seen that the derived energy function from Lemma 3.18 was quite useful. Figure 3.9 shows as an example the energy function (3.70) including its first derivative (3.74) in a bounded domain of thickness $L = 5$. The scattering coefficient is set to $\mu_s = 0.9$ and the considered Poisson-like distribution (3.34) is characterized by $\varrho = 0.4$ and $x_0 = 3$. In accordance with the theoretical predictions, the energy function decreases monotonically and converges for $t \to \infty$ against the final value $E(\infty) = s_0^2/(2L) = 0.1$. In addition, the green dashed line shows the upper bound of the energy inequality (3.71).

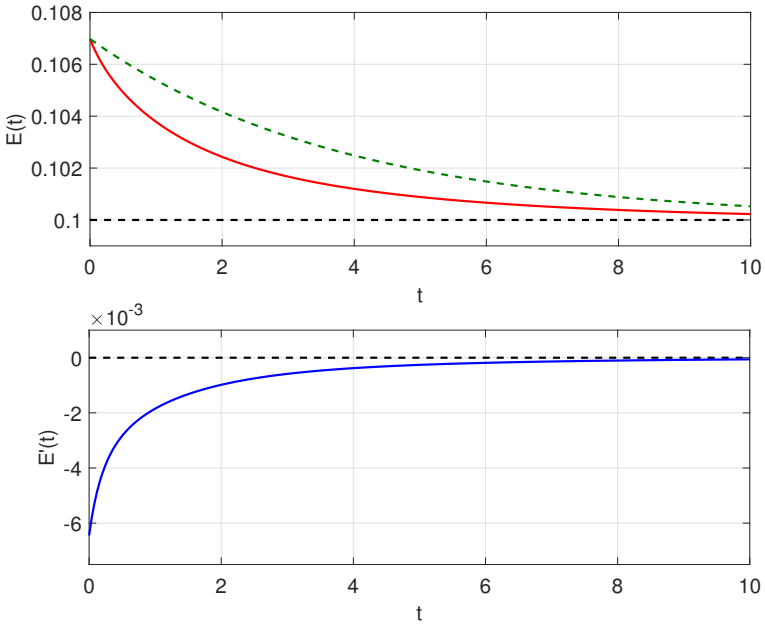

Figure 3.9: Energy function and its first derivative associated with the time-dependent SP_3 equations on a bounded domain.

The last numerical experiment is carried out in the frequency domain. For this, we consider a medium of size $L = 10\,\text{mm}$ with optical properties $\mu_a = 0.01\,\text{mm}^{-1}$ and $\mu_s = 1.0\,\text{mm}^{-1}$. We note that these values for the absorption and the scattering coefficient are typical for biological tissue in the near-infrared (NIR) spectral range [20]. The sample is illuminated by a sinusoidally modulated point light source located at $x_0 = 5\,\text{mm}$ and the resulting fluence $\phi_0 = |\phi_0|e^{i\theta}$ is detected at a certain distance $d := |x - x_0|$. The speed of light in the medium is set to $c = 300\,\text{mm/ns}$. Figure 3.10 shows the modulation M and the phase shift θ according to (3.97) for a typical frequency range. The red solid lines display the fluence belonging to the time-harmonics SP_3 equations (3.93). Note that this is just the kernel function $\hat{\mathcal{K}}_0$ from (3.89) evaluated for $\eta = x_0$ and $s = \mu_a - i\omega/c$. Alternatively, one can use (3.94) for $q_n = \cos(\omega_n x_0)$. For illustration purposes, we additionally have included the exact transport theory fluence (black dashed lines) and the solution to the often used SP_1 equation (blue dashed lines). The latter one can be obtained by the method of images applied to $\hat{G}_0(x, \mu_a - i\omega/c)$ from (3.88). Concerning the transport theory, we can directly use the derived fluence expression (2.22) for $q_n = \cos(\omega_n x_0)$ and $s = \mu_a - i\omega/c$. As shown in Figure 3.10, for the larger distance $d = 2\,\text{mm}$, all theories are in relative good agreement (especially in the case of the modulation M). However, for $d = 0.1\,\text{mm}$, we observe the mentioned problems of the classical diffusion approximation near sources and/or high modulation frequencies.[14] Of course, the SP_3 fluence indeed performs better, but also starts to deviate from the (desired) transport theory data.

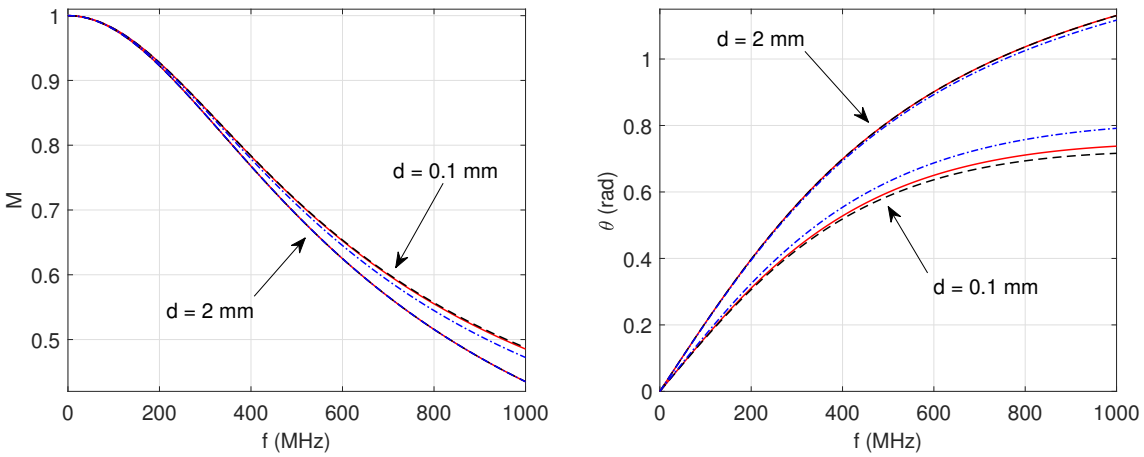

Figure 3.10: Modulation M (left figure) and phase shift θ (right figure) for the frequency domain fluence ϕ_0 in a bounded domain.

[14] See also [20, Chapter 3] regarding the applicability of the diffusion equation in biomedical optics.

4 Conclusion

In this thesis, we have reported about some known as well as some new (or at least not well-known) results on the time-dependent simplified spherical harmonics equations. Let us summarize in this conclusion the findings we have obtained regarding these equations. The starting point, the derivation of the SP_N equations, was basically known to relevant scientists, but without the separation of the absorption. However, as shown in (3.58), this small modification ensured the convergence of the SP_3 fluence (in the long-time limit) against the exact transport theory quantity. In the further course, we have confirmed the parabolic nature of the SP_N equations by determining their characteristics. We now come to the main objective of this thesis, namely the derivation of exact solutions to the SP_3 equations. To accomplish this task successfully, we started with some considerations in the infinite medium. Here, we have derived an analytical solution to the SP_3 equations in Fourier space. The obtained moments (3.50) belonging to the fundamental solution could be uniformly bounded by the Gaussian function e^{-ak^2t}, with $a = \left(\frac{3}{7} - \frac{2}{7}\sqrt{\frac{6}{5}}\right)/\mu_s$ being the smaller eigenvalue of the diffusion matrix $\mathcal{D}$ from (3.45). Based on this, we were able to bound the SP_3 fluence (caused by a δ-source) by the square root function (3.54). This is similar as for the classical heat kernel. Some of the results obtained for the infinite medium could be directly used in the next Subsection 3.4.2, in which we considered the more realistic case of a bounded domain. Here, we started with the derivation of a formal solution under the use of the finite cosine transform, which led to the same initial value problem as for the infinite medium. In proving the well-posedness of the obtained series solution, we have introduced Lemma 3.18 as preparation. It is mentionable that the derived energy inequality (3.71) has the same form as that for the classical heat equation under homogeneous Neumann conditions. The existence and uniqueness as well as the C^∞ regularity (on $\overline{\Omega} \times (0, \infty)$) were then shown with Theorem 3.20. As a consequence of the analysis carried out so far, we could prove the continuous dependence on the initial data as well as the exponential decay (in time) to the equilibrium state (Corollary 3.21). In Subsection 3.4.3, we derived alternative closed-form expressions in Laplace space, which are particularly useful in the context of the time-harmonic SP_3 equations, which have been considered in Subsection 3.4.4. For illustration and verification purposes, we have implemented the obtained solutions for the infinite medium and the bounded domain within Matlab. The numerical experiments outlined in Section 3.5 have shown different things. On the one hand, we could successfully verify the derived series solution (3.76) with the numerical inversion of the expression (3.89) by means of the Post-Widder formula. On the other hand, the considered numerical experiments indicated the improvements achieved by the SP_3 equations (compared to the diffusion theory) especially in the neighbourhood of sources. In some figures, we additionally included the results obtained from the more exact P_3 equations. However, at least in the cases shown, these strongly oscillating results were not really better (compared to transport theory) than those obtained by the SP_3 equations. In view of concrete applications, this can become a decisive point since the SP_3 equations are easier to solve than the (hyperbolic) P_3 equations. As for a future work, it would be interesting to consider and solve the time-dependent SP_3 equations in a layered medium (piecewise constant coefficients), because this is an often assumed model within biomedical optics applications.

Bibliography

[1] I. SenGupta and M. C. Mariani, "Spherical harmonics approach to parabolic partial differential equations," *Analysis and Mathematical Physics*, vol. 2, pp. 461–471, 2012.

[2] N. H. Asmar, *Partial differential equations with Fourier series and boundary value problems*. Courier Dover Publications, 2016.

[3] A. Kirsch and F. Hettlich, *The Mathematical Theory of Time-Harmonic Maxwell's Equations*. Springer, New York, 2015.

[4] J. J. Duderstadt and W. R. Martin, *Transport theory*. Wiley-Interscience, New York, 1979.

[5] S. R. Arridge, "Optical tomography in medical imaging," *Inverse Problems*, vol. 15, pp. R41—R93, 1999.

[6] M. Machida, G. Y. Panasyuk, J. C. Schotland, and V. A. Markel, "The Green's function for the radiative transport equation in the slab geometry," *Journal of Physics A: Mathematical and Theoretical*, vol. 43, no. 6, p. 065402, 2010.

[7] E. M. Gelbard, "Simplified spherical harmonics equations and their use in shielding problems," *Tech. Report WAPD-T-1182*, 1961.

[8] M. Chu, K. Vishwanath, A. D. Klose, and H. Dehghani, "Light transport in biological tissue using three-dimensional frequency-domain simplified spherical harmonics equations," *Physics in Medicine & Biology*, vol. 54, no. 8, p. 2493, 2009.

[9] J. B. Domínguez and Y. Bérubé-Lauzière, "Diffuse light propagation in biological media by a time-domain parabolic simplified spherical harmonics approximation with ray-divergence effects," *Applied Optics*, vol. 49, no. 8, pp. 1414–1429, 2010.

[10] E. Olbrant, E. W. Larsen, M. Frank, and B. Seibold, "Asymptotic derivation and numerical investigation of time-dependent simplified P_N equations," *Journal of Computational Physics*, vol. 238, pp. 315–336, 2013.

[11] M. Frank, A. Klar, E. W. Larsen, and S. Yasuda, "Time-dependent simplified P_N approximation to the equations of radiative transfer," *Journal of Computational Physics*, vol. 226, no. 2, pp. 2289–2305, 2007.

[12] A. D. Klose and E. W. Larsen, "Light transport in biological tissue based on the simplified spherical harmonics equations," *Journal of Computational Physics*, vol. 220, no. 1, pp. 441–470, 2006.

[13] D. Lee, T. Kozlowski, and T. J. Downar, "Multi-group SP_3 approximation for simulation of a three-dimensional PWR rod ejection accident," *Annals of Nuclear Energy*, vol. 77, pp. 94–100, 2015.

[14] A. Carreño, A. Vidal-Ferràndiz, D. Ginestar, and G. Verdú, "Time-dependent simplified spherical harmonics formulations for a nuclear reactor system," *Nuclear Engineering and Technology*, vol. 53, no. 12, pp. 3861–3878, 2021.

[15] C. Fiorina, M. Hursin, and A. Pautz, "Extension of the GeN-Foam neutronic solver to SP_3 analysis and application to the CROCUS experimental reactor," *Annals of Nuclear Energy*, vol. 101, pp. 419–428, 2017.

[16] A. Carreño, A. Vidal-Ferràndiz, D. Ginestar, and G. Verdú, "Frequency-domain models in the SP_N approximation for neutron noise calculations," *Progress in Nuclear Energy*, vol. 148, p. 104233, 2022.

[17] H. Zheng and W. Han, "On simplified spherical harmonics equations for the radiative transfer equation," *Journal of mathematical chemistry*, vol. 49, pp. 1785–1797, 2011.

[18] R. G. McClarren, "Theoretical aspects of the simplified Pn equations," *Transport Theory and Statistical Physics*, vol. 39, pp. 73–109, 2010.

[19] M. F. Modest and S. Mazumder, *Radiative heat transfer*. Academic press, 2021.

[20] F. Martelli, T. Binzoni, S. Del Bianco, A. Liemert, and A. Kienle, *Light propagation through biological tissue and other diffusive media: theory, solutions, and validations*. SPIE Press Bellingham, Washington, 2022.

[21] W. M. Stacey, *Nuclear Reactor Physics*. John Wiley & Sons, 2018.

[22] L. Wang, S. L. Jacques, and L. Zheng, "MCML–Monte Carlo modeling of light transport in multi-layered tissues," *Computer Methods and Programs in Biomedicine*, vol. 47, pp. 131–146, 1995.

[23] D. Balsara, "Fast and accurate discrete ordinates methods for multidimensional radiative transfer. Part I, basic methods," *Journal of Quantitative Spectroscopy and Radiative Transfer*, vol. 69, pp. 671–707, 2001.

[24] F. Asllanaj and S. Fumeron, "Modified finite volume method applied to radiative transfer in 2D complex geometries and graded index media," *Journal of Quantitative Spectroscopy and Radiative Transfer*, vol. 111, pp. 274—-279, 2010.

[25] B. D. Ganapol, "P_1 approximation to the time-dependent monoenergetic neutron transport equation in infinite media," *Transport Theory and Statistical Physics*, vol. 9, no. 4, pp. 145–159, 1980.

[26] R. Carminati and J. C. Schotland, *Principles of scattering and transport of light*. Cambridge University Press, 2021.

[27] G. Yuan, "Convergence of P_N approximation for the neutron transport equation with reflective boundary condition," *Journal of Mathematical Physics*, vol. 41, pp. 867–874, 2000.

[28] A. D. Poularikas and A. M. Grigoryan, *Transforms and applications handbook*. CRC press, 2018.

[29] L. Debnath and D. Bhatta, *Integral transforms and their applications*. Chapman and Hall/CRC, 2007.

[30] K. N. Liou, Q. Fu, and T. P. Ackerman, "A simple formulation of the delta-four-stream approximation for radiative transfer parameterizations," *Journal of Atmospheric Sciences*, vol. 45, no. 13, pp. 1940–1948, 1988.

[31] G. B. Folland, *Fourier analysis and its applications*, vol. 4. American Mathematical Soc., 2009.

[32] A. M. Cohen, *Numerical methods for Laplace transform inversion*, vol. 5. Springer Science & Business Media, 2007.

[33] J. Palmeri, "Exact solutions to the time-dependent Lorentz gas Boltzmann equation: the approach to hydrodynamics," *Journal of statistical physics*, vol. 58, no. 1, pp. 885–921, 1990.

[34] N. Bleistein and R. A. Handelsman, *Asymptotic expansions of integrals*. Dover Publications, 1986.

[35] A. Mandelis, "Green's functions in thermal-wave physics: Cartesian coordinate representations," *Journal of applied physics*, vol. 78, no. 2, pp. 647–655, 1995.

[36] R. C. McOwen, *Partial differential equation, second edition, Methods and Applications*. Prentice Hall, Upper Saddle River, NJ, 2003.

[37] S. I. Heizler, "Asymptotic telegrapher's equation (P_1) approximation for the transport equation," *Nuclear science and engineering*, vol. 166, no. 1, pp. 17–35, 2010.

[38] B. Fischer, *Polynomial based iteration methods for symmetric linear systems*. SIAM, 2011.

[39] E. Zauderer, *Partial differential equations of applied mathematics*. John Wiley & Sons, 2011.

[40] Y. Ilyashenko and S. Yakovenko, *Lectures on analytic differential equations*, vol. 86. American Mathematical Soc., 2008.

[41] W. Arendt and K. Urban, *Partial Differential Equations: An Introduction to Analytical and Numerical Methods*, vol. 294. Springer Nature, 2023.

[42] C. Heil, *Introduction to Real Analysis*, vol. 280. Springer, 2019.

[43] A. Einstein, *Investigations on the Theory of the Brownian Movement*. Courier Corporation, 1956.

[44] A. Liemert, F. Martelli, and A. Kienle, "Analytical solutions for the mean-square displacement derived from transport theory," *Physical Review A*, vol. 105, no. 5, p. 053505, 2022.

[45] T. Durduran, A. G. Yodh, B. Chance, and D. A. Boas, "Does the photon-diffusion coefficient depend on absorption?," *JOSA A*, vol. 14, no. 12, pp. 3358–3365, 1997.

[46] D. J. Durian, "The diffusion coefficient depends on absorption," *Optics letters*, vol. 23, no. 19, pp. 1502–1504, 1998.

[47] W. Cai, M. Xu, M. Lax, and R. R. Alfano, "Diffusion coefficient depends on time, not on absorption," *Optics letters*, vol. 27, no. 9, pp. 731–733, 2002.

[48] R. Pierrat, J.-J. Greffet, and R. Carminati, "Photon diffusion coefficient in scattering and absorbing media," *Journal of the Optical Society of America A*, vol. 23, no. 5, pp. 1106–1110, 2006.

[49] H. K. Kim, L. D. Montejo, J. Jia, and A. H. Hielscher, "Frequency-domain optical tomographic image reconstruction algorithm with the simplified spherical harmonics (SP_3) light propagation model," *International Journal of Thermal Sciences*, vol. 116, pp. 265–277, 2017.

[50] S. L. Jacques and B. W. Pogue, "Tutorial on diffuse light transport," *Journal of Biomedical Optics*, vol. 13, no. 4, pp. 041302–041302, 2008.